Model Analysis for Optimal Operation – A Heat Integrated Distillation Case Study

Li, Hong Wen; Jørgensen, Sten Bay

Publication date:
2006

Document Version
Publisher's PDF, also known as Version of record

Model Analysis for Optimal Operation - A Heat Integrated Distillation Case

Hong Wen Li

Ph. D - Thesis

April 2006

CAPEC

Department of Chemical Engineering

Technical University of Denmark

DK – 2800 Lyngby

Denmark

Preface

This thesis is submitted as partial fulfillment of the requirement for the Ph.D. degree at Technical University of Denmark.

The work has been carried out at Department of Chemical Engineering from November 2001 to January 2006 under the supervision of Professor Sten Bay Jørgensen and Professor Rafiqul Gani.

First, I would like to express my gratitude to Professor Sten Bay Jørgensen and Professor Rafiqul Gani for giving me the opportunity to work on such an interesting project, and for their inspiration and cooperation on the research presented in this thesis. Their involvement, encouragement and enthusiasm for scientific research have always been an invaluable source of inspiration for me, and I've won many thanks to them for all the fruitful discussions throughout the project, especially for their careful proofreading of this manuscript. I am also very grateful for OPERA for funding this project.

I would also like to thank all the students and co-works at the Computer Aided Process Engineering Center (CAPEC) at the Department of Chemical Engineering at Technical University of Denmark for helping me during my time in CAPEC.

Finally I would like to thank my family and friends for their support and understanding throughout the project. There have been times when moral support was needed and I have had little time for other things than work. This is gratefully acknowledged.

Hong Wen Li

Lyngby - Denmark, January 2006

Abstract

The motivation of this thesis is to ensure optimal operation while respecting nonlinear consequences of process integration and optimality. The thesis develops a model based methodology for investigation the dynamic behaviour, optimal operation, and control structure design for the energy integrated chemical processes.

The work has contributed to ensuring optimal operation of integrated process plants through development of a procedure for control structure synthesis for optimal plant operation. The theoretical and methodological work has focused on development of a systematic methodology for determining a control structure which can be used as a basic structure upon which model based control may be implemented to manipulate the basic control loop setpoints to achieve optimal operation. This procedure also has the ultimate aim to facilitate integration of process design and control structure design. The procedure encompasses the following main steps:

1. Theoretical analysis of how the operational degrees of freedom may be used through control to cover the desired operating window such that it is revealed which underlying process connectivity can give rise to static and dynamic complications.
2. Determining an optimal plant operation mode and its relation to the accessible degrees of freedom provided by the basic control structures.
3. Control structuring at the basic levels to account for and possibly exploit the underlying connectivity by replacing constrained degrees of operational freedom with more easily accessible degrees of freedom. Thus control is used to move the degrees of freedom in a most suitable manner for plant efficiency and operability.
4. Demonstration of model based control to exploit the accessible degrees of freedom through validation both by simulation and experiment.

For optimal column operation it is demonstrated that it is important to consider the pressure sensitivity of the mixture to be separated. It is shown that the pressure should be maintained at the proper end of the column depending upon the pressure sensitivity of the mixture. Significantly higher separation efficiency and also higher capacity may be obtained through controlling the pressure at the suitable location.

Dansk resumé

Motivationen bag denne afhandling er at gennemføre modeludvikling med henblik på at kunne sikre optimal operation mens de ulineære konsekvenser af proces operation respekteres. I afhandlingen udvikles en model baseret metode til at undersøge konsekvenserne af proces integration for processernes dynamik og dermed for en ønskelig regulator struktur med henblik på at kunne sikre optimal drift.

Det teoretiske og metodiske arbejdet i afhandlingen er centreret omkring udvikling af en procedure til at strukturere basale regulatorer i et proces anlæg således at de basale regulator sløjfers reference signaler kan manipuleres med henblik på at sikre optimal operation af et anlæg. Proceduren sigter mod integration af proces design og af regulator struktur design. Procedure omfatter følgende hoved trin:
1. Teoretisk analyse af hvorledes de operationelle frihedsgrader kan anvendes til at dække det ønskelige operations vindue således at det afsløres hvilke underliggende proces koblinger der kan give anledning statiske eller dynamiske komplikationer.
2. Bestemmelse af optimal operation og dennes relation til de frihedsgrader der stilles til rådighed af den basale reguleringsstruktur.
3. Modifikation af den basale regulator struktur med henblik på at udnytte underliggende proces koblinger til at opnå enklere kombinationer af eventuelt begrænsende frihedsgrader. Hermed anvendes regulering til at flytte frihedsgrader med henblik på at opnå høj effektivitet og operabilitet for et anlæg.
4. Anvendelse af model baseret regulering til at udnytte et anlægs frihedsgrader valideres ved simulering og i afhandlingen også eksperimentelt.

Et specifikt resultat af arbejdet, der er generelt for destillation er at det vises at følsomheden overfor kolonne trykket kan have væsentlig indflydelse på operationen af en kolonne. Det er således væsentligt hvor i en kolonne man fastholder trykket under operation af kolonnen. Man kan opnå væsentlig højere effektivitet af en destillationskolonne ved at regulere trykket på et hensigtsmæssigt punkt i kolonnen.

Contents

1
Introduction

1.1 Motivation

Process integration is increasingly used to ensure a higher utilization of energy and raw materials, thereby obtaining a more sustainable production and lower impact on the environment. However process integrated plants often become more difficult to operate than plants without integration. Therefore the goal of this project is to develop a method which can ensure smooth operation of process integrated plants even when they are operating near plant operating regions where operation may become difficult due to existence of complex behaviors such as multiple steady or periodic dynamic states. The theoretical work of this project has mainly focused upon development of basic understanding of operational consequences of process integration and on subsequent development of control structures to circumvent complex behaviors. The purpose of the control structures is to enable exploitation of the operational degrees of freedom of the plant to ensure optimal operation while respecting nonlinear consequences of process integration and optimality.

1.2 Background

Distillation is by far the most widely used industrial separation technique, but it is also a very energy consuming process. Mass and energy integration of chemical plants has been proven to possess high potential for reducing energy consumption and environmental impact. However, the increase in complexity caused by mass and the energy couplings thus introduced may change plant characteristics drastically, such that multiple states, limit cycles and other more complicated behaviors including chaos and thereby great impact on suitable operability and on control configuration selection for the plant.

The literature on distillation control research is vast and comprehensive (see e.g. Skogestad (1992) for an extensive reference list) counting thousands of articles and monographs. The study of the distillation control area can be concluded into three aspects, modeling for design and control, dynamic analysis of the process, model

based control that includes linear and nonlinear control to satisfy optimal operation and control requirements. The modeling of the process is obviously important for design and control. A simplified model that can incorporate the most important dynamic behavior of the process is very useful tool for dynamic analysis because the computation demands are usually quite small when compared to a complex model. Recently, as computer technology has developed drastically, model-based multivariable control strategies have been studied and in many cases such control systems have been reported successfully implemented on standard distillation columns in the chemical process industry. But it is needed to point out that the influence of pressure control on conventional distillation column operation is not well understood. Therefore this aspect requires a close investigation more both theoretically and experimentally.

For the nonlinear control aspect of the chemical process, there has been a significant increase in the number of control system techniques that are based on nonlinear systems concepts during the past five years. A number of papers have provided insight into operational and control problems created by nonlinearities in chemical process. Recent research efforts have concentrated on providing control system design techniques to handle the nonlinear chemical process. Adaptive control (Segorg et al., 1986) was promoted as a technique to solve the nonlinear problem by "relinearizing" the process model as the process moved into different "linear" operating regions, as well as to estimate time-varying parameters (generally linear system based). Robust control system design techniques (Doyle and Stein, 1981; Doyle, 1982) were developed to account for model uncertainty. Internal model control (IMC) (Garcia and Morari, 1982) was developed to provide a transparent framework for process control system design and to explicitly handle manipulated variable constraints. Morari (1987) reviewed the three critiques (Foss, 1973; Lee and Weekman, 1976; Kerstenbaum et al., 1976) and concluded that the most promising and widely open areas are control of nonlinear systems and adaptive control. Foss (1973) and Morari (1987) pointed out the need for studying basic control structures. Such a study becomes especially relevant when bifurcations appear close to or within the desired operating region since near bifurcation pointes undesirable behaviors may appear. Even though some studies hereof have appeared then consideration of the effect of bifurcations seem not to be addressed in recently advocated methods for control structuring (Luyben et at, 2000 and Skogestad, 2004). To address the issues related to the occurrence of simple fold bifurcations are investigated in the thesis.

The reason to investigate nonlinear phenomena in chemical process is that most processes are highly nonlinear, thus potentially making use of linear models a rather poor approximation for design of model-based control. This may especially be valid for optimizing control.

From the brief review above it appears that two aspects in optimizing control are neglected: one is how to structure the control loops to operate an integrated plant within the desired operating window especially when operation is in the bifurcation region? Another aspect of optimizing distillation column control is how to control column pressure in an optimal way? Hence the goal of this thesis is to build up a methodology to systematically study the behavior of the indirect vapor recompression distillation pilot plant (IVaRDiP)chemical process to reveal possible nonlinear dynamic behavior, consequences of optimal operation and their resulting control implications.

1.3 Contents of the thesis

The thesis starts with the model formulation that is to build up a process model for model analysis; bifurcation analysis and process control. Then it follows model analysis, which is to determine degrees of freedom, to select actuators and measurements. The next step is to find the optimal operation region. After that the bifurcation analysis is performed to investigate the potential dynamic behavior. Having found the bifurcation behavior, a basic control loop is proposed to stabilize the unstable branch. Finally it is to validate the control structure experimentally. The results are summarized into the following chapters:

Chapter 2 A model based methodology is developed to investigate related process design, process dynamics, process control and issues of integrated process.

Chapter 3 A key question for any model based control is to understand the available degrees of freedom or which should be included at the design stage for maneuvering the plant within the operating window. The degrees of operational freedom of the indirect vapour recompression distillation pilot plant (IVaRDiP) are determined. In the case of a single distillation column these are three at steady state, as directly revealed from an analysis of the simplified model. In the case of the IVaRDiP the number of degrees of freedom is unchanged, but some of the handles are moved to the heat pump. Thus instead of directly using the heating and cooling rate for the reboiler and condenser as in conventional distillation, the high and low pressures of the heat pump are conveniently used as actuators for the IVaRDiP. The available model knowledge for structuring the lower level controls may be revealed through a detailed simulation of the different parts of the model to understand the interconnectivity and their gains. Thereby it was demonstrated to be possible to reveal relationships between key actuators in IVaRDiP and key column operating variables. Part of the result of the analysis is also to envision how to combine key actuators into a more suitable actuator structure than previously applied. It is demonstrated through

simulation that a suitable combination is to use the sum of low and high pressures in the heat pump as actuators to control the distillation column pressure while the difference between high and low pressures in the heat pump is used as actuator to control the vapor flow rate in the column. Thereby nearly independent actuation on each of the specified control goals (set-points) is obtained and a possible set of actuator combinations at the middle control level for IVaRDiP have been defined.

Chapter 4 To demonstrate the applicability of model based control it is decided as a primary goal to experimentally attempt to verify the control structure obtained in previous chapter in binary distillation, since such an experiment involves moving the plant over a significant part of the operating window through varying the vapor flow rate. In this experiment it is decided to use model based control at the middle control level of the control hierarchy to implement the control of vapor boil-up and column pressure using a suitable combination of high and low heat pump pressures. The analysis has pointed out that the sum of these pressures controls the column pressure while the pressure difference should be used to control the vapor boil-up. The selected methodology uses an ARMAX model of the plant. To accommodate to approximations of model over the wide operation range a multivariable controller with three pressure measurements in the heat pump and two in the column plus and the vapor flow rate are used as measurements. The actuators for the multivariable controller are the high and low pressures in the heat pump, while the setpoints for the multivariable controller are vapor boilup rate and column pressure.

Chapter 5 The profit landscapes are obtained. It is demonstrated that for a measure of optimal productivity the IVaRDiP indeed exhibits a fold bifurcation relatively close to optimal productivity.

Chapter 6 Bifurcation analysis is carried out and fold bifurcations are found in the IVaRDiP. It is shown that how the lower level controls should be structured to possibly avoid the influence of complex nonlinear behaviors. Clearly it is advisable to use a suitable control structuring, i.e. one where a specific basic loop controller can maintain stable operation even if an unstable branch is entered.

Chapter 7 Experiments are carried out to validate the optimizing pressure control structure. At the optimization level three degrees of freedom are available; those are the purities of the end products and the optimizing column pressure. That the influence of the pressure sensitivity upon distillation is analyzed in general using model knowledge and it is shown that the desired location of the measurement for pressure control depends upon the type of pressure sensitivity for the mixture to be separated. If the relative volatility of the mixture to be separated increases with decreasing pressure then the pressure measurement should be located at the bottom of the separation section of the distillation column. If the relative volatility of the mixture to be separated decreases with decreasing pressure then the pressure

measurement should be located at the top of the separation section of the distillation column. Thus for the mixture to be separated in the distillation pilot plant where the key mixture components are methanol and isopropanol for which the relative volatility increases with decreasing pressure the pressure sensor should be located at the column bottom.

Chapter 8 The conclusions of the thesis and future work are given. The developed methodology is validated experimentally on IVaRDiP at the Department of Chemical Engineering at DTU through the usage of model based control.

1.4 Publication and conference presentations

Publications:

1) Li, H. W. Gani, R. and Jorgensen, S. B. (2003), "Process-Insights-Based control Structuring of an Integrated Distillation Pilot Plant", Ind. Eng. Chem. Res, Vol. 42, p4620-4627

2) Li, H. W. Gani, R. and Jorgensen, S. B. (2006), "Operating Pressure Sensitivity of Distillation Control Structure Consequences", Submitted for Ind. Eng. Chem. Res.

3) Li, H. W. Gani, R. and Jorgensen, S. B. (2003), "Integration of Design and Control for Energy Integrated Distillation", ESCAPE-13 proceeding, Computer-aided Chemical Engineering, p449-454, Finland

4) Li, H. W. Gani, R. and Jorgensen, S. B. (2004),"Analysis of Optimal Operation of Energy Integrated Distillation Plan", Process Systems Engineering 2003, Computer-aided Chemical Engineering, p940-945, China

5) Li, H. W. Gani, R. and Jorgensen, S. B. (2004), "Actuator Selection Based upon Model Insighs for an Energy Integrated Distillation Column", 7th ADCHEM Symposium proceeding, p135-141, Hong Kong, China

6) Li, H. W. Gani, R. and Jorgensen, S. B. (2004), "Nonlinear Behavior Analysis of Heat Integrated Distillation", ESCAPE-14 proceeding, Computer-aided Chemical Engineering, p691-696, Lisbon, Portugal

Conference Presentations:

1) Li, H. W. Gani, R. and Jorgensen, S. B. (2002), "Integration design and control for heat integrated distillation column", Distillation/Absorption Conference, Baden-Baden, Germany, 1-3 October 2002

2) Li, H. W. Gani, R. and Jorgensen, S. B. (2003), "Integration of Design and Control for Energy Integrated Distillation", ESCAPE-13, Finland, 1-4 June, 2003

3) Li, H. W. Gani, R. Hasen, C. A., and Jorgensen, S. B. (2004), "Analysis of Optimal Operation of Energy Integrated Distillation Plan", Process Systems Engineering 2003, China, 5-10 January, 2004

4) Li, H. W. Gani, R. and Jorgensen, S. B. (2004), "Actuator Selection Based upon Model Insighs for an Energy Integrated Distillation Column", 7th ADCHEM Symposium 2004, Hong Kong, China, 11-14 January, 2004

5) Li, H. W. Gani, R. and Jorgensen, S. B. (2004), "Nonlinear Behavior Analysis of Heat Integrated Distillation", ESCAPE-14, Lisbon, Portugal, 16-19 May, 2004

6) Li, H. W. Gani, R. Hasen, C. A., and Jorgensen, S. B. (2004),"Actuator structure and optimal operating region of an energy integrated distillation", NPCW11, Trondheim, Norway, 9-11 January, 2003

7) Li, H. W. Gani, R. and Jorgensen, S. B. (2004), "Optimal control of a heat integrated distillation pilot plant", NPCW 12, Gøtenborg, Sweden, 19-21 August, 2004

8) Li, H. W. Gani, R. and Jorgensen, S. B. (2003), "Integration of Process Control for Energy Integrated Distillation", 2003 Spring AIChE Meeting, USA, 30 March – 3 April, 2003

9) Li, H. W. Gani, R. and Jorgensen, S. B. (2004), "Optimizing Control of Heat Integrated Distillation Pilot Plant", AIChE Meeting, Austin, USA, 7-12 November, 2004

10) Li, H. W. Anderson, T., and Jorgensen, S. B. (2005), AICHE Spring Meeting, Atlanta, USA, April, 2005

References:

Skogestad, S. (1992), Dynamics and Control of Distillation Column – A Critical Survey; IFAC Symposium DYCORD+92, Maryland, April 27-29

Segorg, D. E.; Edgar, T. F., Shah, S. L. (1986), Adaptive control Strategies for Process Control: A Survey. *AIChE J.*, 32 881-913

Doyle, J.; Stein, G. (1981), Multivariable Feedback Design: Concepts for a Classical/Modern Synthesis. IEEE Trans. Auto. Control, AC-26, 4-16

Doyle, J. (1982), Analysis of Feedback System with Structured Uncertainties. IEE Proc., 129, 242-250

Garcia, C. E.; Morari, N. (1986), Internal Model Control. 1. A Unifying Review and Some New Results. Ind. Eng. Commun., 46, 73-81

Holt, B. R.; Morari, M. (1985), Design of Resilient Processing Plants. V. The Effect of Deadtime on Dynamic Resilience. Chem. Eng. Sci., 40, 1229-1237

Morari, M. (1987), Three Critiques of Process Control Revisited a Decade later. *In* Shell Process Control Workshop, 306-321

Foss, A. S. (1973), Critique of Chemical Process Control Theory. AIChE J., 19, 209-214

Lee, W.; Weekman, V. W. (1976), Advanced Control Practice in the Chemical Process Industry: A View from Industry. AIChE J., 22, 27-38

Kestenbaum, A.; Shinna, R.; Thau, F. E. (1976), Design Concepts for Process Control. Ind. Eng. Chem. Process Des. Dev., 15, 1-13

Clausen, K. (2002), Nonlinear Dynamics of Distillation Plants, Master thesis, Technical University of Denmark

Koggersbøl, A. (1995), Distillation Column Dynamics Operability and Control, Ph.d thesis, Technical University of Denmark

2

Methodology

Abstract: *Energy saving has through the years grown to become an issue of great importance for chemical industry as for the rest of society. For chemical production and refinement plants energy integration represents a significant potential for energy savings. However, the increase in complexity caused by tighter energy couplings may change plant characteristics drastically and thereby impact on operability and on selection of the most suitable control configuration for a process plant. Thus the introduction of complex nonlinear dynamics constitutes an undesirable effect of process integration. The goal of herein proposed methodology is to develop a methodology that can ensure smooth operation of process integrated plants even when they are operating near regions where operation may become difficult due to the existence of complex behaviours such as multiple steady or periodic dynamic states.*

2.1 Introduction

Control structure selection may be important to ensure exploitation of the full potential of energy and mass integration without significantly jeopardizing operability and dynamic performance. A general model based analysis methodology has been developed. The purpose of this methodology is to develop a sequence of problem formulations to reveal operational complexities and to develop an efficient method that can enable smooth operation despite the existence of complex behaviours.

2.2 The outline of the methodology

A methodology is built up for optimal design and control synthesis for indirect vapor recompression distillation pilot plant (IVaRDiP)chemical process as shown below in Figure 2.1.

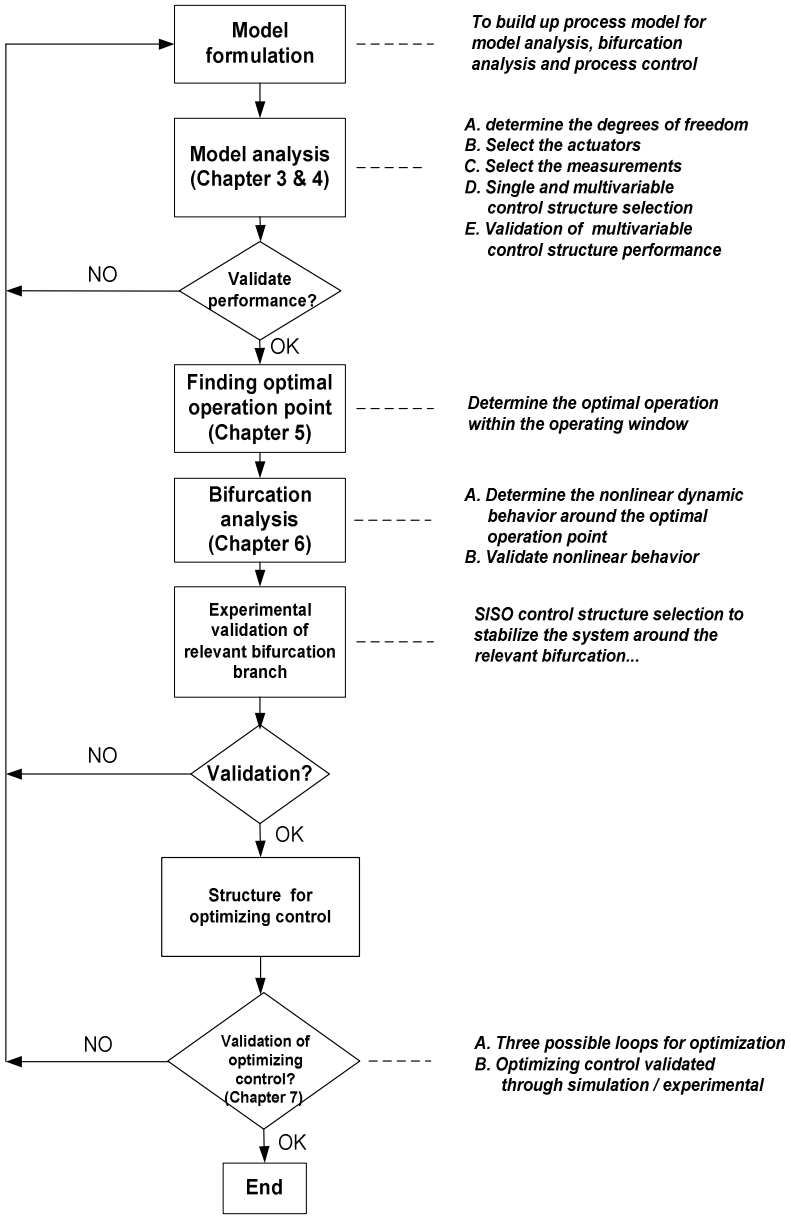

Figure 2.1: Outline of the methodology for development of (optimizing) control structure for IVaRDiP

The details of the methodology will be explained in the following.

2.3 Methodological details

2.3.1 Model formulation

The methodology starts from process model formulation. The models are composed of balance equations, constitutive equations and conditional equations shown in Figure 2.2. The balance equations include mass balance, energy and momentum balances. The constitutive equations are composed of phenomena models that are usually as a function of intensive variables.

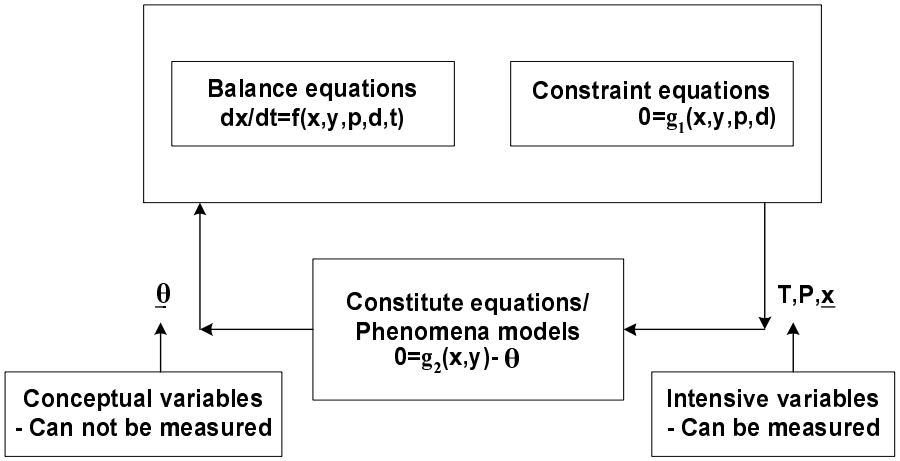

Figure 2.2 Chemical process models

2.3.2 Model analysis

The model analysis identifies the important constitutive equations, their dependent process variables and the corresponding derivative information. This knowledge is used to identify the existence of non-linear terms in the balance equations and to decouple the balance equations and the constitutive relations.

The model analysis first determines the available degrees of freedom for design and for control. The analysis of the decoupled balance equations and the constitutive equations generate information related to process sensitivity, process feasibility, design constraints and provide solutions for design and control sub-problems. If the results from the model analysis are validated, eg. through simulation using a more detailed model then the procedure moves to the next step; otherwise it goes to back to modify the model formulation.

2.3.3 Determine optimal operation

The basis for analysis of optimal operation is the type of operation upon which an application focuses. In this part the attention is on achieving close to optimal economical benefit of a continuous or batch wise operating plant. The optimal operation region for the plant is visualized through the profit landscape of the process.

2.3.4 Bifurcation analysis

One method to reveal possible nonlinear phenomena is to perform a bifurcation analysis within an operating region around optimal operation using a dynamic process model. A bifurcation diagram displays the changes in the nonlinear characteristic of a physical system and is therefore very important method in investigating integrated process systems.

In order to analyze for occurrence of such behaviours a continuation method can be used to trace nonlinear behaviours throughout the operating window. Such a continuation method has been implemented to enable such continuation calculations. With a simplified model of the energy integrated distillation plant a bifurcation diagram has been determined. The next step is to validate experimentally the results from the bifurcation analysis. If the results from the model analysis are validated, then the procedure proceeds to the next step; otherwise it goes back to one of the previous steps depending upon the cause behind the invalidation. In figure 2.1 the backtracking for simplicity is illustrated to the model formulation.

2.3.5 Optimizing control structure

The control structure in a chemical plant is structured hierarchically into several layers see Figure 2.3, each operating on a different time scale. Typically, layers include scheduling (weeks), site-wide (real-time) optimization (day), local optimization (hours), supervisory control (minutes) and stabilizing and regulatory control (seconds); The layers are interconnected through measurement and setpoints for the controlled variables.

At the optimization layer there are two key approaches developed of an optimizing control structure. One it is self-optimizing control structure, which with constant set points yields near optimal performance during typical operational disturbances. Another it is real-time optimizing control that enables optimization performed regularly; e.g. every four hours. Here the stationary optimal operations model is updated every four hours for a static process model. The on-line control task is then to track the optimal operations model. If the optimal operations model is updated, more often, e.g. most frequently which could be every sampling instant (say every 10 minutes), but then using a dynamic non-

linear model for optimization. In this case the optimizing control can be classified as on-line optimizing control, however the control design task for this case leads to a computationally intractable problem, therefore the application of real-time optimizing control have become wide spread.

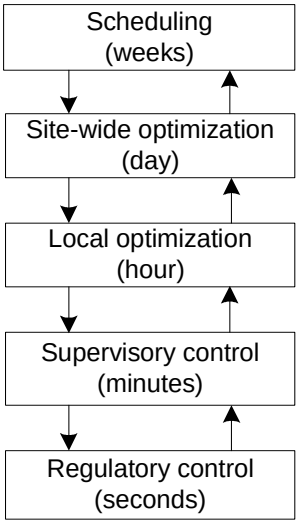

Figure 2.3 Typical control hierarchy in a chemical pilot plant

The approach taken in the process optimization part of this thesis is to investigate one special aspect of optimizing distillation column control, which has been neglected in most papers on distillation control. Therefore the influence of the operating pressure sensitivity upon distillation will be analyzed using model knowledge. The location of the measurement for pressure control depends upon the type of pressure sensitivity of the mixture to be separated. The influence of where to control column pressure will also be investigated experimentally.

3

Model Analysis for Control Structure Selection

Abstract *The proposed simple model analysis provides a connection between process design and control design, which identifies the optimization variables in process design as possible actuator variables for control design. The model analysis thereby provides the important selection of actuator variables which also define the plant operating window. Thereafter pairing of actuator variables with measurements can be analyzed. On this basis control structuring questions can be addressed. The results of the simple model analysis are based upon simple knowledge of process interconnections. The resulting control structures are validated using rigorous simulation using the full model. In this chapter, this analysis is applied to an energy integrated distillation pilot plant to identify the set of common variables that have important roles in design as well as in control structure definition. This identified set of variables is used to develop an actuator structure for the pilot plant for the purpose of optimizing control by exploiting interactions between plant design and control design. The process model is first presented, followed by a model analysis, which directly leads to the coupling between process design, process sensitivity and actuator structure. Furthermore, the analysis reveals how the heat pump should operate the pilot plant, using a set of actuators on the heat pump side to achieve mainly independent control of boil-up flow rate and column pressure.*

3.1 Introduction

Chemical process plant design and operation based on combining mathematical models with computer science have the potential to significantly increase the efficiency of manufacturing systems by integrating the design with the planning of operation. At the level of chemical plant units, integrating systems means coupling several physical processes either within the same piece of equipment or between units, which perform different physical/chemical tasks. Full economic potential of such novel integrated processes can only be exploited if they can be operated efficiently.

To achieve a suitably operable plant it is essential to investigate operability of integrated processes at the design stage in order to enable suitable design modifications as early as possible. A systematic computer aided pre-solution analysis of the process model for integration of design and control presented by Russel et al.(2002) is extended in this chapter for the purpose of definition of suitable actuator structures on an energy integrated distillation pilot plant. The process model equations are classified in terms of balance equations, constitutive and conditional equations. Analyses of the phenomena models, which represent the constitutive equations, identify relationships between important process and design variables. These relationships help to understand, define and address issues related to integration of design and control decisions. The analysis enables identification of a set of process (control) variables and a set of design (actuator) variables that may be employed with different objectives in a process design context versus in a control actuator design context. Consequently these sets play an important role in formulating an integrated design and control problem. Russel et al.(2002) and Tyreus (1993) have proposed interesting model analysis approaches for identification of dominant variables for control purpose. More generally, the issue of selecting controlled variables is the first subtask in the control structure design problem (Foss (1973), Skogestad et al (2000)). In partially related works, Agrawal et al (1999) have proposed new thermally coupled schemes from a steady state analysis only, while Hernández et al (1999) have analyzed the controllability of thermally coupled distillation plants.

This chapter investigates design and control of an energy integrated distillation pilot plant through an analysis of parts (mainly different sub-sets of constitutive equations) of the model equations and validates the analysis results through rigorous simulations. The energy integrated pilot plant consists of a distillation column section and a heat-pump section. The model of distillation column section is first presented, followed by an analysis for this section, which is then followed by an extended analysis for the heat pump section. The analysis directly leads to identification of a

feasible actuator structure for the distillation pilot plant, wherein design optimization may be carried out, and wherein the heat pump section should operate the pilot plant, using a set of actuators designed as a part of the heat pump. The insights obtained through the analysis lead to a modification of the actuator set for the integrated distillation pilot plant.

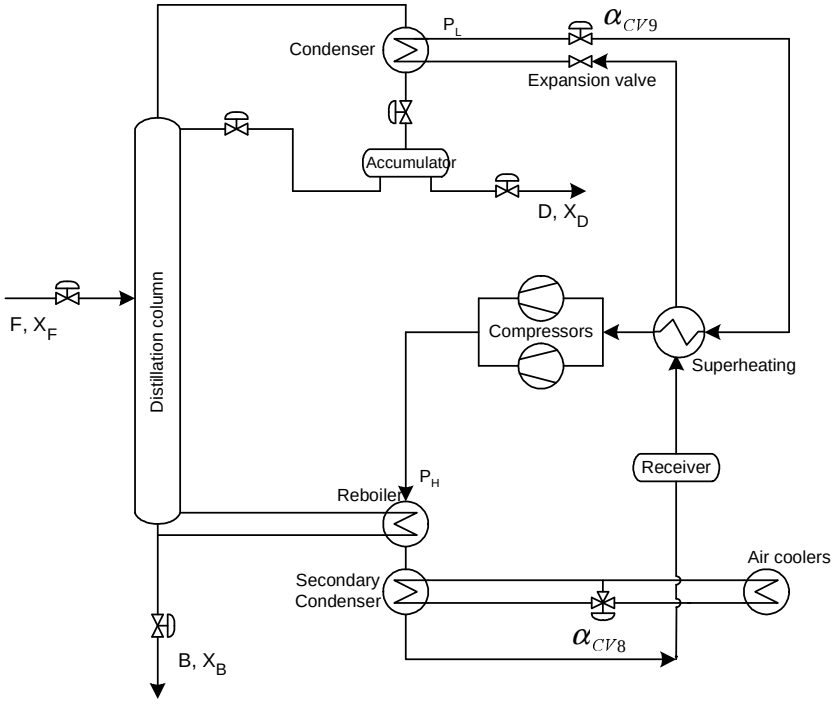

Figure 3.1. Flow sheet for the indirect vapor recompression distillation pilot plant (IVaRDiP)

3.2 Short description of the IVaRDiP

The starting point for the model analysis is to use an appropriate process model. The IVaRDiP, shown in Figure 3.1 (1998), contains two main parts, namely a distillation column section and a heat pump section. The heat pump section is physically connected to the distillation column through the condenser at the top and the reboiler at the bottom of the column. The column consists of 19-sieve trays with a total height of 10.5m and an internal diameter of 0.47m. It is designed to separate a mixture of methanol and isopropanol containing a small amount of water. The refrigerant flow circulating within the heat pump is freon-R114. Figure 3.2 shows the operating window of the IVaRDiP with one of its operating points. A more detailed description

is available in Eden et al (2000). The process model equations of the two sections are presented individually below.

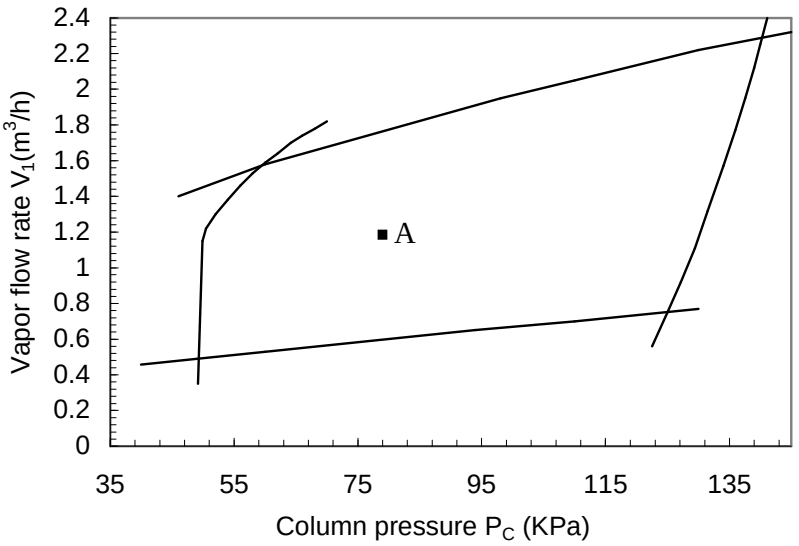

Figure 3. 2: Operating window of the IVaRDiP (Point A is the nominal operation point). The vapor flow rate unit is for condensed vapor. Ref. to Koggersbøl (1995)

3.3. Model description

3.3.1 Process model equations for distillation column section

The process model equations for the distillation column section are given below:
Component balance equations (each ideal stage j, j=1,NP; where NP is the total number of ideal stages):

$$\frac{d(M_j x_{i,j})}{dt} = F_j Z_{i,j} + L_{j-1} x_{i,j-1} + V_{j+1} y_{i,j+1} - L_j x_{i,j} - V_j y_{i,j} \qquad i=1,NC;\ j=1,NP \qquad (3.1)$$

Where, accumulator for total condensation in the condenser:

$$\frac{dM_D}{dt} = V_1 - (L_0 + D) \qquad (3.2)$$

When there are two liquid phases, the compositions of L_0 and D would be different. The equations are shown only for the case of a single liquid phase in the accumulator.

Where, for total reboiler,

$$\frac{dM_B}{dt} = L_{NP} - (V_B + B) \tag{3.3}$$

Energy balance:

$$0 = F_j H_j^F + V_{j+1} H_{j+1}^V + L_{j-1} H_{j-1}^L - V_j H_j^V - L_j H_j^L \qquad \text{j=1,NP} \tag{3.4}$$

$$0 = V_1 H_1^V - (L_0 + D) H_D^L - Q_C \qquad \text{(total condenser)} \tag{3.5}$$

$$0 = (L_{NP} - B) H_{NP}^L - V H_B^V + Q_B \qquad \text{(total reboiler)} \tag{3.6}$$

Constitutive equations:

$$H_j^L = f_1(T, x_{i,j}) \qquad \text{i=1,NC; } j\text{=1,NP} \tag{3.7}$$

$$H_D^L = f_2(T, y_1) \tag{3.8}$$

$$H_j^V = f_3(T, y_{i,j}) \qquad \text{i=1,NC; } j\text{=1,NP} \tag{3.9}$$

$$H_B^V = f_4(T, x_{NP}) \tag{3.10}$$

$$y_{i,j} = K_{i,j} x_{i,j} \qquad \text{i=1,NC; j=1,NP} \tag{3.11}$$

$$K_{i,j} = f_5(T, P, x_{i,j}, y_{i,j}) \qquad \text{i=1,NC; j=1,NP} \tag{3.12}$$

$$M_j = f_6(L_j, V_j, P_j, T_j) \qquad \text{j=1,NP} \tag{3.13}$$

Conditional equations (j=1,NP)

$$0 = \sum_{i=1}^{NC} x_{i,j} - 1 \qquad \text{i=1,NC; j=1,NP} \tag{3.14}$$

$$0 = \sum_{i=1}^{NC} y_{i,j} - 1 \qquad \text{i=1,NC; j=1,NP} \tag{3.15}$$

$$P_j - P_{j-1} = \Delta P \qquad \text{j=1,NP} \tag{3.16}$$

In the above model, Eq.(3.1)-Eq.(3.3) represent the mass balance for NC components in the distillation column. These equations are shown for ideal stages. However, by introducing tray efficiencies into the model (Eq.3.11), profiles for real stages can be generated. Eq.(3.4)-Eq.(3.6) represent the energy balance on each stage. Q_c and Q_B are the heat removed in the condenser and heat added in the reboiler, respectively. The energy balances for the column, condenser and reboiler, assume quasistationary due to the very high rate of energy transport compared to the rate of mass transport in the

column. This assumption is reasonable for continuous operation; however, for startup energy balances for condenser and reboiler should be dynamic. Eq.(3.7)-Eq.(3.13) represent the phenomena models for enthalpy, gas-liquid equilibrium condition and the so-called equilibrium constant. Eq.(3.14) and Eq.(3.15) represent the conditional equations related to mole fractions. Eq.(3.16) represents the pressure drop on each stage. Subscripts i and j represent component and stage, respectively.

3.3.2 Process model for the heat pump section

The heat pump shown in Figure 3.3 (Eden et al, 2000) consists of four heat exchangers, two compressors, one expansion valve, a refrigerant reservoir called receiver, two control valves with valve opens α_{CV8} and α_{CV9}, respectively. While the refrigerant circulates within the heat pump it changes phase, and through absorbing heat of vaporization at low pressure and releasing it again at high pressure it carries heat from the column condenser to the column reboiler. A model of the heat pump is presented for the purpose of model analysis.

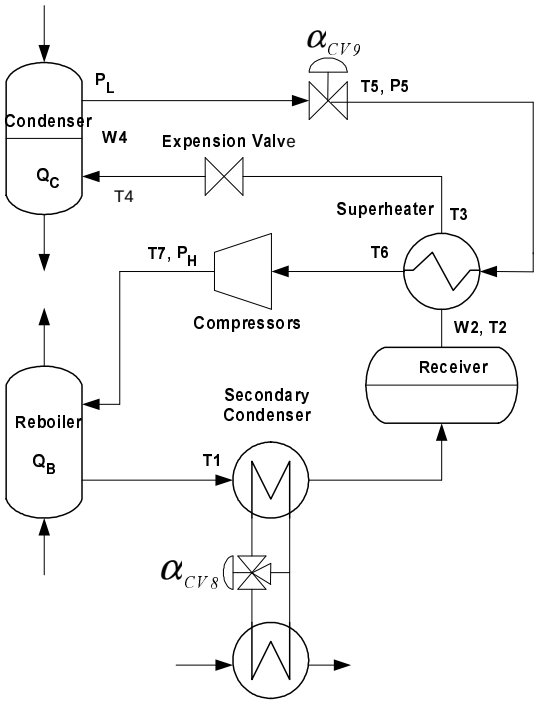

Figure 3.3: Flow sheet of the heat pump

For the heat pump section (Figure 3.3), the variables related to this problem are the following twenty-one variables; W_4, $P_4=P_L$, T_4, P_5, T_5, P_6, T_6, P_3, T_3, $P_1=P_H$, T_1, W_2, T_2, L_W, T_W, T_W^{in}, Q_B, Q_C, L_{EXP}, L_{COMP}, W_W. The model equations are:

Expansion valve:

$$L_{EXP} = f_7(P_3, P_4) \tag{3.17}$$

$$T_2 = f_8(T_3) \tag{3.18}$$

Condenser:

$$\frac{dW_4}{dt} = L_{EXP} - L_{COMP} \tag{3.19}$$

$$Q_C = f_9(W_4, T_4, L_{EXP}, L_{COMP}) \tag{3.20}$$

$$P_4 = f_{10}(T_4) \tag{3.21}$$

Control valve α_{CV9}:

$$T_4 = T_5 \tag{3.22}$$

$$L_{COMP} = f_{11}(P_4, P_5) \tag{3.23}$$

Compressor:

$$P_1 = f_{12}(P_6, T_6) \tag{3.24}$$

$$T_1 = f_{13}(P_1) \tag{3.25}$$

Reboiler:

$$Q_B = f_{14}(T_1, L_{COMP}, P_1) \tag{3.26}$$

$$P_1 = f_{15}(T_1) \tag{3.27}$$

Secondary condenser:

$$\frac{dW_w}{dt} = f_{16}(L_W, T_W^{in}, T_1, T_W) \tag{3.28}$$

$$T_W = f_{17}(T_1, L_{COMP}, P_1) \tag{3.29}$$

Receiver:

$$\frac{dW_2}{dt} = f_{18}(T_1, T_2, L_{COMP}, L_{EXP}) \tag{3.30}$$

Cross-flow heat exchanger before compressor:

$$T_3 = f_{19}(T_2, T_6, T_5, P_5) \tag{3.31}$$

3.4. Model analysis

The model analysis first determines the available degrees of freedom for design and for control. The analysis subsequently identifies the important constitutive equations, their dependent process variables and the corresponding derivative information. The analysis of the balance equations and the constitutive equations generate information related to process sensitivity, process feasibility, design constraints and provide solutions for design and control sub-problems. Note that the analysis only uses parts of the model equations and is therefore, very easy to perform and does not need solution of all the model equations. First the analysis is carried out for the distillation column; thereafter the heat pump is introduced into the analysis.

3.4.1 Process model analysis for the distillation column

In the above distillation column model, there are 4NC*NP+9NP+13 variables ($x_{i,j}$, $y_{i,j}$, $z_{i,j}$, $K_{i,j}$, F_j, H^F_j, L_j, V_j, H^V_j, H^L_j, T_j, P_j, M_j, M_D, M_B, L_0, V_B, P_0, ΔP, H^L_D, H^V_B, Q_C, Q_B, D, B, NP), 3NC*NP+7NP+6 independent equations(Eq.(3.1)-Eq.(3.16)). So the degrees of freedom are NP*NC+2NP+7. For one feed, the number of variables are 3NP*NC+NC+7NP+15+NF, where there are 3NC*NP+7NP+6 independent equations. The difference between all the variables and the independent equations are NC+NF+9. The variables related to the feed, the number of stages and the pressure drop ($z_{i,j}$, F, HF, NP, ΔP, NF) are NC+NF+4 variables, which are considered known variables during design. So there are five variables that remain to be specified in order to solve the 3NC*NP+7NP+6 independent equations. This means that in this distillation column section, five process variables (control variables) are related to five actuator variables (design variables). Out of the five control variables, two of them, i.e., the hold-ups in the reboiler and the accumulator, are first selected to be specified as controlled variables to stabilize the reboiler and accumulator level.

The variables (P, T, $x_{i,j}$) are the intensive process variables from which three of them may be chosen as control variables. The following variables Q_B, Q_C, D, L_0 and B are design (specified) variables and could be considered as actuator variables. Variables $K_{i,j}$ and $H_{i,j}$, which are constitutive variables (see Eq.(3.12)) are functions of pressure P, which then in turn determine the vapor composition $y_{i,j}$ (the pressure dependence of H^L_j in many cases may be neglected). This indicates that the pressure

in the distillation column directly affects the mass balance and indirectly affects the energy balance (Eq.(3.7)-Eq.(3.10)) for all types of equilibrium model. The nonlinear terms in the balance equations are related to the constitutive variables $K_{i,j}$, which generally depends on the intensive variables *T, P,* $x_{i,j}$ and $y_{i,j}$. With these nonlinear couplings at every stage and only three available control handles it is not possible to attempt to compensate for the nonlinear behaviors in general using control. The operational goals are assumed to be related to the top and bottom purities and to ensure a desired pressure level in the column. Thus the end compositions (X_B, X_D) can be controlled using two handles. And finally, for the remaining control variable to select, pressure is chosen at one location in the column, which will then also fix the temperature profile for a binary system. The above selection of controlled variables depends on the actual control problem to be solved. The above selection is made here to illustrate the model analysis procedure in the sequel.

The next step is to discuss integrated design and control with the control variables P, X_D and X_B. As stated above the optimization design variables are assigned as Q_B, Q_C, D, L_0 and B. Assuming the hold-ups in the reboiler and the accumulator are controlled separately by manipulating design variables B and L_0, the remaining design variables, Q_B, Q_C and D are the variables that need to be adjusted in order to match the design and can also serve as variables to manipulate the column conditions to reach desired values for the above selected set of measured variables P, X_D and X_B. In the design problem, values of Q_B, Q_C and D are usually calculated for specified values for three of the process variables (P, X_D and X_B). In the control problem, the process variables (P, X_D and X_B) are controlled through manipulation of three actuator variables (Q_B, Q_C and D). Thus, the same set of variables (P, X_D, X_B and/or Q_B, Q_C, D) may be used in different roles for design and control design purposes. For a conventional distillation column one of the typical decentralized control structures is that the control variables X_D, X_B and P are controlled by manipulating three actuator variables D, Q_B and Q_C. Hence an integrated design and control problem may be formulated that can be solved simultaneously.

3.4.2 Model analysis for the heat pump section.

The heat pump section is described by Eq.(3.17)-Eq.(3.31). There are twenty-one variables on the heat pump side, while there are fifteen equations. So the degrees of freedom are six. Variables T_W and L_W are considered as known variables, while the reboiler heat duty Q_B and the condenser heat duty Q_C are decided from the column section requirements. This means that there are two degrees of freedom on the heat

pump side. From Figure 3.4A and Figure 3.4B one can see that two process variables, the high pressure P_H and the low pressure P_L on the heat pump section, are good choices as control variables because there exists a nonlinear dependence between pressure, temperature and enthalpy. Two valves α_{CV8} and α_{CV9} are considered as actuators. Note that for the IVaRDiP these control variables (P_H and P_L) are related to the pressure and vapor flow rate in the column section through reboiler and condenser.

3.4.3 Sensitivity analysis.

In the analysis above, the distillation column section and heat pump section have been considered separately. Note that the heat pump is integrated with the distillation column through the condenser and the reboiler. In both cases, the streams undergo phase changes. On the heat pump side, disturbances in the heat exchange effects the P-V-T (pressure-volume-temperature) relationship since a pure gas is being condensed and vaporized. Figure 3.4A shows plots of pure component pressure-enthalpy diagram for the refrigerant freon-R114; while Figure 3.4B shows plots of pure component heats of vaporization, enthalpies and vapor pressure

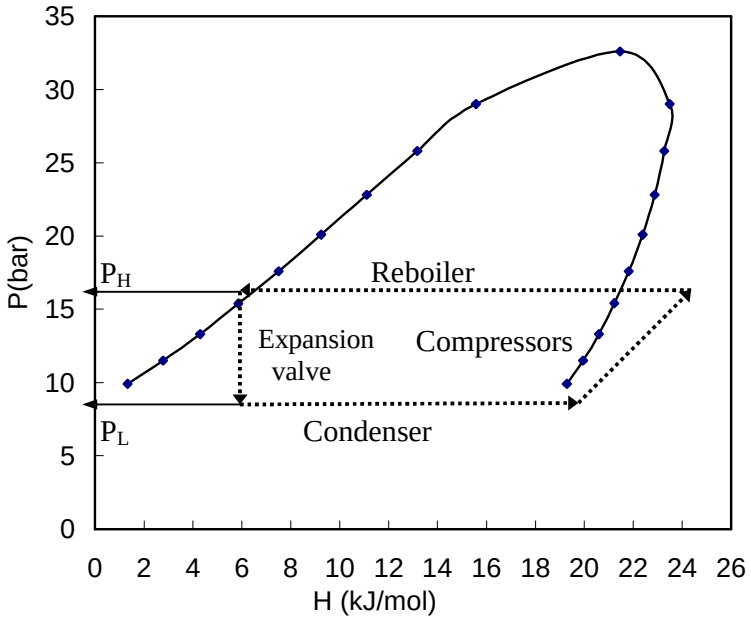

Figure 3. 4A: P-H diagram of freon-R114

for freon-R114, methanol and isopropanol. Analysis of the energy balance equation for the reboiler on the distillation column section and the heat pump section shows that small changes in pressure on the heat pump side may cause large changes in temperature on this side because of the P-V-T relation (see vapor pressure curves on Figure 3.4B). Consequently, a large change in the vapor boil-up may be produced since a change in the temperature causes a change in vaporization rate (see heat of vaporization curves in Figure 3.4B) assuming the residence time for vapor is negligible. A similar analysis for the condenser on the distillation column side and heat pump side shows that the change in temperature on the heat pump side is sensitive to small changes in pressure, but the reflux rate is less sensitive to changes in the temperature (at lower temperatures, the heat of vaporization is almost constant as shown in Figure 3.4B). Also, a change in temperature may cause a change in condensation, but since the residence time for a liquid is significantly larger than that of vapor, the liquid (reflux) flow rate is less sensitive than the vapor (boil-up) flow rate. Based on this analysis, the column pressure and vapor flow rate is sensitivity to the high pressure P_H and low pressure P_L on the heat pump section so the pressures on the heat pump side need to be controlled at both ends in order to ensure a specific static operating point for the total process. So for a indirect vapor recompression distillation pilot plant (IVaRDiP) Q_B, Q_C cannot be manipulated to control X_B and P as on a conventional distillation column, but the high pressure P_H and low pressure P_L on the heat pump section can be considered as the manipulated variables, which in turn are controlled by control valves α_{CV8} and α_{CV9}. But as the operating temperature approaches the critical temperature of freon-R114, the controller may fail and the operation may become infeasible.

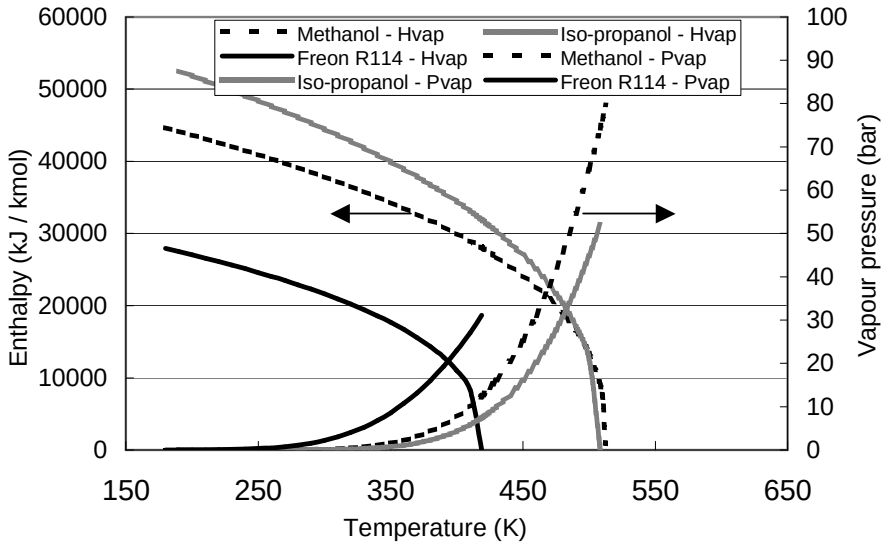

Figure 3.4B: Heat of vaporization and vapor pressure as functions of temperature for refrigerant and column components.

3.4.4 Control structure analysis for the IVaRDiP

3.4.4.1 Control structure analysis on the heat pump section.

From analysis of the process sensitivity, the pressures on the heat pump side needs to be controlled at both ends in order to ensure a specific static operating point for the total process. How to pair these two variables and two control valves play a very important part in stabilizing the integrated distillation pilot plant. However let us discuss how disturbance affects the heat pump high pressure P_H and low pressure P_L before the pairing problem is considered.

Consider, for example, the pilot plant operating at steady state with only liquid level controllers for the reboiler and the condenser implemented. If suddenly the energy balance is disturbed by a small amount δH, for instance, due to a disturbance in the feed preheater or in the feed composition or perhaps in the temperature of the cooling medium in the secondary condenser, then the changed heat input starts to accumulate in the column. If the disturbance reduces the cooling rate this will immediately affect the high pressure P_H such that P_H begins to increase. Thereby the compression work is continuously increased. The increase in the high pressure affects boil-up flow rate, and as a result of the column pressure and the heat pump low pressure P_L simultaneously increase, consequently the heat pump high pressure also increases. That is, positive feedback occurs in the integrated distillation pilot plant.

Assuming that the enthalpy of the column feed remains constant after the disturbance, the behavior of the entire column may become unstable. Therefore, a small disturbance in the overall energy balance can initiate a drift of the pilot plant towards increasing or decreasing column pressures depending on the sign of the disturbance. To reject the disturbance so as to stabilize the system, the high pressure P_H and low pressure P_L should be controlled by manipulating suitable actuators. In theory either the low pressures or the high pressure could be paired with α_{CV8} and thereby stabilize the system. However, the gain from α_{CV8} to the low pressure is relatively small (Koggensbøl, 1995), hence, if α_{CV8} is to be used for stabilization it should preferably be paired with the measurement of P_H.

The valve α_{CV9} does not directly affect the energy balance but it can be used to stabilize the pilot plant if it is paired with a suitable measurement. Suppose that P_L is stabilized by manipulating the valve α_{CV9} then a disturbance, which tends to increase P_L, will be neutralized by the valve opening being increased by the controller. This way P_L is maintained at set point. Furthermore, α_{CV9} is a butterfly valve which has a rather unpleasant nonlinear valve characteristics, hence the suggested loop will also serve to effectively linearize the valve characteristics. Not using such a local linearizing loop would seriously affect the column behavior due to the nonlinear valve characteristics.

The above analysis is based on linear arguments, which is sufficient for local purposes. To investigate nonlinear issues related to the consequences of process integration, however, it is necessary to resort to a nonlinear analysis.

3.4.4.2 Qualitative analysis for actuator selection for the IVaRDiP

To simplify the analysis, total-reflux operation is assumed by not including feed and product conditions for the steady state energy balance of the IVaRDiP:

$$0 = A_B U_B (T_1(P_H) - T_B) - A_C U_C (T_C - T_4(P_L)) \tag{3.32}$$

For the same reason the heat loss of IVaRDiP is also neglected. These are not important for the conclusion. $A_B U_B$ and $A_C U_C$ are coefficients containing information about heat transfer area and heat transfer coefficients for the reboiler and the condenser. T_1 and T_4 are temperatures of saturated freon-R114 at the given pressure on the heat pump side, and T_B and T_C are the temperatures on the column side of the reboiler and the condenser, respectively. The energy balance equation (Eq.(3.32)) states that the heat transfer rate in the reboiler must be equal to that in the

condenser. Otherwise the column would obviously accumulate or loose energy. The boil up rate (measured as the volumetric flow rate of condensed over-head vapor V_1) and column pressure (measured in the condenser P_C) are related to the variables in Eq.(3.32) knowing the heat of vaporization and composition on the column section in the condenser. This gives Eq.(3.33) and Eq.(3.34), where $f_{20}(T_C, x_{D,i})$ should be a function calculating the pressure in the condenser (bubble-point pressure in case of a total condenser) based on the temperature and the composition. To complete the picture a correlation for the pressure drop from bottom to top stage is assumed, and furthermore, it is for simplicity assumed that the column ends are so pure that dew and bubble points here are independent of composition. The set of relations connecting the heat pump pressures P_H and P_L to the column pressure and vapor flow rate are thus:

$$V_1 \Delta H = A_B U_B (T_1(P_H) - T_B) = A_C U_C (T_C - T_4(P_L)) \tag{3.33}$$

$$P_C = f_{20}(T_C) \tag{3.34}$$

$$P_B = f_{21}(T_B) = P_C + \Delta P \tag{3.35}$$

From Eq.(3.33) to Eq.(3.35) one can see that if P_H is increased at constant P_L this will affect first the temperature difference in the reboiler. This causes the vapor flow rate to increase. To accommodate the higher vapor flow rate the pressure in the column top increases until the temperature difference in the condenser satisfies the energy balance. So the high pressure has positive gain to both boil-up flow rate and column pressure. If instead P_L is increased at constant P_H the temperature difference in the condenser is decreased. This causes the vapor flow rate to decrease. To accommodate the lower vapor flow rate the pressure in the column increases until the temperature difference in the reboiler satisfies the heat balance. So the low pressure has positive gain to column pressure but the negative gain to the vapor flow rate. Based on this analysis, both the high pressure P_H and low pressure P_L affect the column pressure and vapor flow rate, but they have different gains. These results obtained from the model analysis will be further investigated through rigorous simulation.

3.5 Verification and further analysis

3. 5.1 Analysis of the movement of the operation point.

Through analysis of the phenomena models with respect to the properties of the pure components, a sensitivity analysis of the IVaRDiP and the actuator structure has been obtained. Rigorous simulation with the simulation program of Koggensbøl (1995) is carried out to validate the analysis results. First, simulations are done as listed in Table 3.1, where the heat pump low pressure P_L is kept constant at 500kPa while P_H is decreased in steps of 25kPa. The column pressure (top stage) and the boil-up flow rate are given in Table 3.1. For these simulations the feed composition of methanol X_F is 0.4950(mole fraction) and feed flow rate is 3096mole/hr. Further the heat pump high pressure P_H is kept constant at 1075kPa; P_L is decreased in steps of 25kPa. The simulation results are listed in Table 3.2. These results are plotted in Figure 3.5, where branch A corresponds to the results in Table 3.1 and branch B corresponds to the results in Table 3.2.

Table 3.1 (Branch A)

Point	P_H (kPa)	P_L (kPa)	P_C (kPa)	V_1 (m^3/h)
1	1175	500	81.22	1.423
2	1150	500	78.98	1.184
3	1125	500	76.55	0.950
4	1100	500	73.88	0.720
5	1075	500	70.87	0.505

Table 3.2 (Branch B)

Point	P_H (kPa)	P_L (kPa)	P_C (kPa)	V_1 (m^3/h)
5	1075	500	70.87	0.504
6	1075	475	69.94	0.782
7	1075	450	68.34	1.040
8	1075	425	66.38	1.286
9	1075	400	64.13	1.516

From Figure 3.5 one can see that the column pressure and vapor flow rate are very sensitive to high pressure P_H and low pressure P_L on the heat pump section, in accordance with the results obtained earlier from the sensitivity analysis. Decreasing P_H at constant P_L move the operation points along branch A from operation point 1 to 5. When decreasing P_L in two single loops at constant P_H, the operation points move along branch B from operation point 5 to 9. Both branch A and branch B are

nonlinear and sensitive to the pressure change of the heat pump side. Hence direct usage of P_H and P_L to maintain constant column pressure and vapor flow rate is not advisable due to interactions between these two variables.

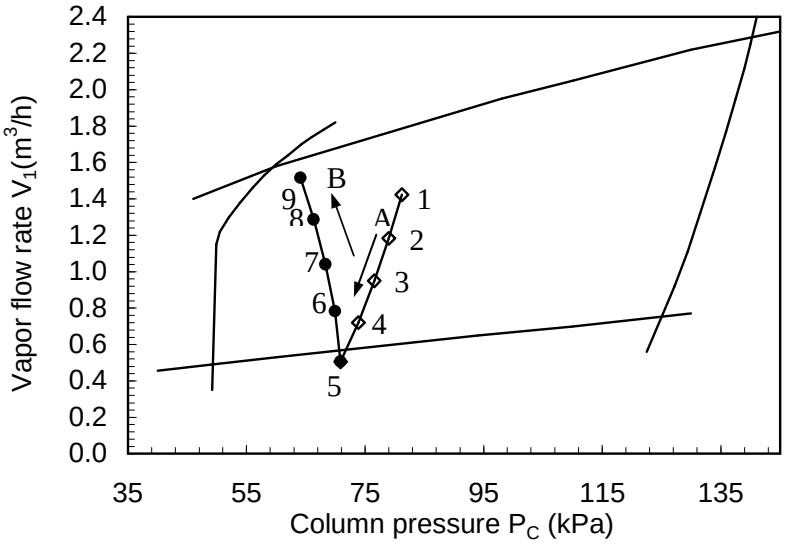

Figure 3.5: Operation point movement- top stage pressure versus vapor boil-up flow rate.
Branch A: Constant P_L=500kPa, decrease in P_H by steps of 25kPa
Branch B: Constant P_H=1075kPa, decrease in P_L by steps of 25kPa

In order to determine a more suitable actuator configuration the gain from PH and PL to the column pressure and vapor flow rate will be investigated through simulation. The results are shown in Figure 3.6 from which one can see that PH has positive gain to column pressure and

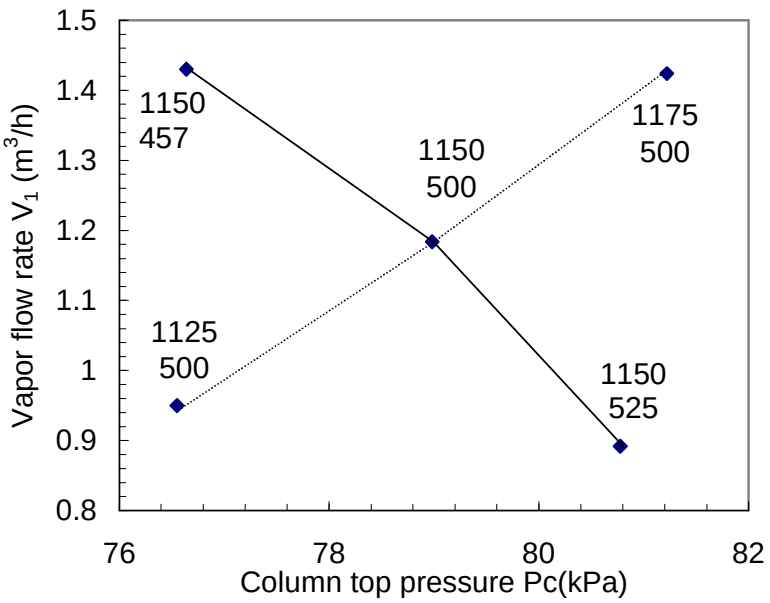

Figure 3.6: The gain for positive and negative changes in the heat pump pressures Steps $\pm 25kPa$ *in high and low heat pump pressures (on simulation plot:* P_H *over* P_L *in kPa)*

vapor flow rate while P_L has positive gain to column pressure but negative gain to vapor flow rate, which confirm the results from the model analysis. From this understanding it is seen that in order to increase the column pressure at constant boil-up flow rate one must increase both actuators, while if the boil up flow rate is to be increased at constant column pressure (either P_B or P_C) one must increase P_H and/or reduce P_L. So it is clear that specifying the two heat pump pressures P_H and P_L is equivalent to specifying boil-up flow rate and column pressure and hence it should be possible to configure a control system manipulating the set points to the high and low pressure (or perhaps the control valves α_{CV8} and α_{CV9}) directly such that the operator can manoeuvre the process through the operating region using the actuators P and V of a conventional distillation pilot plant. The selection of the above actuators (P_H+P_L) for column pressure and (P_H-P_L) for vapor flow rate ensures a simple mapping to the conventional actuators P, V.

3.5.2 The static actuator configuration

To confirm the control issues discussed above, rigorous dynamic simulations have again been performed with the simulation program of Koggerbøl (1995). The simulation result are plotted in Figure 3.7, where curve A in Figure 3.7 represents

constant P_H+P_L, while P_H-P_L change. From curve A one can see that column pressure is nearly constant for constant P_H+P_L for many different values of P_H-P_L. From curve B one can see that the vapor flow rate is nearly the same at constant P_H-P_L in spite of different values of P_H+P_L. This confirms the design and control issues stated above that one could control the vapor flow rate in the integrated distillation pilot plant by manipulating the pressure difference between the high pressure and the low pressure of the heat pump side and the column pressure by manipulating the sum of the two heat pump pressures.

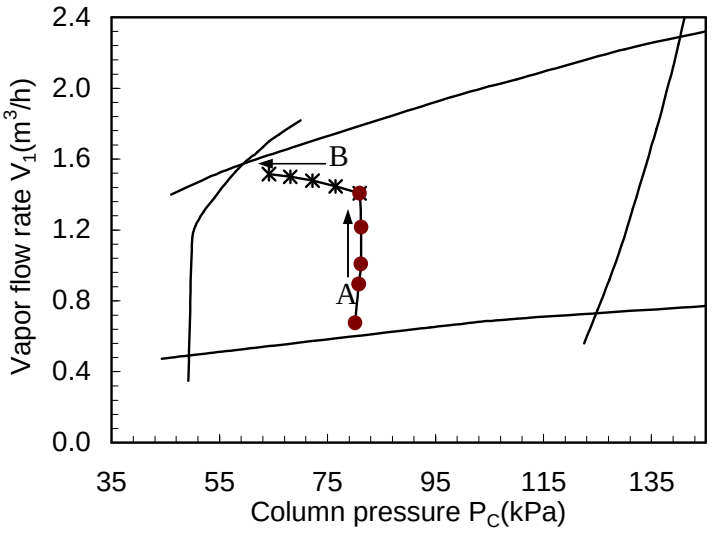

Figure 3.7: Top stage pressure versus vapor boil-up flow rate
Curve A: P_H +P_L at constant, P_H-P_L Change;
Curve B: P_H-P_L at constant, P_H +P_L change

3.6 Conclusions

A model-based analysis method has been used for the design and control actuator selection for an integrated distillation pilot plant. The analysis method employs a sub-set of the total model equations according to the sub-problem being analyzed and therefore, does not need to solve the total set of model equations. The results demonstrate that with this method an integrated design and control problems could be defined correctly and consistently with respect to the process behavior and the selected process model. Rigorous simulation results verify this analysis, confirming that it may be possible to generate good estimates of the optimal solution before a

rigorous solution of the model equations is attempted. The model analysis method provides useful insight to relations between process design and control structuring for control. The resulting control structure can operate the plant within an identified operating window. The suggested control structuring methodology fits the industrial plant design paradigm. However it is pointed out that a nonlinear analysis may be required for proper analysis of the nonlinear dynamic implications. The control structuring method also demonstrates how to use process insights developed from model analysis for achieving flexible plant operation.

Symbles:

A_BU_B : Heat transfer area and heat transfer coefficients for the reboiler, kJ/K

A_CU_C : Heat transfer area and heat transfer coefficients for the condenser, kJ/K

B: Bottom product flow rate, mol/hr

C_p : Heat capacity of refrigerant, kJ/mol.K

D: Top product flow rate, mol/hr

F_j : Feed flow rate, mol/hr

f_1- f_{19}: Function

g_g: Gas density (kg/m^3)

g_l: Liquid density (kg/m^3)

H_D^L: Enthalpy on the column side at the condenser, kJ/kmol

H_B^V: Enthalpy on the column side at the reboiler, kJ/kmol

H_j^F: Enthalpy of liquid on feed stage, kJ/kmol

H^H_{vap}: Heat of vaporization of freon, kJ/kmol

$H_{i,j}$: Component enthalpy on stage j, kJ/kmol

H_j^L: Enthalpy of liquid on stage j, kJ/kmol

H_j^v: Enthalpy of vapor on stage j, kJ/kmol

ΔH: Heat of condensation in the reboiler, kJ/kmol

$K_{i,j}$: Equilibrium constant of component i on stage j

L_0: Reflux flow rate, mol/hr

L_{COMP}: Flow rate out of secondary condenser, mol/hr

L_{EXP}: The flow rate of refrigerant on heat pump side, mol/hr

L_j : Liquid flow rate from stage j, mol/hr

L_W: Molar flow rate of water in heat pump section, mol/hr

NC: The total number of components

NF: The stage of feed

NP: The total number of stages

P_1: High pressure at reboiler on heat pump side, kPa

P_3: Pressure before expansion valve at condenser, kPa

P_4: Pressure after condenser, kPa

P_5: Pressure after α_{CV9}, kPa

P_6: Pressure before compressor, kPa

P_B: Pressure on the column bottom, kPa

P_c: Pressure at the column top, kPa

P_H: High pressure on the heat pump side, kPa

P_j: Pressure on stage j, kPa

P_{j-1}:Pressure on stage j-1, kPa

P_L: Low pressure on the heat pump side, kPa

ΔP: Pressure drop over each stage, kPa

Q: Heat exchange before compressor, mol/hr

Q_B: Heat add to the reboiler, mol/hr

Q_c: Heat removed from the condenser, mol/hr

Q_j: Heat added or removed from stage j, mol/hr

t: Time, hr

T: Temperature, K

T_1: Temperature of reboiler on heat pump side, K

T_2: Temperature in the receiver, K

T_3: Inlet temperature of expansion valve, K

T_4: Temperature of condenser on heat pump side, K

T_5: Temperature after control valve CV9, K

T_6: Inlet temperature of the compressor, K

T_B: Temperature in the reboiler on the column side, K

T_C : Temperature in the condenser on the column side, K

T_j: Temperature on the stage j, K

T_W: Temperature of cooling water leaving secondary condenser, K

T_W^{in}: Inlet temperature of cooling water at secondary condenser, K

$\Delta T_{Condenser}$: Temperature difference between both sides in the condenser, K

$\Delta T_{Reboiler}$: Temperature difference between both sides in the reboiler, K

V_B: Vapor flow rate of the column at the bottom, m^3/hr

V_1: Vapor flow rate on top stage, m^3/hr

V_j: Vapor flow rate on stage j, m^3/hr

W_2: Molar hold up in the receiver, mol

W_4: Molar freon hold-up in the condenser, mol

W_w: Molar hold up in the secondary condenser, mol

X_D: Methanol composition on the top of the column, mole fraction

X_B: Methanol composition at the bottom of the column, mole fraction

$X_{i,j}$: Mole fraction (liquid) of component i on stage j, mole fraction

$Y_{i,j}$: Mole fraction (vapor) of component i on stage j, mole fraction

$Z_{i,j}$: Feed composition, mole fraction

References

Russel, B. M.; Henriksen, J. P.; Jørgensen, S. B.and Gani, R. (2002), Integration of Design and Control through Model Analysis. Comput. and Chem. Eng. 26(2), 213-225.

Tyreus, B. D.; Luyben, W. L. (1993), Dynamics and Control of Recycle System. 4. Ternary systems with one or two recycles streams. Ind. Eng. and Chem. Res., 32, 1154-1162

Foss, A. S. (1973), Critique of Chemical Process Control Theory. AIChE, 19(2), 209-214.

Skogestad, S. (2000), Plantwide Control: the Search for the Self-optimizing Control Structure. Proc. Contr., 10, 487-507.

Agrawal, R.; Fidkowski, A. T. (1999), New Thermally Couple Schemes for Ternay Distillation, AIChE, 45, 3, 485.

Hernández, S.; Jiménez, A. (1999), Controllability Analysis of Thermally Coupled Distillation System. Ind. Eng. Chem. Res., 38, 3957.

Hansen, J. E.; Jørgensen, S. B.; Heath, J.; Perkins, J. D. (1998), Control Structure Selection for Energy Integrated Distillation Column. Proc. Contr., 8(2), 185-195.

Eden, M. R.; Køggersbøl, A.; Hallager, L.; Jørgensen, S. B. (2000), Dynamics and Control during Startup of Heat Integrated Distillation Column. Comput. and Chem. Eng., 24, 1091-1097.

Koggersbøl, A. (1995), Distillation Column Dynamics, Operability and Control. Ph. D thesis, Technical University of Denmark, Denmark.

4

Experimental Validation of Flexible Multivariable Control Structure for IVaRDiP

Abstract *Control of boil-up and internal flows of the IVaRDiP requires a rethinking of the conventional binary distillation control problem since the actuators are shifted from the conventional energy inputs and outputs to heat pump actuators. Actuator analysis reveals that a set of combined heat pump actuators advantageously can be used to decouple interaction between pressure and boilup in binary distillation. This structure is implemented in a flexible multivariable controller, which utilizes multiple measurements. Application of this rectangular multivariable controller for controlling distillation pressure and boilup flow rate is validated experimentally. In the experimental validation the column is operated over a range of internal flows.*

4.1 Introduction

For a chemical process the general control task is to maintain some process outputs at given setpoints and make set points tracking with at least as many inputs when these setpoints are changed. The literature of these control problems on distillation research is vast and comprehensive (Skogestad, 1992) counting thousands of articles and monographs of which many of them are concerning actuator selection to decouple the interaction of the manipulated variables. In general the fundamental problem in multivariable control includes the following:

1. Selection of controlled variables

   The selection of control variables must be based on good knowledge of the process to be controlled. There is usually a difference between the quantities that one primarily want to control and the variables that are easily available for measurement without any time delay. A set of variables is to be controlled to achieve a set of specific objectives. In many cases, it is clear from a physical understanding of the process what the controlled outputs should be. In other cases it is less obvious because each control objective may not be associated with a measured output variable. Then the controlled variables are selected to achieve the overall system goal, and may not appear to be important variables in themselves.

2. Selection of manipulated variables

   A set of variable can be manipulated and measured for control purposes. In some cases there is a large number of candidate measurements and/or manipulation. The selection of manipulation is to stabilize the system, to reject disturbances and to track reference changes, which have a strong relationship with the controlled output.

3. Selection of the control configuration

   A structure interconnects measurements and manipulated variables

4. Selection of the controller type

   Control law specification, e.g. PID-controller, decoupler, LQG

From above one can see that a fundamental problem in multivariable control is to select measurements, actuators and the pairing of these variables. For multivariable control system the interaction between actuators is existing and decoupling has been studying though the years by using theory for design multivariable systems. To simplify the complex of decoupling the actuator of multivariable system, a new approach in previous chapter to decouple the interaction of the actuators by using the combination of the actuators is suggested, which is implemented into the IVaRDiP.

The purpose of this chapter is to experimentally investigate the practical feasibility of selecting a control structure, which renders the IVaRDiP behaviour similar to that of a conventional distillation column, i.e. without heat integration. In particular it is relevant to investigate what are the key differences between these two alternatives and which role of these differences do play for the selection and function of a decoupling control structure.

The structure of the chapter is as following: first it is the control of distillation column introduced, then the basis for the control structure is briefly given and the actual implementation of the decoupling control structure is presented and finally experiment that is carried out to validate this control structure is shown and the results are discussed.

4.2 A short description of IVaRDiP

Figure 3.1 shows a schematic of an IVaRDiP suitable for separating a mixture of methanol and isopropanol with a little impurity water. The plant consists of a distillation column, a thermosiphone reboiler, a total condenser and a reflux drum. The column has 19 sieve trays. In order to reduce energy consumption, the reboiler and condenser are energy integrated through a heat pump. The heat pump transfers the energy released from the condenser to the reboiler.

A schematic of the main pieces of equipment is given in Figure 3.1 and Figure 3.3. Feed is introduced via two pumps, mixed and preheated in a heat exchanger. It may be fed into the column at 5 different positions. At the bottom of the column liquid is withdrawn partly as bottoms product via a pump and partly evaporated in the reboiler and reintroduced into the column as vapour. From the top of the column the vapour is led to the condenser, where it is condensed. The liquid is pumped to a decanter via a pump. In this study the decanter simply is an accumulator. From the decanter a part is withdrawn as top product and a part is returned as reflux to the top of the column. The tank park contains seven tanks in sizes from 1.5 to 4.0 m^3/hr, which are connected to the plant in a manner, which allows flexible usage of the tanks and of distillation mixtures. For binary distillation experiments a methanol-isopropanol system is currently used. The heat pump system depicted in Figure 3.3 has been designed for large heat transfer load variations. It used Freon 114 as the heat transfer medium and utilizes two 8-cylinder piston compressors. The heat pump works as follows: most of the heat pump fluid vapour is condensed in the reboiler. An extra condenser removes an amount of heat roughly corresponding to the heat introduced by the compressors. Three air fan coolers pass on this heat to the environment. The condensed heat pump

fluid passes to a receiver and through a heat exchanger to the heat pump fluid evaporator. This heat exchanger serves to superheat the heat pump fluid gas before it enters the compressors, to prevent condensation during compression. After the evaporator a demister prevents liquid from passing on to the compressors and enables the heat pump fluid evaporator (or distillate condenser) to operate as a thermosiphon reboiler.

On tray 1,5,10, 15and 19 PT100 temperature sensors are located in the liquid hold-up. In combination with pressure measurements (located in the column bottom, on tray 10 and in the column top) the temperature measurements are used for concentration estimates. All flows in and out of the system and the reflux flow rate are measured on a mass basis. Feed, bottom product, and distillate are sampled manually at each steady state for off-line gas chromatography analysis.

The basic control configuration for the plant is as follows: the column pressure and column vapor flow are control by Multivariable Selftuning Control (MIMOSC). The accumulator level is controlled by reflux flow rate L and reboiler level is controlled by bottom product flow rate B. The concentration profile is manipulated in the high gain direction by distillate flow rate D.

4. 3 Computer system

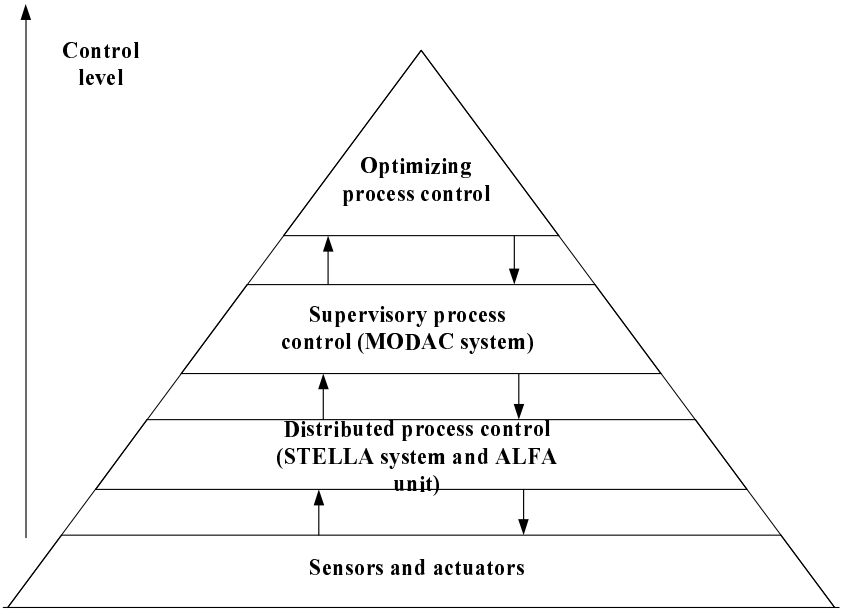

Figure 4.1: Computer systems corresponding to the different levels of IVaRDiP control hierarchy

A control hierarchy of the IVaRDiP is shown in Figure 4.1, where three conceptual control levels are organized. The lowest level of the control structure is the distributed process control level. The task of this level is to keep the measurements at their setppoints, which are either specified by the operators or the higher levels in the control scheme. The next level in the control hierarchy is termed supervisory process control level. The tasks of this level are to coordinate several alternative manipulated variables in order to avoid saturation in critical loops at the distributed control level, and maintain the measurements at their setpoints or within maximum and minimum limits. The top level is the optimizing process control level. This level simultaneously calculates the optimal plant conditions for part of the plant or the entire plant. A flexible multivariable controller is implemented into the above IVaRDiP, which is equipped with a large quantity of measurements and actuators.

The structure of the basic control loops relevant for the IVaRDiP is described in Table 4.1 and Figure 4.1. From this table it may be observed that the top section of the distillation column may be operated in both a D and in a L configuration. Depending on the configuration the actuator in loop 19 changes. In D-configuration loop 19 passes a setpoint to FM6, i.e. loop6, while in the L-configuration the setpoint is passed to FM4, i.e. loop 4.

Table 4.1: Distillation process and heat pump control loops relevant for start-up purposes

Loop	Sensor	Actuator	Set-point	Remarks
1	FM1	PF1	Feed flowrate 1	
2	FM2	PF2	Feed flowrate 2	
3	FM3	PB	Bottoms product flowrate	Inner cascade to loop 18
4	FM4	CV2	Distillate flowrate	Inner cascade to loop 19
6	FM6	PR	Reflux flowrate	Inner cascade to loop 19
8	P10	CV8	Heat pump high pressure	Supervisory level setpoints
9	P8	CV9	Heat pump low pressure	Supervisory level setpoints
11	FMSM	CV5	Preheater steam flowrate	
18	DP1	SP FM3	Reboiler level	Outer cascade to loop 3
19	L1	SP FM6/4	Accumulator level	Outer cascade to loop 6 or 4

After completing the start-up, i.e. the system is close to normal operating conditions; it is possible to introduce P-V control in the form of an algorithm called MIMOSC, Multi Input Multi Output Selftuning Controller (Brabrand et al. 1991).

The control structure showed in Table 4.2 fulfills the three levels of the control hierarchy, which compares to the conventional distillation column and the heat-integrated distillation pilot plant.

Table 4.2: Control structure level of the IVaRDiP

Lower level Measurements		Lower level Actuators		Middle level Actuators		Optimizing level Actuators	
Conventional	Improved	Conventional distillation	Heat integrated distillation plant	Heat integrated distillation plant	Conventional distillation	Measure-ments	Actuators
$\hat{D}$ or $\hat{L}$	Same	Valve opening	Valve opening	D_{sp} or L_{sp}	D_{sp} or L_{sp}	x_D	D_{sp} or L_{sp}
$\hat{V}$	Same	Valve opening	CV9 for P_L	P_H - P_L	V_{sp}	x_B	V_{sp}
P_T	$P_{B\ or\ T}$	Valve opening	CV8 for P_H	P_H + P_L	P_{sp}	$P_{B\ or\ T}$	P_{sp}

Table 4.2 lists measurements and actuator variables for control structuring at three levels for conventional and IVaRDiP binary distillation with three static degrees of freedom. Note subscript sp stands for setpoint while other subscripts refer to the specific IVaRDiP. When reference is made to a valve opening as an actuator, this may also be a pump speed.

4.4 Control system (MIMOSC)

A short description of the control system, i.e. MIMOSC is introduced, which operates within the OS/2 based MODAC data acquisition and control system. The control algorithm in MIMOSC is LQ-controller based on a receding horizon state space representation of the identified multivariable ARMAX model. The idea behind MIMOSC is to perform one or more iterations on the Ricatti equation every time the parameters in the ARMAX model have been updated, starting with the result of the last iteration of the Ricatti equation from the previous sample period. In this way the controller adapts smoothly to changes in the controlled process.

The controller part of MIMOSC applies an LQ-controller to a non-minimum state representation of the ARMAX-model or rather the ARX- part of ARMAX-model. The state space equation is written as follows:

$$z(t+1) = Az(t) + Bu(t) \tag{4.1}$$

where

$$z(t) = \begin{bmatrix} y'(t) \\ y'(t-1) \\ \vdots \\ y'(t-NA) \\ u'(t-1) \\ u'(t-2) \\ \vdots \\ u'(t-NB) \end{bmatrix} \tag{4.2}$$

where:

$y(t)$: vector of the process output variables measured at time t

$u(t)$: vector of manipulated process input variables measured at time t

$y'(t)$: vector of the process output differenced variables measured at time t

$u'(t)$: vector of manipulated process input differenced variables measured at time t

A , B : parameter matrices to be estimated in the ARMAX-model

NA, NB : number of respective parameter matrices to be estimated in the ARMAX-model

The optimal criterion to minimize is:

$$J = z^T(t+N)Q_Z z(t+N) + \sum_{i=1}^{N-1} z^T(t+i)Q_Z z(t+i) + u'^T(t+i)Q_u u'(t+i) \tag{4.3}$$

Where Q_Z , Q_u are diagonal weighting matrices. The user chooses a weight for each process output, manipulated variable and integral state. The feedback gains are calculated making iterations of the Ricatti equations. The output variables are the setpoints of the high pressure and low pressure on the heat pump section.

The measurement matrix z:

$$z = \begin{bmatrix} P_1 \\ P_3 \\ P_8 \\ P_9 \\ P_{10} \\ V\_est \end{bmatrix}$$

Where:

P_1 : bottom column pressure (abs), kPa

P_3 : top column pressure (abs), kPa

P_8 : low heat pump pressure before α_{CV9}, kPa

P_9 : low heat pump pressure after α_{CV9}, kPa

P_{10} : high heat pump pressure, kPa

V_est : column reboiler-up vapor flow rate, m^3/hr

The input u:

$$u = \begin{bmatrix} P_8\_est \\ P_{10}\_est \end{bmatrix}$$

4.5 Experiment

With this flexible variables control system are implemented into the computer system to control the IVaRDiP. During this experiment, lasting a total of more than 168 hours, 12 steady states were obtained. The experiment was separated into two phases, phase B and phase C. During phase B the top pressure is controlled at 100 kPa. The initial set point for the boil up is 1.12m^3/hr. For both phases, the composition on tray 15 was controlled at 0.75 (Methanol mole fraction). When steady state conditions have been reached samples of the feed and products are sampled for later analysis on a gas chromatograph. The boil up flow rate is decreased by setpoints changes according to Table 4.3, and steady state conditions are obtained for each boiler up flow rate. When all steady states in phase B has been obtained, the pressure control scheme is changed i.e., phase C starts. During phase C the column bottom pressure is controlled. The boil up flow rate is then increased again according to the Table 4.2 lists, and steady state conditions are obtained for each boil up flow rate. In Table 4.2

the list of experiments is given together with number of steady state obtained, column pressure, vapour flow rate, the higher pressure and low pressure on heat pump section during the experiments. After each set of steady state conditions has been reached samples of the feed and top and bottom products are collected for off-line analysis.

4.5.1. Experimental procedure

Start up is made and the system is brought to a "steady" operation at high pressure 1180 kPa and low pressure 400 kPa. MIMOSC is activated with setpoints equal to process values. Setpoint to column top pressure is changed to 100 kPa. 1-point composition control is activated with setpoint for the molefraction on tray 15 (XPTT15) equal to 0.75 (mol/mol). Initial setpoint for the boil up (V_est) is 1.09 m^3/hr. When steady state conditions have been reached samples of the feed and products are collected. The boil up flow rate is decreased according to the Table 4.3, and steady state conditions are obtained for each boil up flow rate.

Table 4.3: Experimental setpoints for the multivariable controller

Phase	Steady State	P_1 (Top) (kPa)	P_3 (Bottom) (kPa)	V (m^3/hr)
Phase B	1	100		1.09
	2	100		0.981
	3	100		0.868
	4	100		0.739
	5	100		0.661
	6	100		0.538
Phase C	7		100	0.536
	8		100	0.660
	9		100	0.738
	10		100	0.860
	11		100	0.979
	12		100	1.083

4.5.2 Experimental results and discussion

The experiment results related to the control structure validation are shown and discussed. The column pressure and boil-up flow rate are the two measurements to be controlled from which the setpoints of the high and low pressure on the heat pump

section are set by MIMOSC. The actuator of the high pressure on the heat pump is control valve CV8; while the actuators of the low pressure on the heat pump is control valve CV9.

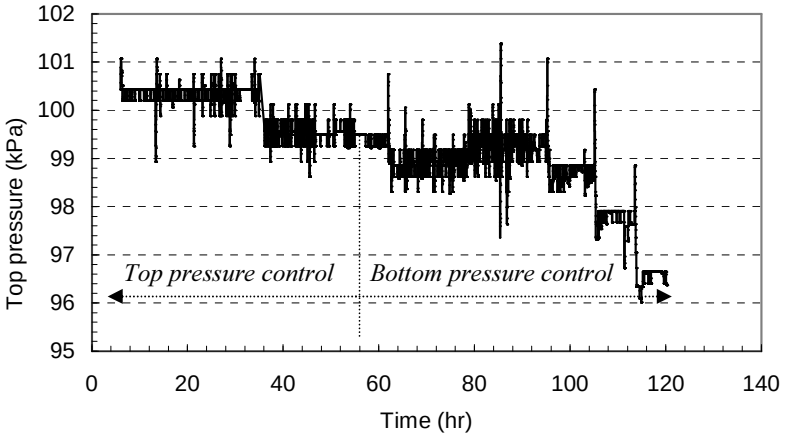

Figure 4.2: Column top pressure during the experiment

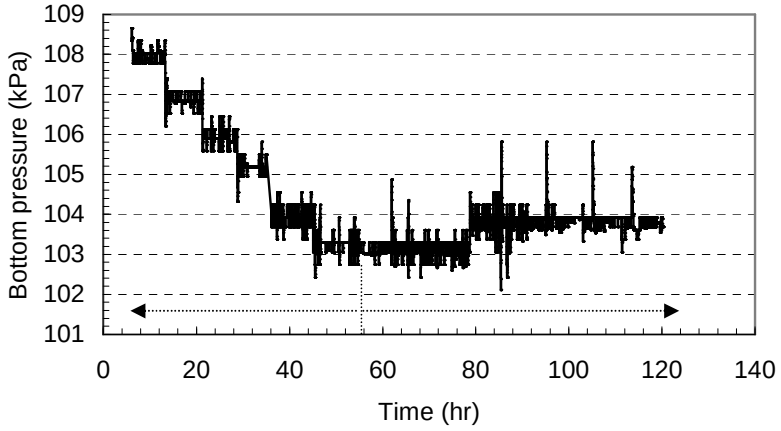

Figure 4.3: Bottom pressure during the experiment

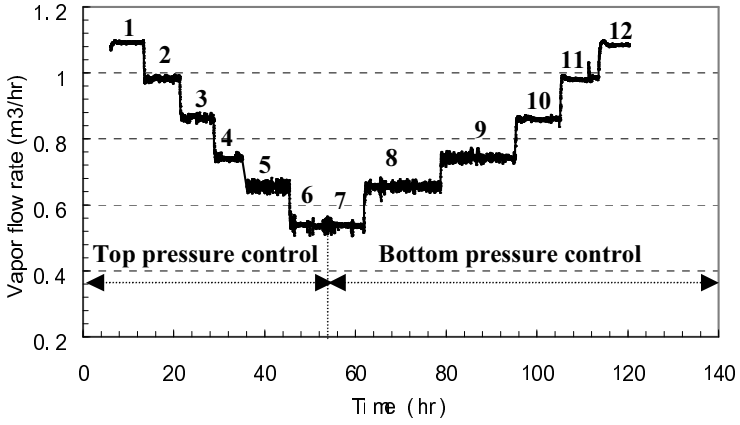

Figure 4.4 Vapor flow rate (m'/hr) during the experiment

From Figure 4.2, Figure 4.3 and Figure 4.4 one can see that the column pressure and column boiler-up vapor flow rate are well controlled with the suggested flexible multivariable control structure implemented into the computer.

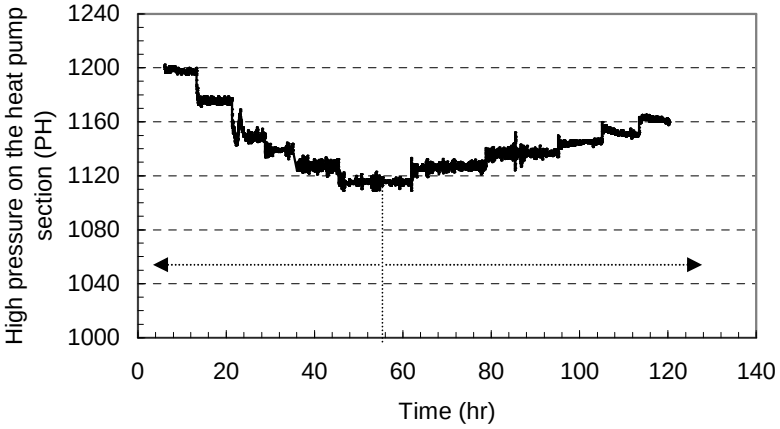

Figure 4.5: High pressure (kPa) on the heat pump during the experiment

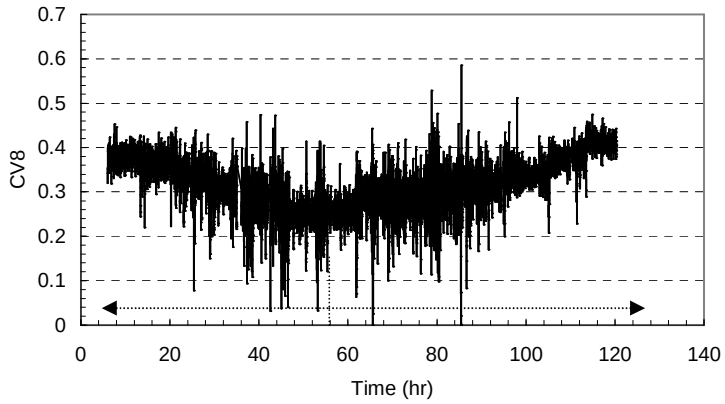

Figure 4.6: The actuator of high pressure on heat pump, CV8

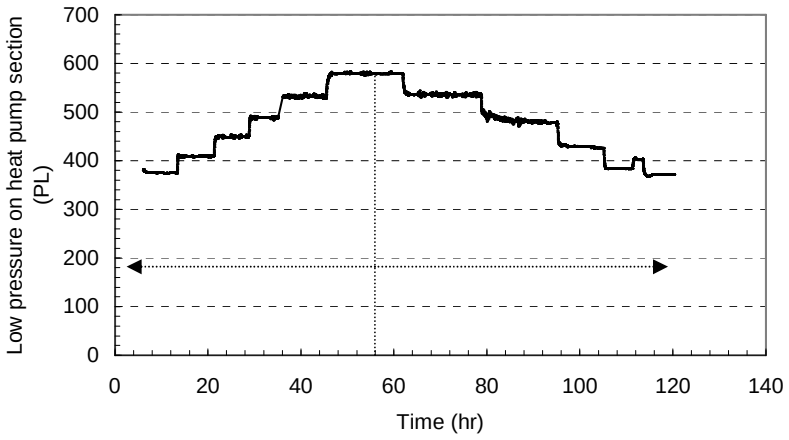

Figure 4.7: Low pressure (kPa) on the heat pump during the experiment

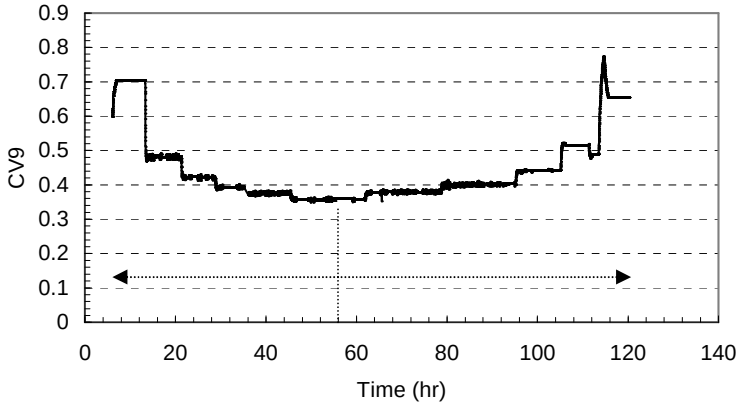

Figure 4.8: The actuator of low pressure on the heat pump, CV9

When the vapor flow rate decrease from 1.2 m^3/hr to 0.5 m^3/hr at top pressure control part from time 7.3 hr to 56 hr, the high pressure on the heat pump decrease see Figure 4.5 and the low pressure on the heat pump increase seeing Figure 4.7, which cause the sum of the high and low pressure on the heat pump keeps almost constant (seeing Figure 4.12), where the deviation of this sum is 9.5%, but the difference of high and low pressure on the heat pump section decrease (seeing Figure 4.10). When the vapor flow rate increase from 0.5 m^3/hr to 1.2 m^3/hr, i.e. time from 56 hr to 120 hr, the high pressure increase and the low pressure decrease that can be seen from Figure 4.5 and Figure 4.7, which result the sum of the high and low pressure almost constant (seeing Figure 4.12) and difference of the high and low pressure increase (seeing Figure 4.10). These behaviors validate the results from model analysis (Li et al 2003).

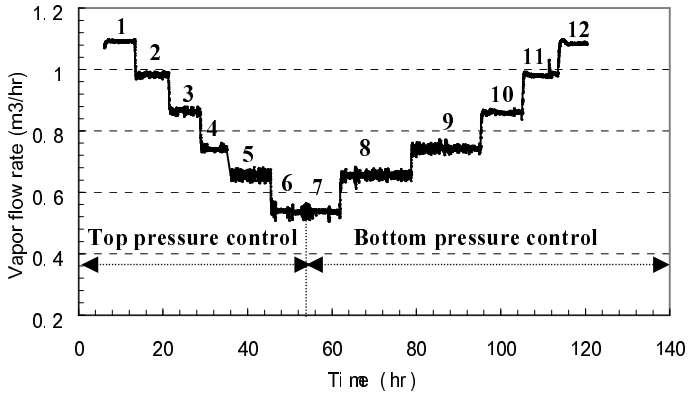

Figure 4.9: Boiler-up vapor flow rate during the experiment

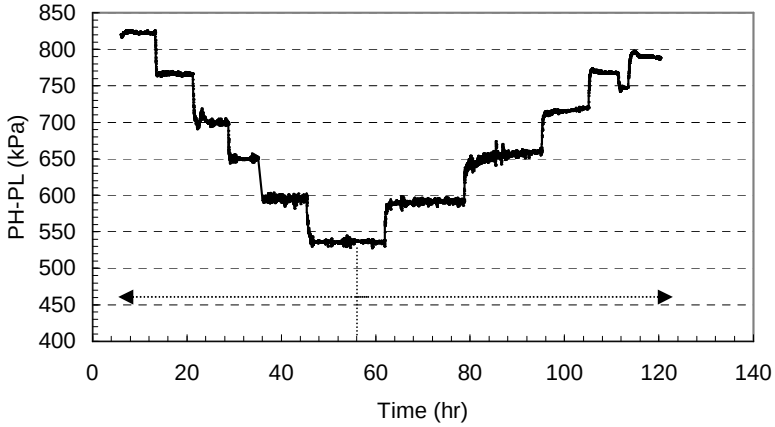

Figure 4.10: Pressure difference between high and low pressure on the heat pump during the experiment

The pressure behaviour and the difference between the high and low pressure are shown in Figure 4.9 and Figure 4.10. One can see that as vapour flow rate decreases, the difference between the high and low pressure decreases; and when vapour flow rate increases, the difference between the high and low pressure increases, which validates the result obtained from the model analysis, i.e, the difference between the high pressure controls the column vapour flow rate.

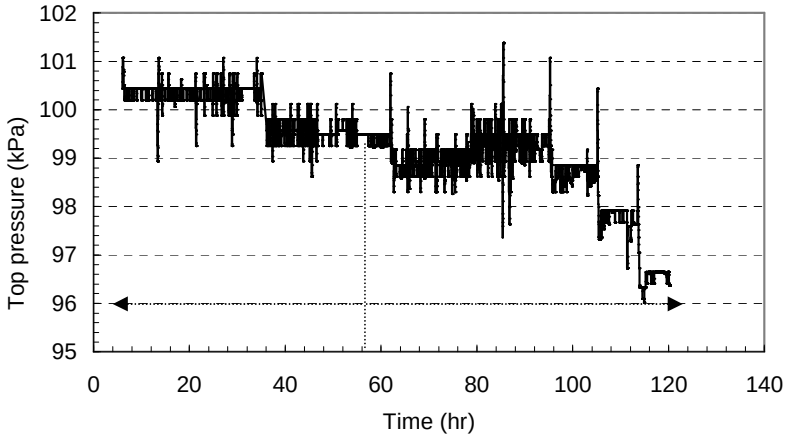

Figure 4.11: Top pressure in column

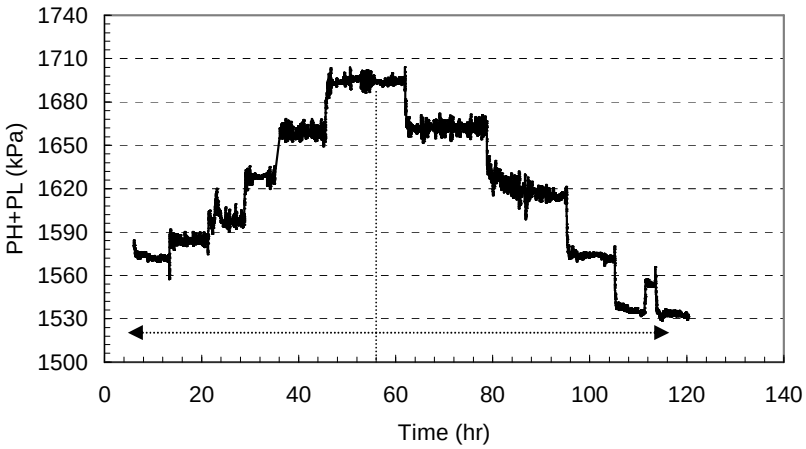

Figure 4.12: Top pressure and the sum of high and low pressure on the heat pump during the experiment

So as to see clearly, both the pressures in the column and sum of the high and low pressure are shown in Figure 4.11 and Figure 4.12.

From Figure 4.11 and Figure 4.12 one can see that when the vapour flow rate decrease the high pressure decrease and low pressure increase; while the vapour flow rate increase the high pressure increase and low pressure decrease. That means the controller try to keep the sum of the high pressure and low pressure constant so as to

control the column pressure constant in spite of the vapour flow rates change. The biggest deviation of this sum throughout the experiment is 9.5%, which can say that the sum of the pressure on the heat pump is kept at constant so as to control the column pressure constant while the vapour flow rates change.

4.6 Conclusions

A flexible multivariable control structure, i.e., MIMOSC control structure, is implemented into the computer system to control the IVaRDiP. The experiment is carried out and the actuator selection obtained form the model analysis is validated. The experimental results where the plant behaviour has been investigated over a broad range of internal flow rates have been presented. It is shown that the rectangular multivariable controller indeed implements the intended decoupling over most of the investigated range. The experimental results show that the column pressure and boilup flow rate are well controlled with this flexible multivariable control structure.

Symbols:

A, B: parameter matrix to be estimated in Eq. (5-1)
CV2: control valve for distillate flow rate
CV5: control valve for preheater steam flow rate
CV8: control valve for heat pump high pressure
CV9: control valve for heat pump low pressure
DP1: reboiler lever, kPa
D_{SP}: setpoint for distillate flow rate, ton/hr
FM1: feed flow rate, ton/hr
FM2: feed flow rate, ton/hr
FM3: bottom product flow rate, ton/hr
FM4: distillate flow rate, ton/hr
FM6: reflux flow rate, ton/hr
FMSM: preheater steam flow rate, m^3/hr
J: object function in Eq. (5-3)
L1: accumulator level, mA
L_{SP}: setpoint of reflux flow rate, ton/hr
NA, NB: number of respective parameter matrix in Eq. (5-2)
P1: column top pressure, kPa
P3: column bottom pressure, kPa
P8: heat pump high pressure, kPa
P8_est: setpoint of heat pump high pressure, kPa
P9: heat pump low pressure after CV9
P10: heat pump low pressure, kPa
P10_est: setpoint of heat pump low pressure, kPa
PB: bottom product pump
PF1: feed pump 1
PF2: feed pump 2
PR: reflux pump
P_B: column bottom pressure, kPa
P_H (PH): heat pump high pressure, kPa
P_L (PL): heat pump low pressure, kPa
P_{SP}: setpoint of column pressure, kPa
P_T: column top pressure, kPa
Q_Z,Q_U: diagonal weighting matrix in equation (5.3)
SP FM3: setpoint for bottom product pump, ton/hr

SP FM6/4: setpoint for reflux pump or top product pump, ton/hr

$u(t)$: vector of input variable

$u'(t)$: vector of input differenced variable

V: vapor flow rate, m^3/hr

Vsp: setpoint of vapor flow rate, m^3/hr

V_est: setpoint of vapor flow rate, m^3/hr

x_D : top product composition, mole fraction

x_B : bottom product composition, mole fraction

XPTT15: setpoint of composition on tray 15, mole fraction

$y(t)$: vector of output variable

$y'(t)$: vector of output differenced variable

References

Li, H. W.; Gani, R and Jørgensen, S. B. (2003), "Process-Insights-Based control Structuring of an Integrated Distillation Pilot Plant". Ind. Eng.Chem.Res., 42, p4620-4627

Brabrand, H.; Jensen, N.; Jørgensen; S. B. (1991): "MIMOSC – A Tool for Real-Time Multivariable Identification and Adaptive Control of Chemical Processes", Nordic Process Control Workshop, Copenhagen, Denmark.

Eden, M. R.; Løppenthien, C.; Skotte, R. (1999): "Distillation Column Startup Manual", Department of Chemical Engineering, Technical University of Denmark.

Hallager, L.; Toftegård, B. (1986): "A Distillation Plant with Indirect Heat Pump for Experimental Studies of Operation Form, Dynamics and Control", In Proc. of IFAC Symposium on Dynamics and Control of Chemical Reactors and Distillation Columns, Bournemouth, England.

Hangos, K. M.; Csáki, Zs.; Jørgensen, S.B. (1992): "Qualitative Model-Based Intelligent Control of a Distillation Column", Engng. Applic. Artif. Intell., Vol. 5, pp. 431-440.

Koggersbøl, A. (1995): "Distillation Column Dynamics, Operability and Control", Ph.D. Thesis, Department of Chemical Engineering, Technical University of Denmark.

Ruiz C. A.; Cameron, I. T.; Gani, R. (1988): "A Generalized Dynamic Model for Distillation Columns - III. Study of Startup Operations", Comput. Chem. Eng., 12, pp. 1-14.

Skogestad, S. (1992) "Dynamics and Control of Distillation Columns - A Critical Survey", IFAC Symposium, DYCORD 92, University of Maryland, USA.

Yasuoka, H.; Nakanishi, E.; Kunigitta, E. (1987): "Design of an On-line Startup System for a Distillation Column Based on a Simple Algorithm", Int. Chem. Eng., 27, pp. 466-472.

Yazdi, H. (1997): “Control and Supervision of Event-driven Systems”, Ph.D. Thesis, Department of Chemical Engineering, Technical University of Denmark.

Årzen, K.E. (1994): “GRAFCET for Intelligent Supervisory Control Application”, Automatica, 30(10), pp. 1513-1525.

5

Optimal Operation

Abstract *The efficiency of manufacturing systems can be significantly increased through diligent application of control based on mathematical models thereby enabling more tight integration of decision making with systems operation. In the present chapter analysis of optimal operation of energy integrated distillation plant is investigated more closely with the purpose of elucidating essential decisions behind planning experiments, which are suitable for identifying models and constraints. The basis for analysis of optimal operation is the type of operation upon which an application focuses. In this chapter the attention is on achieving close to optimal economical benefit of a continuously operating plant. The optimal operation region for the plant is visualized by the profit landscape of the example process. The nonlinear dynamic behavior within the optimal operation region is studied through bifurcation analysis. Thereafter a series of decisions have to be made concerning the experimental design for revealing the plant steady states and dynamics within the optimal operating region. However in this chapter the focus is upon revealing the possible nonlinear behaviors around the optimal operating region and their influence upon the further decisions behind the experimental design. An energy-integrated distillation column, which may exhibit fold bifurcations, is used as a relevant example process.*

5.1 Introduction

Chemical process plants usually operate at a productivity of 70-80% if one does not use advanced multivariable control. Further 10-15% can be gained if linear MPC is implemented, and a further increase in productivity is obtained if optimising and perhaps also nonlinear MPC is implemented to a plant. Maciejowski (2001)'s book provides a systematic and comprehensive study for MPC control. In a study of the Tenessee Eastman challenge problem, Ricker (1996) notes that when applying MPC, one needs to make critical decisions without quantitative justifications. This chapter attempts to address decisions related to uncovering possible nonlinear dynamic behaviours within the optimal operation region with the underlying aim of implementing optimising model predictive control. This aim will be achieved through mapping the optimal operation region and analysis of the nonlinear dynamic behaviour within this region.

5.2 Process description

The IVaRDiP, shown in Figure 3.1 (Hansen et al, 1998), contains two main parts, a distillation column section and a heat pump section. It separates a mixture of methanol and isopropanol, which contains a low concentration water impurity. The column is a sieve tray column with 19 trays. The heat pump section is physically connected to the distillation column through the condenser at the top and the reboiler at the bottom of the column. A more detailed description is available in Eden et al (2000). The model used in this chapter for bifurcation study is a simplified version of the model implemented by Koggersbøl (1995).

5.3 Profit landscape

5.3.1 The objective function

In this chapter the objective is to optimize the following profit function:

$$Profit = D \cdot c_1 + B.c_2 - B \cdot (1 - x_B) \cdot c_3 - D \cdot (1 - x_D) \cdot c_4 - V \cdot c_5 \qquad (5.1)$$

Where D is the distillate flow rate, B is the bottom product flow rate, V is the vapor flow rate and x_D and x_B is the molar fractions of methanol. The constants c_1, c_2, c_3, c_4 and c_5 are describing either the prize of methanol (in \$), isopropanol or the prize of

energy($ joule^{-1}) c_1 and c_2 are functions of the compositions of product streams. This means that the unit of the profit is $ hour^{-1}.

5.3.2 The simulation condition

For steady state of the IVaRDiP there are three degrees of freedom that relate three control variables and three actuators, which are distillate flow rate, vapor flow rate and column pressure. So the landscape of the profit is drawn as the function of vapor flow rate, distillation flow rate and column pressure for the IVaRDiP, steady state simulations is performed with the simulation program of Koggerbøl (1995). A ternary mixture of methanol, isopropanol and a little impurity water is considered to be separated in the IVaRDiP with 19 stages and the feed entering at stage 10 (counted from the bottom). Nominally, the feed contains 49.5mol% of methanol and 49.5mol% of isopropanol and is saturated liquid and the nominal feed flow rate is 0.86095 mol/.sec.

5.3.3 The simulation results

Three pressure ranges are examined, i.e. 84-88kPa, 105-109kPa and 122-129kPa named low pressure range, middle pressure range and the high pressure range. In Figure 5.1 the profit is plotted as a function of the vapor flow rate, distillate flow rate and the bottom pressure. This figure shows how the profit at different column pressure ranges varies with distillate flow and the vapor flow rate. The figure demonstrates a distinct maximum for each column pressure range. Thus an optimal operation region corresponding to optimum distillate flow rate and column pressure range is pinpointed. To compare the profits at different pressure ranges a projection onto the profit versus distillate flow rate is shown in Figure 5.1(b). This figure shows that the column pressure does not affect the profit very much at these pressure ranges.

From Figure 5.1 one can also see that distillate flow rate is the most significant optimal variable. The optimal distillate flow is between 0.35 and 0.45 (mol.sec^{-1}) for all the three pressures ranges. The profits do not change much at this optimal distillation range. But considering the operation fee and operation control the middle pressure, which is close to atmosphere pressure in the column, is a favorable optimal pressure. So far the optimal operation condition is obtained.

When using operating an integrated process it is important to know the nonlinear dynamic behavior around the optimum. If the optimum is near a bifurcation point, e.g. with an unstable branch it would be essential for any control design to understand such behavior a priori.

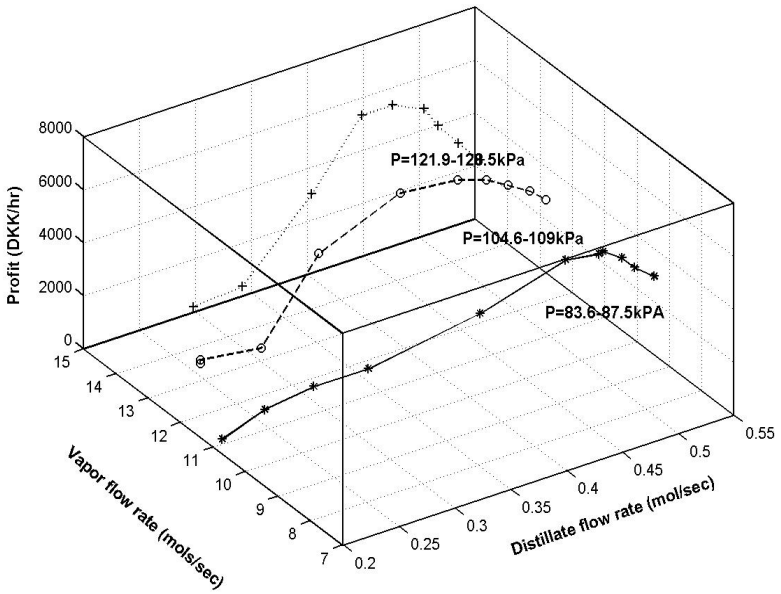

(a)

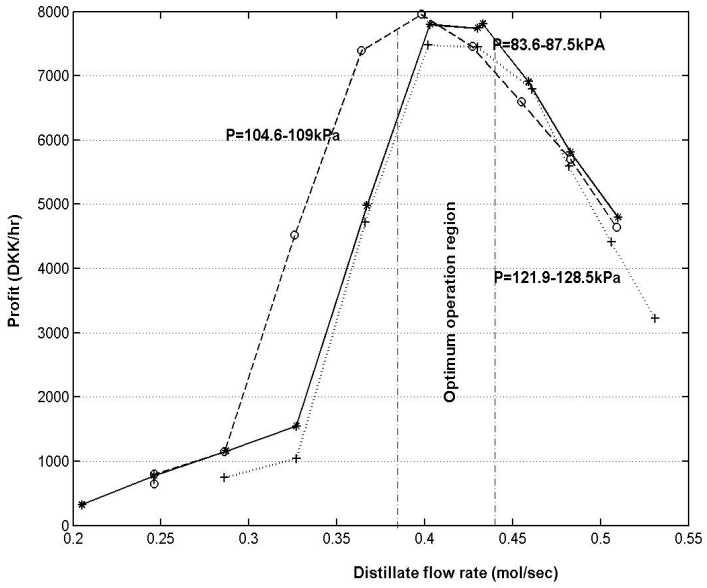

(b)

Figure 5.1: a) Landscape of profit as function of vapor flow rate and distillate flow rate at different pressure region. b) Projection onto the profit versus distillate flow rate plane

5.4 Bifurcation analysis

Knowing the position of the optimum of this IVaRDiP from the landscape movement, it is important to investigate the dynamics of the system in this area. One method is to do a bifurcation analysis of a dynamic model. Bifurcation diagrams can be used to investigate the dynamic behavior of nonlinear physical systems. A bifurcation diagram shows the changes in the dynamics of a physical system and is therefore very important in investigating integrated process systems. A two-dimensional bifurcation diagram is a map of a system variable as a function of small changes of a system parameter, where all stable and unstable states are determined and hence shown. By performing a bifurcation, or continuation analysis one can depict how the plant behaves along a branch of a single (or two) operation parameters. Given this information one can determine the location of the bifurcation points, and therefore their location relative to the optimum conditions.

Normally small changes in the bifurcation parameter produce small changes in the system dynamics. When a system reaches a bifurcation point a change in the bifurcation parameter causes the system to undergo a qualitative change. There are several different types of bifurcations. Some of the most common is the Hopf-bifurcation, the fold-bifurcation and the pitchfork bifurcation. The Hopf-bifurcation occurs in a system with two or more system variables. A system goes from a stable fix point to an unstable point by a change of sign in the real part of one of the eigenvalues. A fold bifurcation, which is a common when dealing with these types of nonlinear problems, occurs when a stable and unstable fix point meets. The values of the dependent and independent variables the bifurcation diagrams have been calculated by using the program continuation program CONT developed by Schreiber et al (2000) where the models are solved in MOT (Russel, 2000). Note that the bifurcation diagrams have been made by using the simplified model of the integrated distillation column, as described above. If optimum is close to a bifurcation point it could be necessary to operate the column at values just below the optimum. When using these methods it is important to have a good understanding of the behaviors of the system. This is due to constraints in the system that could affect the optimum or alter the positions of the bifurcation points.

From Figure 5.2 it is clear that there is a fold bifurcation point around a distillate flow rate of 0.54 mole sec^{-1}. This means that the optimum operation range is not from a possible unstable branch. Due to the relatively close location of the bifurcation point to the optimal operation range it is desirable to further investigate both the sensitivity of the optimal operation range and of the bifurcation diagram to process disturbances.

Furthermore it is most relevant to investigate the validity of the process model near and within the optimal operating region.

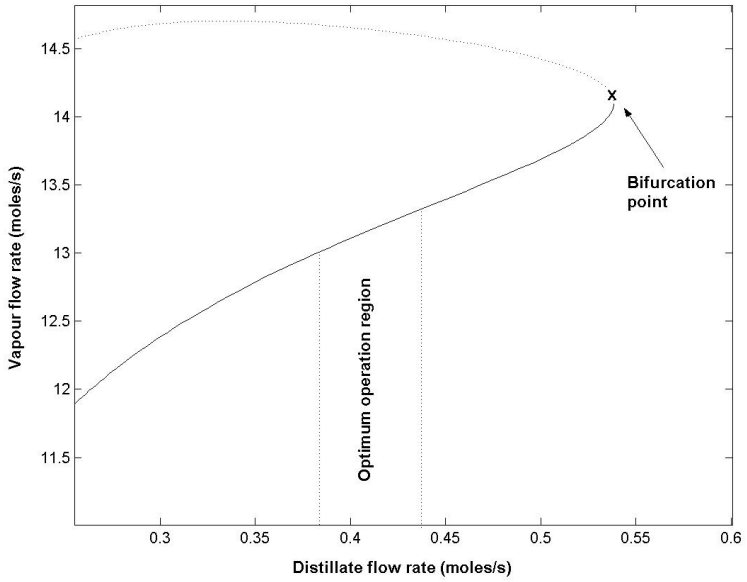

Figure 5.2: Bifurcation diagram with the distillate flow rate as bifurcation parameter

5.5 Sensitivity to disturbance

5. 5.1 Profit landscape

For this IVaRDiP the disturbances mainly come from the feed flow rate and the feed composition. The sensitivity of the optimum within the profit landscape is investigated with the existence of both disturbances at the middle pressure range, i.e. the optimal pressure. The amount and the sign of these disturbances are listed in Table 5.1.

The results are plotted in Figure 5.3 where (a) is three-dimensional figure and (b) is the projection onto the profit versus distillate flow rate plane. From Figure 5.3 we can see that the landscapes toward an increase in the distillate flow rate when both disturbances are positive

Table 5.1: List of the disturbances and landscape name

Disturbances	Feed flow rate		Feed composition		Feed flow rate and feed composition		No
Disturbance sign and amount	F↑25%	F↓25%	X_F↑25%	X_F↓25%	F↑ 12.5% X_F↑12.5%	F↑ 25% X_F↓25%	No
Landscape name	C1	C5	C2	C6	C3	C4	C

(See C1, C2 and C3). While a negative disturbance is added to the system the optimal operation point moves toward a decrease in the distillate flow rate (see C5 and C6). For C4 one may notice that with a positive disturbance in one parameter and a negative disturbance in another the landscape moves toward a decrease in the distillate flow rate. The result shows that disturbances affected the profit landscape of the IVaRDiP when the control loops are opened. Clearly also the sensitivity of the bifurcation analysis to disturbances need to be investigated.

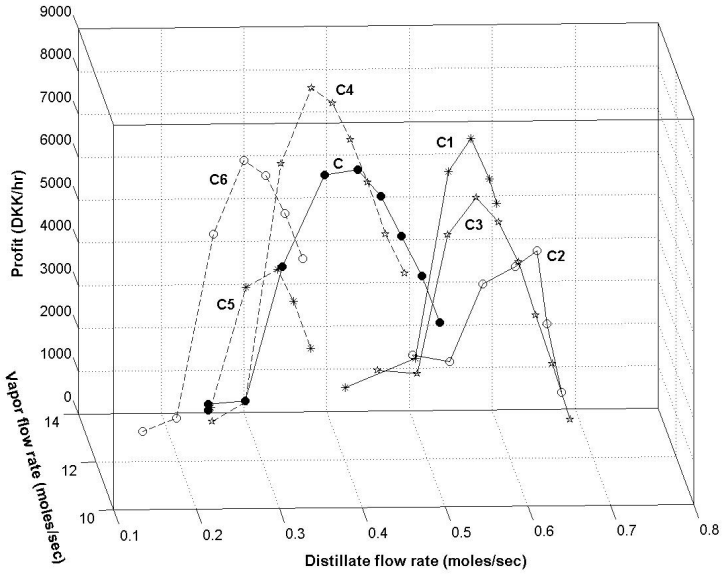

(a) Three dimensional figure

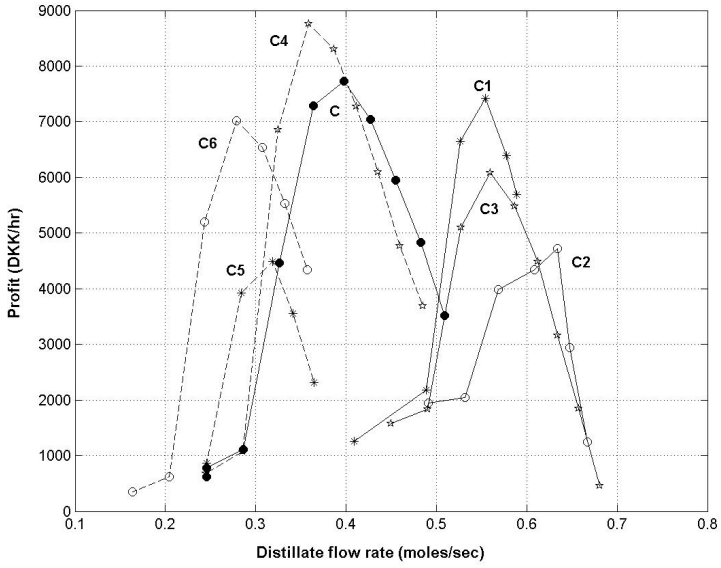

(b) Projection of profit versus distillate flow rate

Figure 5.3: Movement of the profit function with different disturbances C1-C6 explained in Table 5.1

5.5.2 Bifurcation diagram

In order to compare results bifurcation diagrams using the same step sizes as the landscapes was made. This shows if a disturbance will have the same effect on the position of the bifurcation points as it has on the optimum. The results are shown in Figure 5.4.

A positive step in both feed flow rate and feed composition results in a higher position of the bifurcation as a function with respect the distillate flow rate. But it seems that the optimum region is closer to the bifurcations. With a negative step the position of the bifurcation is at a lower value of the distillate flow rate but further from the optimum region. A positive disturbance in one parameter and a negative disturbance in another do not affect the position of the bifurcation point. Understanding the dynamic behavior around the optimal operation of this integrated distillation column an experiment design can be started.

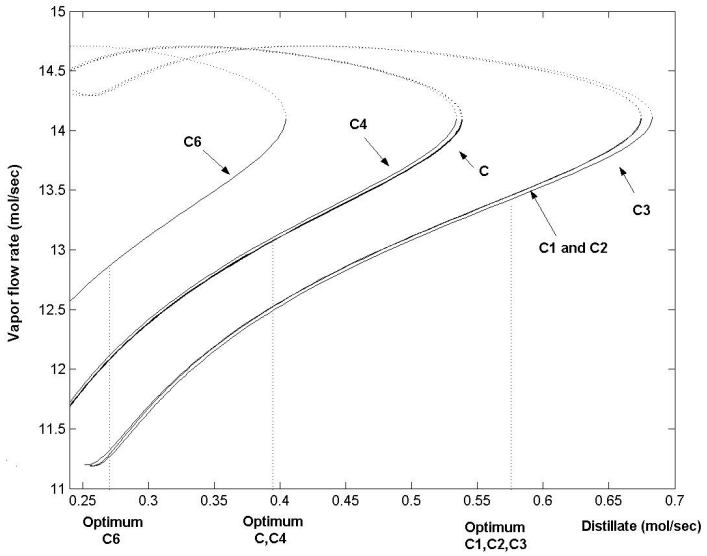

Figure 5.4: Bifurcation diagrams for the different disturbances C1- C6

5.6 Conclusions

The focus in this chapter on determining the behaviour of the optimal operation region relative to possible nonlinear behaviours for an IVaRDiP. The purpose of the investigation is to provide background information for planning experimental investigation of model performance as a pre-example to implementing model predictive control. The profit landscape is drawn for a specific profit function. Subsequently a nonlinear bifurcation analysis is carried out to reveal the possible nonlinear behaviours in the optimal operating region. The IVaRDiP reveals that a fold bifurcation is located relatively close to the optimal operating region. Thus special precautions have to be taken to verify the modelled behaviour before implementing optimising model predictive control on the actual plant.

Symbols:

D: distillate flow rate, mol/s

B: bottom product flow rare, mol/s

V: vapour flow rate, mol/s

X_D: mole fraction of the methanol in the top product

X_B: mole fraction of isopropanol in the bottom product

X_F: mole fraction of methanol in the feed

References

Maciejowski, J. M. (2001), Provide Control with Constraints, Pearson Education under the Prentice Hall imprint.

Ricker, N. L. (1996), J. Proc. Cont., 205-221.

Hansen, J. E.; Jørgensen, S. B.; Heath, J. and Perkins, J. D. (1998), J. Proc. Contr., 8, 185-195.

Eden, M. R.; Køggersbøl, A.; Hallager, L.; and Jørgensen, S. B. (2000), Comput. and Chem. Eng., 24, 1091-1097.

Koggersbøl, A. (1995), Distillation column dynamics, operability and control, Ph. D thesis, Technical University of Denmark, Denmark.

Ipsen, M. and Schreiber, I. (2000), Chaos,10(4), 791-802.

Russel, B.M.; Henriksen, J. P.; Jørgensen, S. B.and Gani, R. (2000), Comput. Chem. Eng. 24(2), 967-973.

6

Nonlinear Behavior Analysis

Abstract *The efficiency of manufacturing systems can be significantly increased through process integration combined with diligent application of control based on model analysis thereby enabling more tight integration between decision-making and process operation. The principal objective of this study is to investigate the nonlinear behavior, which is relevant for designing optimizing control of an IVaRDiP. In this chapter the nonlinear dynamic behavior is investigated in terms of a bifurcation analysis. First, a simple dynamic model capable of capturing the important non-linear behavior has been derived and solved through a computer aided modeling toolbox (ICAS-MoT). Next, the position of control valves, which plays an important role in moving the operation points around within the operation range of the integrated column, are used as bifurcation parameters to analysis open loop operation. In this chapter the focus is on revealing and understanding the possible nonlinear behaviors and their influence upon the further decisions behind the experimental design for validating the process model in the region around optimal operation. Finally, an experiment results are shown and compared with the theoretical analysis results.*

6.1 Introduction

In chemical production and refinement plants energy integration represents a significant potential for energy saving. However, the increase in complexity caused by the introduced couplings may change plant characteristics drastically and thereby have significant impact on operability and on control configuration selection for the plant. Understanding such characteristics is essential for being able to use (multivariable) control as an enabling technology to optimize the operation of chemical plants. Bifurcation analysis is to investigate the nonlinear dynamic behaviour of a process. A huge number of bifurcations have been derived and described. Examples of application oriented approaches are given by Kuznetsov (1998) and Recke et al. (2001). Some of the more common bifurcations reported within the chemical engineering in literature are fold and Hopf bifurcations. The purpose of this chapter is to develop a basic stabilizing control structure for planning experimental investigation of pilot plant performance around optimal operation condition as a first step to implementing optimizing control.

The chapter is organized as follows. A bifurcation analysis is performed on the pilot plant for operation around optimal productivity after introduction of the pilot plant and a suitable simplified model. Then the sensitivity of the fold characteristic behaviour is analyzed and a control structure to stabilize the plant is proposed and validated also using bifurcation analysis. The performance of the suggested control structure is also validated experimentally. Finally it is conducted that the operation over a large part of the operating window indeed occurs on the open loop unstable branch.

6.2 Process description and process model

The IVaRDiP, shown in Figure 3.1 (Hansen et al, 1998), contains two main parts, a distillation column section and a heat pump section. It separates a mixture of methanol and isopropanol, which contains low concentration water as impurity. The column has 19 sieve trays. The heat pump section is physically connected to the distillation column through the condenser at the top and the reboiler at the bottom of the column. Two control valves α_{CV8} and α_{CV9} control the high pressure and low pressure of the heat pump section, respectively. The values of valve coefficients of α_{CV8} and α_{CV9} determine how open the valves are. If α_{CV8} and α_{CV9} equal one then high pressure and low pressure on the heat pump are at their minimum values; otherwise, if α_{CV8} and α_{CV9} equal zero, the high pressure and low pressure reach their maximum values. A more detailed description is available in Eden et al (2000). The

model used in this chapter for bifurcation study is a simplified version of the process (Li et al, 2003), where in Figure 3.1 D is the distillate flow rate, B is the bottom product flow rate, V is the vapor flow rate and x_D and x_B are the molar fractions of methanol. The feed contains 49.5mol% of methanol and 49.5mol% of isopropanol and is saturated liquid and the nominal feed flow rate is 0.86095 mol/sec. In the model used in this chapter the reboiler and accumulator levels are assumed under perfect control.

6.3 Bifurcation analysis

Bifurcation analysis is one way to analyses the dynamic behavior of a system as a parameter is varied. A bifurcation diagram shows the changes in the dynamics of a physical system and is therefore very useful for investigating integrated dynamic behavior of a process operation. A two-dimensional bifurcation diagram is a map of a system variable as a function of small changes of a suitable system parameter, where all stable and unstable states are determined and hence shown. By performing a bifurcation or continuation analysis one can depict how the pilot plant behaves for a number of operation or uncertain parameters. Given this information one can determine the location of the bifurcation points. The bifurcation diagrams have been calculated by using the continuation program CONT (Ipsen and Schreiber, 2000) where the models are solved in MOT (Russel et al, 2000); and the values of parameters are given in Appendix C. The two-control valve openings α_{CV8} and α_{CV9} determine the operating point movement within the operation window of the heat-integrated distillation pilot plant. Hence these two parameters are selected as bifurcation parameters to investigate the nonlinear behavior of the system in this paper. In the bifurcation diagrams shown below, the solid lines denote stable stationary points and the dotted lines denote unstable stationary points. The bifurcation points are located where stable and unstable branches coalesce.

6. 3.1 Bifurcation diagrams

In this chapter the bifurcation analysis performed first with α_{CV8} as bifurcation parameter at constant α_{CV9}=0.4. The bifurcation diagrams of all the important operational variables have been determined and only the one corresponding to the vapor flow rate in the column is shown in Figure 6.1. It can be seen that the system undergoes fold bifurcations at α_{CV8}=0.38, 0.45 and 0.41 marked A, B and C, respectively. Operation on the I-A and B-C branches (solid line) in Figure 6.1 are stable while A-B and C-II branches (dotted line) are unstable. The size of the largest

real eigenvalue corresponding to Figure 6.1 is depicted in Figure 6.2 and it is seen that a single real eigenvalue crosses imaginary axis (between slightly negative and positive) at the three fold bifurcation points, where they are zoomed in so as to see clearly how the eigenvalue change their signs at their bifurcation points.

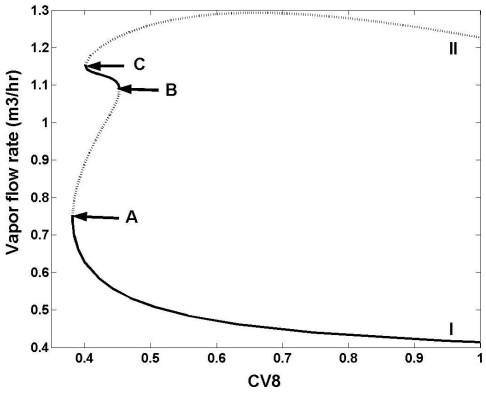

Figure 6.1 Bifurcation diagram with α_{CV8} as bifurcation parameter

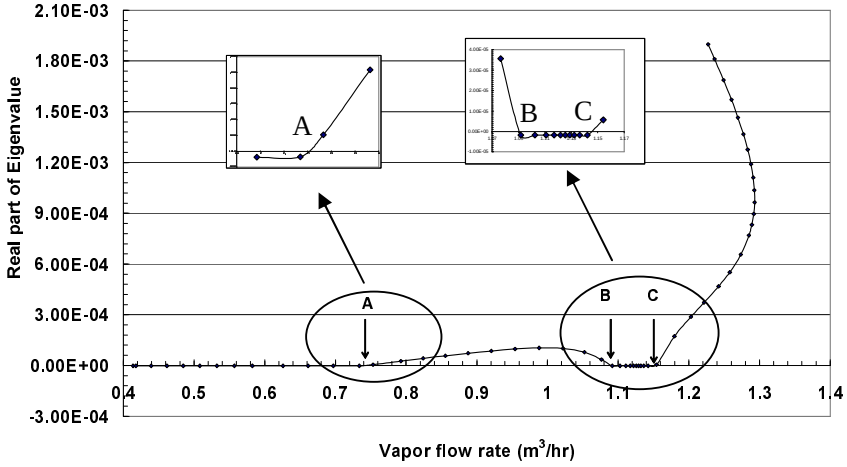

Figure 6.2: the real part of largest eigenvalue plotted as function of the vapour flow rate at constant $\alpha_{CV9}=0.4$

Concerning operation of the pilot plant described by the model it can be concluded that the feasible operation region is located on the part of low vapour flow rate when α_{CV9} is kept constant at 0.4 because the bifurcation points B and C are far beyond the high pressure safety limit (see Figure 6.3) of the distillation pilot plant.

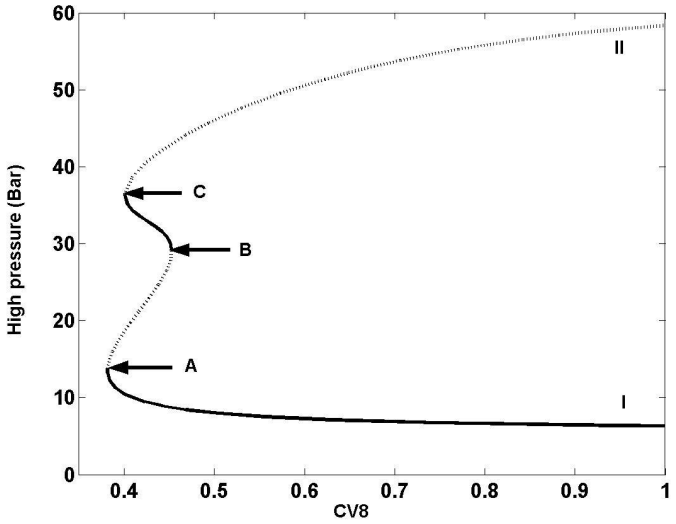

Figure 6.3: High pressure in the heat pump section. The safety limit is 16Bar

6. 3.2 Sensitivity analysis of bifurcation

The theoretical and qualitative analysis of bifurcation diagram Figure 6.1 is the following. The slope of $\partial V/\partial \alpha_{CV8}=\partial V/\partial P_H \partial P_H/\partial \alpha_{CV8}$ changes sign through infinity at bifurcation points A, B and C. It is known that both column pressure and vapor flow rate in the column are sensitive to the high and low pressures in the heat pump section, where high pressure P_H on the heat pump section has positive gain to vapor flow rate in the column (Li et al 2003), i.e. $\partial V/\partial P_H>0$. Thus the sign of $\partial V/\partial \alpha_{CV8}$ should follow the sign of $\partial P_H/\partial \alpha_{CV8,}$ which is the slope of high pressure with respect to α_{CV8} (see Figure 6.3). The total energy balance for IVaRDiP is:

$$d(M_{tot}\cdot H_{tot})/dt=F\cdot H_{feed}- D\cdot H_{top}-B\cdot H_{bot}+W_{comp}-Q_{cool}-Q_{loos} \qquad (6.1)$$

Where $M_{tot}\cdot H_{tot}$ is the total plant enthalpy, H_{feed}, H_{top} and H_{bot} is enthalpy of feed, top and bottom product, Q_{cool} is heat transfer rate out through the air coolers, and W_{comp} is work introduced by the compressor. Q_{loos} is the heat loss rate through equipment and tube surfaces. This latter term can be neglected by ensuring proper insulation of all surfaces.

When valve position α_{CV8} decreases, this will immediately affect the high pressure P_H such that P_H begins to increase. Thereby the compression work is increased, but the cooling rate will also gradually increase as the temperature gradient in the secondary

condenser and in the air coolers will increase with P_H. The increase in the high pressure affects vapor flow rate in the column, and consequently the heat pump low pressure P_L also increases when α_{CV9} is kept constant. The increased in low pressure P_L tends to reduce the compression work. If the resulting effect of P_H and P_L on W_{comp} is positive, the energy flux into the system increases further. And if the compressor work increases faster than the sum of all the outgoing heat flows, the behavior of the entire plant may become unstable, i.e. reach the bifurcation points. So the sign of $\partial P_H/\partial\alpha_{CV8}$ depends on difference between the increase of compressor work and the sum of all the outgoing heat flows.

6. 3.3 Bifurcation diagram with cascade control

From the bifurcation results in Figure 6.1 one can see that branch A-B is unstable. To compare the nonlinear behavior with and without control of the high pressure P_H, a cascade control loop is implemented, where the control valve α_{CV8} now controls the high pressure P_H, the set point of which is given by the vapor flow control loop. The bifurcation analysis is repeated, but now with the vapor flow rate set point as a bifurcation parameter shown in Figure 6.4.

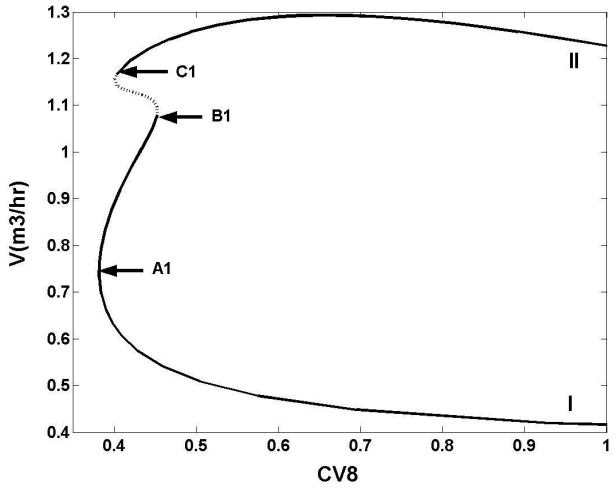

Figure 6.4: Bifurcation diagram with the cascade control: $\alpha_{CV8} \rightarrow P_H \rightarrow V$(where Kp=4, $K\alpha_{CV8}$ =-4)

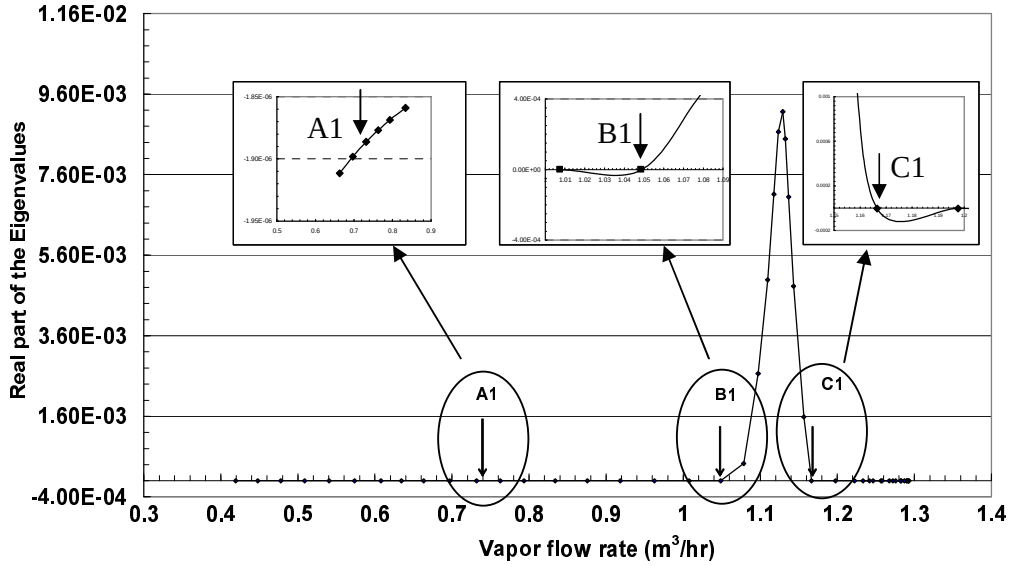

Figure 6.5 The real part of the largest eigenvalue platted as a function of the vapor flow rate at constant α_{CV9}*=0.4 with cascade control implemented (*$\alpha_{CV8} \rightarrow P_H \rightarrow V$*)*

Comparing Figures 6.4 and 6.1 it can seen that the branches A1-B1 and C1-II become stable (solid line) while B1-C1 becomes unstable (dotted line) when the cascade control loop is implemented. The largest real eigenvalue corresponding to Figure 6.1 is shown in Figure 6.5 where the branch B1-C1 is much further into the right half plane than branch A-B in Figure 6.2. This means that the cascade controller indeed ensures the stability of the process within the feasible operating region. The performance of this cascade control loop is shown in Figure 6.6 and 6.7, where Figure 6.6 shows the high pressure to α_{CV8} and Figure 6.7 shows the vapor flow rate to high pressure to high pressure.

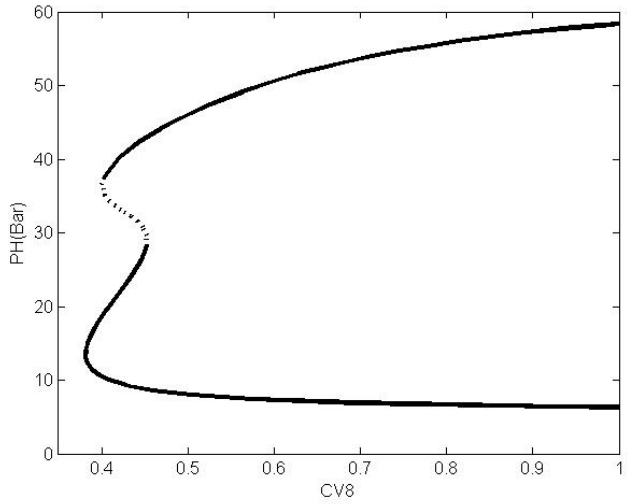

Figure 6.6 High pressure to α_{CV8} with cascade control implemented ($\alpha_{CV8} \rightarrow P_H \rightarrow V$)

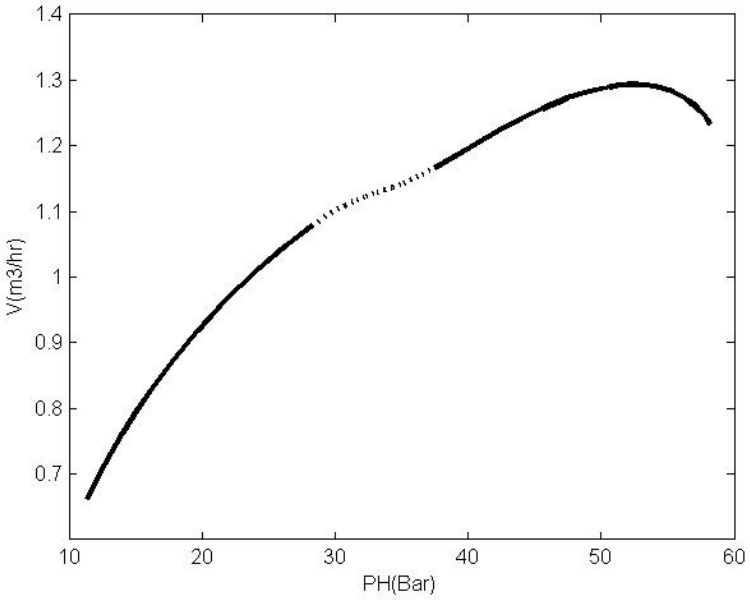

Figure 6.7 Vapor flow rate to high pressure with cascade control implemented ($\alpha_{CV8} \rightarrow P_H \rightarrow V$)

The next step is to tune the cascade control loop, i.e. the value of Kp and $K\alpha_{CV8}$ are changed in the cascade control loop, where Figure 6.8 and 6.9 show the results with Kp=30 and $K\alpha_{CV8}$ =-30 compare to the original values, i.e. Kp=4 and $K\alpha_{CV8}$ =-4.

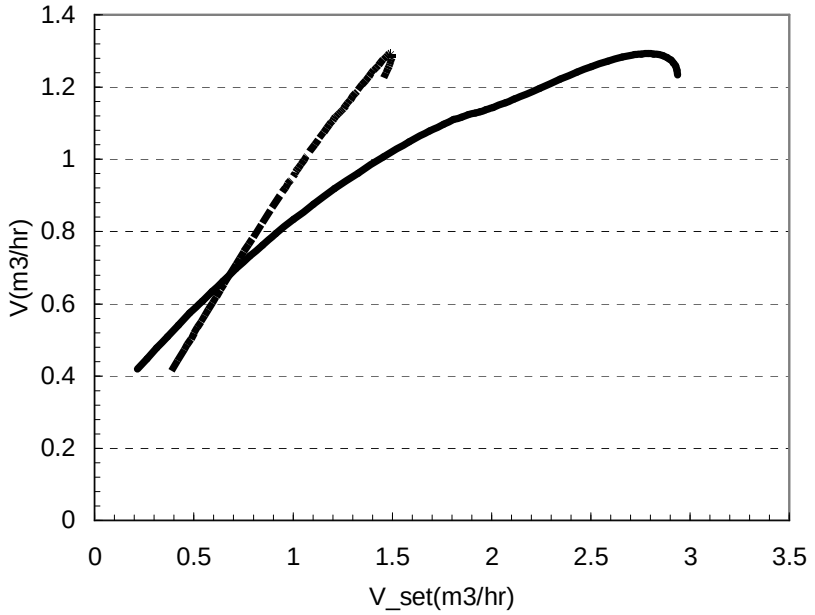

Figure 6.8 Vapor flow rate to setpoint of the vapor flow rate. The solid line is at Kp=4 and $K\alpha_{CV8}$ =-4. The dotted line is at Kp=30 and $K\alpha_{CV8}$ =-30

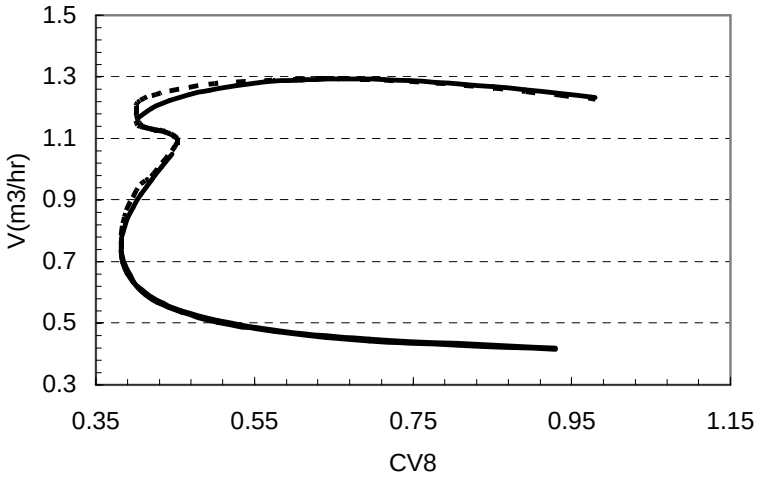

Figure 6.9 Vapor flow rate to α_{CV8}. The solid line is at Kp=4 and $K\alpha_{CV8}$ =-4. The dotted line is at Kp=30 and the $K\alpha_{CV8}$ =-30

From Figure 6.8 and 6.9 one can see that while tuning the cascade controller, the vapor flow rate does not change much, but less bias between setpoint of the vapor flow rate and the vapor flow rate.

6.3.4 Sensitivity investigation for α_{CV9}

The sensitivity of the bifurcation diagram to α_{CV9} shown in Figure 6.10 shows that the vapor flow rate increases as valve α_{CV9} open from 0.4 to 0.5 with the above cascade control loop implemented. Consequently the low pressure P_L will decrease. This is in agreement with the finding that the low pressure P_L has negative gain to column vapour flow rate (Li et al, 2003).

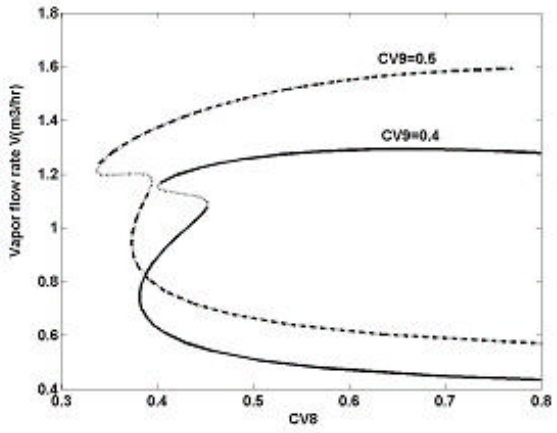

Figure 6.10: Bifurcation diagram V as α_{CV8} sensitivity to α_{CV9} with cascade control ($\alpha_{CV8} \rightarrow P_H \rightarrow V$)

6.3.5 Sensitivity to heat transfer in the reboiler and condenser

The sensitivity of two uncertain parameters, i.e. heat transfer coefficients in the reboiler and condenser is investigated with the same cascade control loop closed. The results of different heat transfer coefficients in the reboiler are shown in Figure 6.11. Clearly the bifurcation curves are somewhat sensitive to the reboiler heat transfer coefficient..

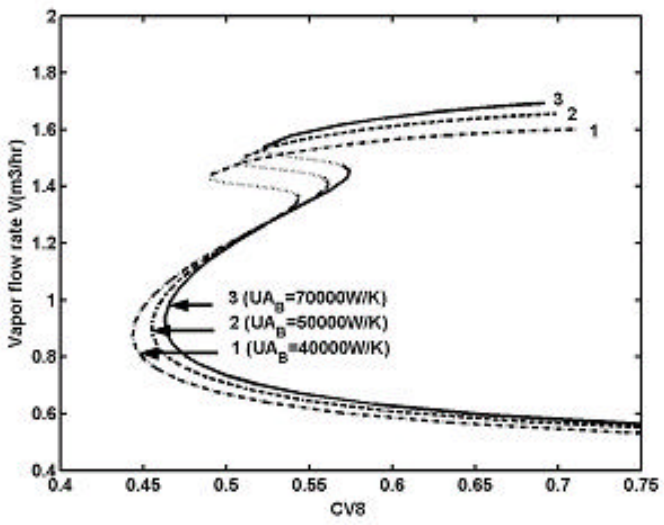

Figure 6.11: Sensitivity to UA_B with cascade control loop ($\alpha_{CV8} \rightarrow P_H \rightarrow V$)

6.4 Experimental validation

6.4.1 Experimental design

To validate the nonlinear analysis an experiment that uses the suggested cascade control structure to permit operation also on the open loop unstable branch of the theoretical bifurcation diagram.

The experiment consisted of three phases. Steady state flow data for phases B & C is shown in the Table 6.1. During phase B the plant is started up subsequently. Plant is operated with control of column composition at tray 15 with constant setpoint $X_{15,sep}$=0.75 while the boil-up flow rate is varied from 1.09 m^3/hr down to 0.538 m^3/hr in six steps. At each boil-up operation achieving steady-state conditions is attempted. During phase B the column pressure is controlled at the column top P_T=100kPa. During phase C column pressure is controlled at the column bottom P_B=103kPa, which corresponds to the actual bottom pressure during the previous steady state (SS6). Thereafter boil-up is increased also in sex steps while steady state conditions are attempted achieved. In average operation during 1-15 hours are necessary to obtain near to steady state operation. At each steady state data was collected for about 2 hours to obtain solid statistical information. At the end of this period samples are collected of feed and product steams for off-line analysis. A more detailed description of the control structure is given in

Table 6.1: Experiment IV with F=0.12±0.0004

Name	Steady state time(hr)	P_1(Top) (kPa)	P_3(Bot)	V (m^3/hr)	F (ton/hr)	D (ton/hr)	B (ton/hr)	L (ton/hr)
SS1	1.5	100		1.09	0.120	0.0349	0.085	0.827
SS2	1.5	100		0.981	0.120	0.0349	0.085	0.742
SS3	1.5	100		0.868	0.120	0.0353	0.085	0.647
SS4	1.5	100		0.739	0.120	0.0353	0.085	0.552
SS5	1.5	100		0.661	0.120	0.0343	0.086	0.484
SS6	1.5	100		0.538	0.120	0.0342	0.086	0.392
SS7	1.5		103	0.536	0.120	0.0339	0.086	0.390
SS8	1.5		103	0.660	0.120	0.0344	0.086	0.483
SS9	1.5		103	0.738	0.120	0.0344	0.086	0.553
SS10	1.5		103	0.860	0.120	0.0344	0.086	0.646
SS11	1.5		103	0.979	0.120	0.0340	0.086	0.744
SS12	1.5		103	1.083	0.120	0.0340	0.086	0.823

6.4.2 Experimental results and discussion

The dynamic behavior of vapor flow rate, control valve α_{CV8} and control valve α_{CV9} during the experiment are shown in Figure 6.8, Figure 6.9 and Figure 6.10. The state states from 1 to 6 are top pressure control, where the vapor flow rates are decreased from 1.09 to 0.538 m^3/hr. The state states from 7 to 12 uses bottom pressure control, where the vapor flow rates are increased from 0.536 to 1.083 m^3/hr shown in Figure 6.12. The dynamic behavior of control valve α_{CV8} and α_{CV9} are shown in Figure 6.13 and Figure 1.14, where one can see that the valves opening are decreased according to decreasing of the vapor flow rate from steady state 1 to 6 and increased according to the increase of the vapor flow rate from steady state 7 to 12. It is also clear that α_{CV8} is used with higher frequency than α_{CV9}. This observation agrees with the low frequency of α_{CV9}, which is a relatively slow moving butter flow valve while α_{CV8} is a primitively operated three way valve, which controls the ration between the bypass water flow and air cooler.

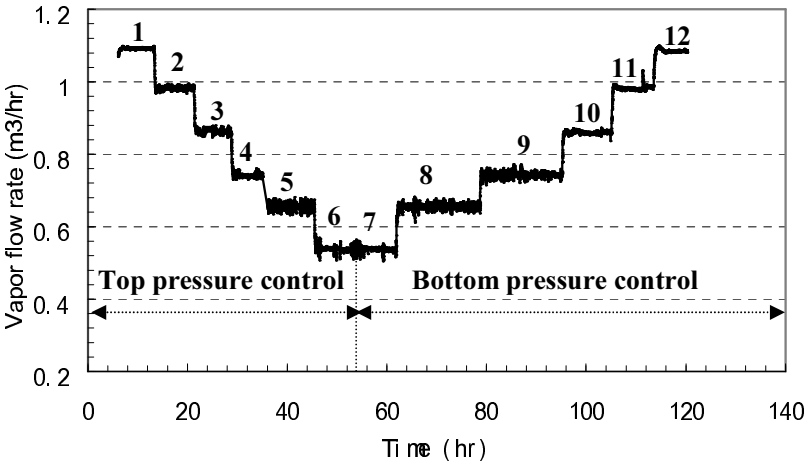

Figure 6.12: Vapor flow rate during the experiment

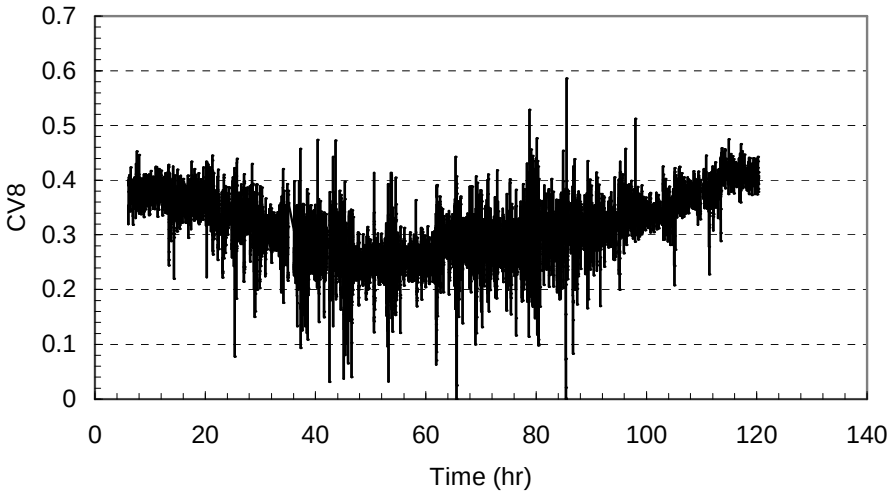

Figure 6.13: Dynamic behavior of control valve α_{CV8} during the experiment

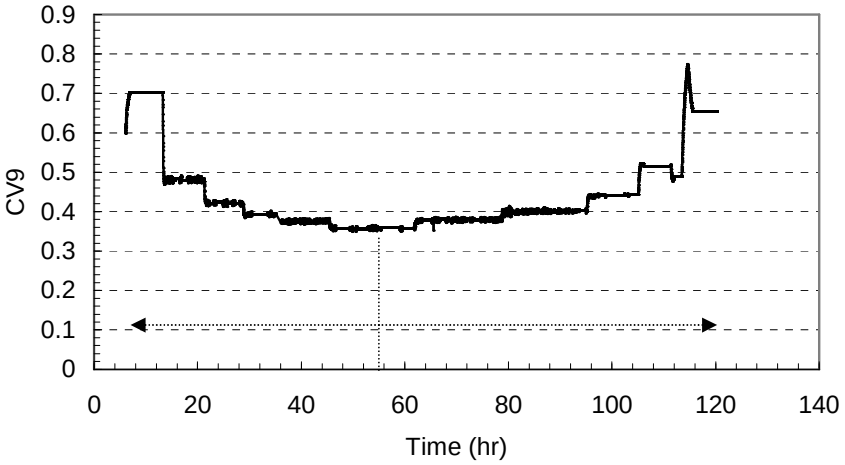

Figure 6.14: Dynamic behavior of control valve α_{CV9} during the experiment

The experimental steady state and theoretical data related to the V_{est}, α_{CV8} & α_{CV9} bifurcation diagram are shown in Figure 6.15 in which the theoretical projections is shown with 0.4 of α_{CV9}. The projections of the experimental data on vapor flow rate and control valve α_{CV8} and α_{CV9} are shown in Figure 6.16 and Figure 6.17.

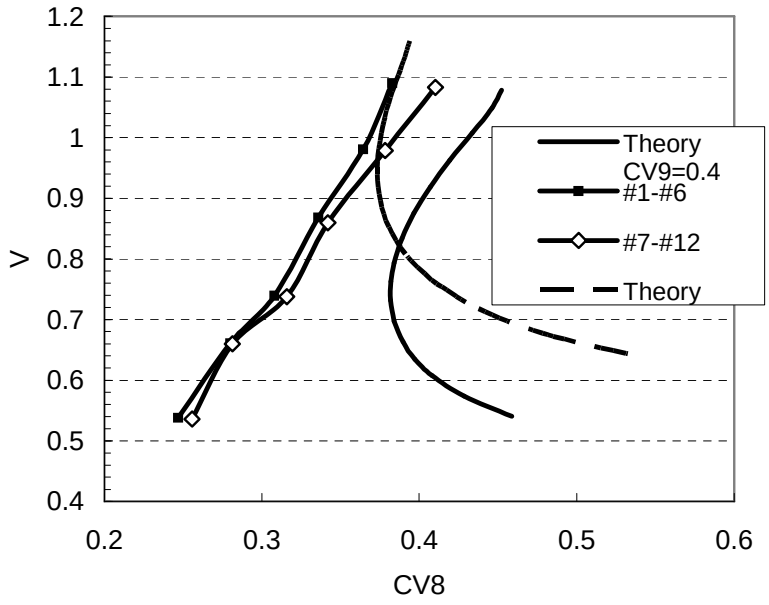

Figure 6.15: Projection of experimental data (with α_{CV9} as shown in Figure 6.16) compared to theoretical data with α_{CV9}=0.4 and with α_{CV9}=0.5

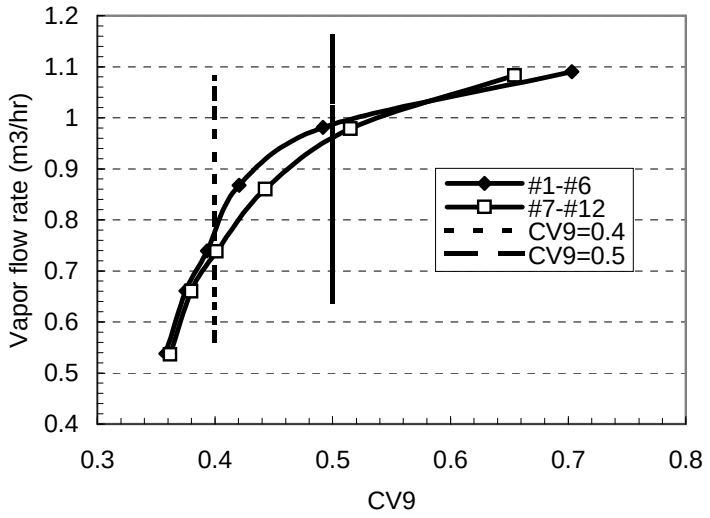

Figure 6.16: Projection of experimental data (with α_{CV8} as shown in Figure 6.15) of the vapor flow rate versus control valve α_{CV9}. The theoretical vapour flow rate for constant α_{CV9}=0.4 and 0.5 are also shown.

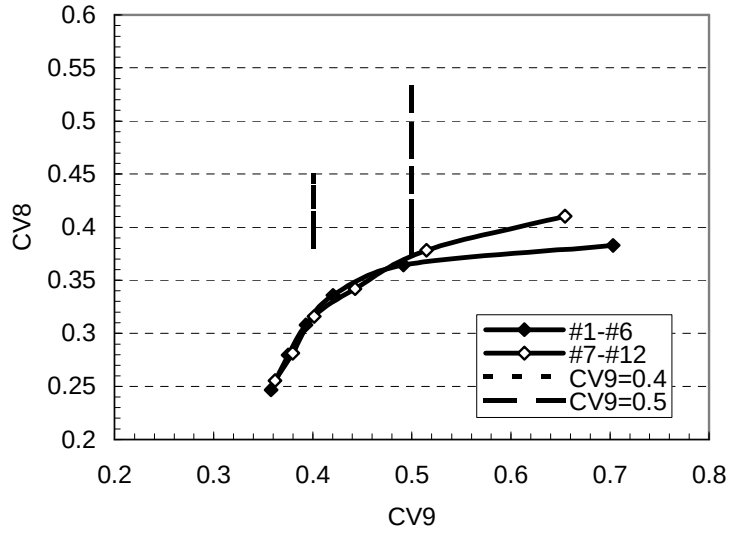

Figure 6.17: Experimental data for the control valve position α_{CV8} versus control valve position α_{CV9}. The theoretical α_{CV8} for α_{CV9}=0.4 and 0.5 are also shown

From Figure 6.15 one can see that the experiment was carried out around the open-loop unstable region, which was stabilized by the cascade loop. The experimental figures show the same trend as the theoretical analysis. The experiment results showed that when both control valves α_{CV9} and α_{CV8} increased, the vapor flow rate in

the column increases, thereby confirming that the plant operates on the open loop unstable surface of a three dimensional bifurcation diagram V (α_{CV8} & α_{CV9}).

Clearly the fold bifurcation is not passed when both α_{CV8} and α_{CV9} varies. In stead the plant operates on the open loop instable surface of the three dimensional bifurcation diagram V (α_{CV8} & α_{CV9}).

Further experiments at higher vapour flow rates are required to get closer to determine the location of the fold bifurcation in the pilot plant. Clearly the precise location of the fold also will depend upon the model approximation while modelling heat transfer in the condenser and especially the rebloiler.

However even with the relatively simple model applied in these study operation on the open loop instable branch over a large part of the operating window is confirmed.

6.5 Conclusions

A nonlinear analysis has been performed on an IVaRDiP to reveal possible complex behaviours. Based upon a relatively simple model a bifurcation analysis shows that a fold bifurcation may be encountered within that feasible operating window. A significant part of the operation would be expected to occur on the unstable branches (or surface) of the bifurcation analysis. Therefore a cascade control structure to stabilize the plant is proposed and investigated. It is shown that special precautions have to be taken before implementing optimising model predictive control on the actual plant. Based on this analysis, a sequence of experiments involving the distillation pilot plant has been planed to validate the model and the plant performance in the operation region.

The nonlinear analysis results are validated through investigation of an extensive experimental. It is demonstrated that operation indeed occurs on the open loop unstable surface of the V (α_{CV8}, α_{CV9}) bifurcation diagram. However the most precise location of the fold bifurcation requires experiments at higher vapour flow rates.

Symbols:

B: bottom product flow rate, ton/hr
CV8: the same as α_{CV8}
CV9: the same as α_{CV9}
α_{CV8}: the value of control valve 8
α_{CV9}: the value of control valve 9
D: top rodust flow rate, ton/hr
F: feed flow rate, ton/hr
H_{feed}: enthalpy of feed, kJ/ton
H_{bot}: enthalpy of bottom product, kJ/ton
H_{top}: enthalpy of top product, kJ/ton
H_{tot}: total enthalpy, kJ/ton
K_P, $K\alpha_{CV8}$: the gains of the cascade controller
M_{tot}: total mass hold up, ton
P_B: column bottom pressure, kPa
P_H: heat pump high pressure, kPa
P_L: heat pump low pressure, kPa
P_T: column top pressure, kPa
Q_{cool}: heat transfer rate through air cooler, kJ
Q_{lost}: heat lost, kJ
UA_B: heat transfer coefficient in the reboiler, W/K
V: vapour flow rate, m3/hr
$X_{15,set}$: set point of methanol molar fraction on tray 15

References

Eden, M. R., A. Koggersbøl, L. Hallager and S. B. Jørgensen (2000), Comp. and Chem. Eng.1091-1097, 24.

Guckenheimer, J. and P. Holmes (1983), Springer Serious in Applied Mathematical Sciences. Springer Verlag, 42, New York.

Hansen, J., S., B. Jørgensen, (1998), Heath and J. D. Perkins, J. Proc. Contr. 185-195,8

Ipsen, M. and I. Schreiber, (2000), Chaos, 791-802, 10(4).

Wiggins. S. (1990), Introduction to Applied Non-linear Dynamical Systems and Chaos.
Springer-Verlag, New York

Kuzetsov, Y. A. (1998), Elements of Applied Bifurcation Theory. Springer-Verlag, Inc.
New York.

Li H. W., R. Gani and S. B. Jørgensen (2003), Ind. Eng. Chem. Res. 4620-4627, 42.

Recke, B and S. B. Jorgensen, (2001), Adv. Contr. Chem. Proc. 569-74, 2.

Russel, B.M., J. P. Henriksen, S. B. Jørgensen and R. Gani (2000), Comp. Chem. Eng. 967-973, 24(2).

7

Operating Pressure Sensitivity of Distillation - Control Structure Consequences

Abstract *The influence of pressure variations upon distillation operation appears not to be well understood in the open literature, as contradicting statements concerning the importance of pressure control on binary distillation are found. In order to minimize energy consumption it is recommended to operate columns at minimum pressure; however, even if column pressure is controlled, instability may still occur when both product purities are controlled in a decentralized control structure. In this chapter operating pressure sensitivity is classified according to the pressure sensitivity of the vapour-liquid equilibrium (VLE) relationship for the mixture being separated. Operating pressure sensitivity is shown to become significant at high internal flow rates. It is furthermore shown that this sensitivity may lead to a situation where different values of internal flow rate may produce the same product purity, which commonly is labeled "input multiplicity" of the separation. This input multiplicity is shown to occur through a theoretical analysis combined with simulation of the case study and an extended series of experiments. The input multiplicity can be explained by two opposing effects from varying internal flow; the first comes from the well-understood effect of changing the slope of the operating lines, while the second is due to the effect of pressure VLE relationship. Understanding the input multiplicity or rather the pressure sensitivity is relevant for efficient exploitation of the separation capacity of the column through proper control structure selection, i.e. for where to place sensors in a distillation column for controlling pressure. It is shown that the distillation column is most efficiently utilized through controlling pressure at*

the column bottom/top for a negative/positive pressure sensitive mixture. It is furthermore concluded that controlling column pressure at the proper end of the column may be crucial to column stability when both product purities are controlled in a decentralized control structure. In an experimental verification it is demonstrated that for separating a mildly negative pressure sensitive mixture the distillation column separation capacity is most efficiently exploited when controlling column pressure at the bottom of the distillation column. For the investigated mixture it is shown that a 20 % higher capacity may be obtained at slightly lower energy expenditure. Thus a significantly (20%) lower energy expenditure per produced unit, is realized through the improved control structure when compared to conventional control of column pressure at the top of the distillation column.

7.1 Introduction

Distillation is by far the most widely used industrial separation technique. To ensure reliable operation of distillation columns a number of variables need to be maintained ideally through application of a suitable control structure where different measurements are paired with relevant actuators. Among the variables to be controlled column pressure is most often listed. The design pressure for distillation is usually determined through analysis of the possibilities for process integration, i.e. to ensure the most efficient exploitation of the available process integration. Pressure sensitivity is thus being exploited regularly in design of distillation sequences, such as in the Linde column system where distillation at two different pressures is employed to achieve thermal integration and also to circumvent azeotropic distillation by eg. increasing pressure. However as already stated by Chin (1979) there is a need for better understanding of distillation pressure control. However little attention has been given to distillation column operating pressure sensitivity in the otherwise vast literature on distillation dynamics (Tolliver and Waggoner (1980) and Skogestad (1992)). Buckly, Luyben and Shunta (1985) claims that most columns do not need tight pressure control and that sometimes it may even be undesirable because sudden changes in column pressure (presumably induced by the operator) may result in either flooding or weeping. On the other hand both Shinskey (1984) and Deshpande (1985) state that column pressure should be controlled in order to avoid sudden rise or fall of pressure, which could result in flooding or weeping if the column is operated near these limits. Additionally, they state, that pressure should be constant such that temperatures can be used to infer composition and because pressure significantly affects the separation capability of the column. Shinskey (1984), however, also suggests to operate distillation columns with a floating pressure to enable minimizing the pressure in order to minimizing energy expenditure. It must be noted that Shinskey (1984) also remarks that this scheme cannot be recommended for certain plants without being more specific.

Column pressure should clearly be observed and controlled carefully when operating near flooding or weeping limits as noted above. This statement is valid for columns operated both with and without composition control. In the following, however, it is shown that tight control of column pressure may be desirable regardless of closeness to flooding or weeping limits. The reason for this necessity is that the relative volatility of the components may be sensitive to pressure. And since the column actuators both affect column pressure as well as the internal flowrates the column separation capability may be more effectively exploited if pressure is

controlled in the proper column end, dependent upon the pressure sensitivity of the mixture being separated.

The purpose of this chapter is to investigate the sensitivity of distillation performance to operating pressure. The implication of this sensitivity upon control structure selection is investigated. First pressure sensitivity for a mixture to be separated is defined. Then an analysis of pressure sensitivity of distillation performance is presented. Here it is argued that for certain mixtures input multiplicity may arise at high internal flow rates. An experimental pilot plant is presented where the input multiplicity first analyzed using simulation and then demonstrated during extensive experiments. The implications of pressure sensitivity upon control structure selection is analyzed and also demonstrated experimentally. The consequence of controlling pressure in the proper end of a distillation column is shown to be a higher capacity and better utilization of the separation potential in the column.

7.2 Methods

7.2.1 Classification of operating pressure sensitivity

Distillation performance is sensitive to the operating pressure. This sensitivity may be investigated through evaluation of the separation factor, which for a binary zeotropic mixture is defined as $S = (y_D/(1- y_D))/(x_B/(1- x_B))$. For pressure sensitive mixtures assuming that constant relative volatility applies then two main types of pressure sensitivity may be defined: A mixture that has $\partial\alpha/\partial P<0$ is said to exhibit negative pressure sensitivity; while a mixture with $\partial\alpha/\partial P>0$ exhibits positive pressure sensitivity. For a negative pressure sensitive mixture, when pressure increases, the separation factor decreases.; while for the positive pressure sensitive mixture the separation factor increases when pressure increases. It will later be shown that for these two system types different decentralized control structures should be used to control pressure in order to exploit the column separation capability most efficiently. Concerning the occurrence of the two types of pressure sensitivity then most of nearly ideal separations belong to the negative pressure sensititive type. However it is interesting to note that if a system has a pressure sensitive azeotrope then both the above two types of pressure sensitivity can be relevant with one on each side of the azeotropic point in the equilibrium diagram until the azeotrope disappears at some pressure. Which dependence will be present in a distillation column thus depends

upon the feed composition relative to the azeotropic composition. Examples of such systems are ethanol-water and isopropanol-water where the azeotrope disappears at higher pressure than atmospheric however with lower relative volatility that present at lower pressures.

7.2.2 Systematic model analysis

Operating pressure affects the separation factor as presented above. At the same time, other variables affect the separation factor, in particular the boil up flow rate. For a negative pressure sensitive system, where separation improves with decreasing pressure, assuming that the column pressure is allowed to float, then an increase in the heat input to the reboiler (keeping all other inputs constant) gives rise to two opposing effects. The effect of slope sensitivity of the operating line may be visualized in a McCabe-Thiele diagram, to give better separation as illustrated in Figure 7.1 (Andersen (2002)). It can been seen here that a saturated liquid feed mixture of composition z_F is separated into two products of composition x_D and x_B. As the vapour flow rate is gradually increased, the slopes of the operating lines approach the diagonal, thus resulting in fewer ideal equilibrium stages necessary to obtain the specified purities. The second effect of equilibrium curve sensitivity is that of increased pressure due to higher internal flow rates, which for negative pressure sensitive mixtures including the one investigated experimentally below flattens the equilibrium curve. This second effect yields a more difficult separation as the relative volatility is decreased for the case illustrated in Figure 7.2.

At low to moderate vapour flow rates an increase in the heat input to the reboiler will give better separation since the operating line sensitivity is dominating. However in search for still higher bottom purity a point will be reached where the operating line is not improved significantly, while column pressure is increased. The equilibrium curve sensitivity may then dominate the operating slope sensitivity such that the separation factor decreases with increasing internal flow rate for a negative pressure sensitive mixture. Hence for two different internal flow rates located on either side of maximum separation the same separation factor (or purity) may be achieved thus leading to input multiplicity, ie. that the same output property, here separation factor may be achieved for different values of the input, ie. the reflux flow rate.

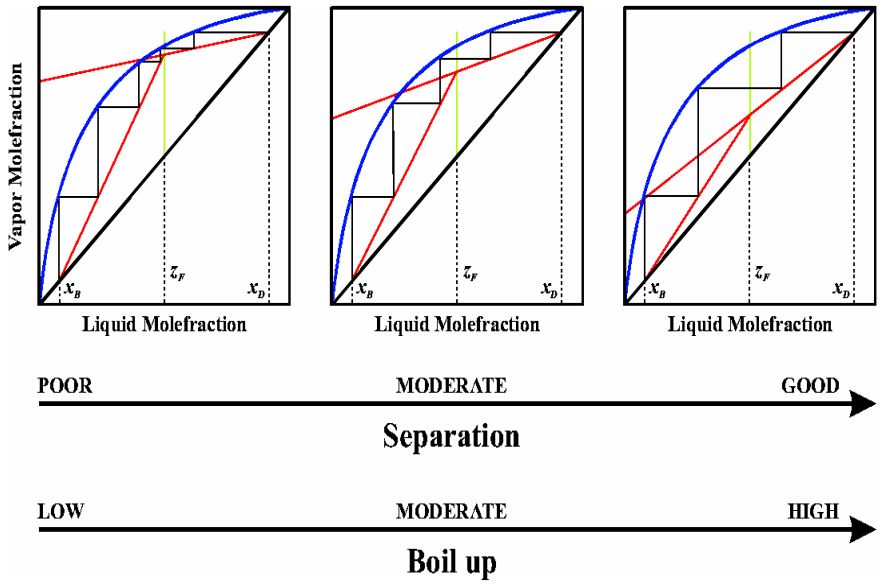

Figure 7.1: Boil up affects the slopes of operating lines visualized in a McCabe-Thiele diagram

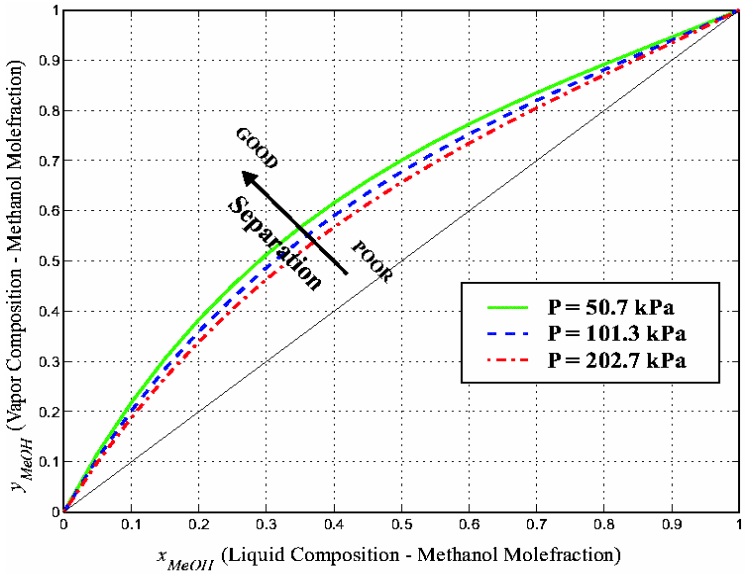

Figure 7.2: Pressure effects on the methanol-isopropanol vapour – liquid equilibrium.

The above analysis was carried out for the separation factor simply because this is most directly compared if a column is operated with a fixed concentration somewhere along the columns length. However the dependence of the top (or bottom) purity would be similar to what is shown for the separation factor above. Following the same arguments as for the separation factor then the top purity dependence of an increasing reflux flow rate will be an increasing function until the working line is almost diagonal then the pressure effect will start to dominate for further increasing reflux flow rate, which for a negative pressure sensitive mixture will lead to a decreasing top purity. These two effects in combination mean that the first term in the sensitivity factor $y_D/(1- y_D)$ is a convex function of the reflux flow rate. Similarly the second term in S also will be a convex function of the reflux flow rate. Since the product of two convex functions also is convex the separation factor indeed is a convex function of the reflux flow rate. This means that if an input multiplicity occurs in the purity then this also will be the case for the separation factor. However the location of the maximum separation factor compared to the maximal purity will depend upon the particular separation. This may be illustrated by differentiating the separation factor with respect to the molar reflux flow rate:

$$\frac{\partial S}{\partial L_M} = \frac{1-x_B}{(1-y_D)^2 x_B}\frac{\partial y_D}{\partial L_M} + \frac{y_D}{x_B^2(1-y_D)}\left(-\frac{\partial x_B}{\partial L_M}\right) \tag{7.1}$$

Thus only for a symmetric separation where the two purity derivatives are numerically equal will the location of the maximum separation factor ($\partial S / \partial L = 0$) and the purity maxima coincide. For non-symmetric separations the maximal separation factor will lie between those of the two-purity extreme. The precise location of the maximum separation factor depends upon the properties of the separation and upon the pressure profile imposed upon the column through the selected operation policy. This aspect will be further studied using simulation of the specific case study.

7.2.3 Description of experimental distillation pilot plant

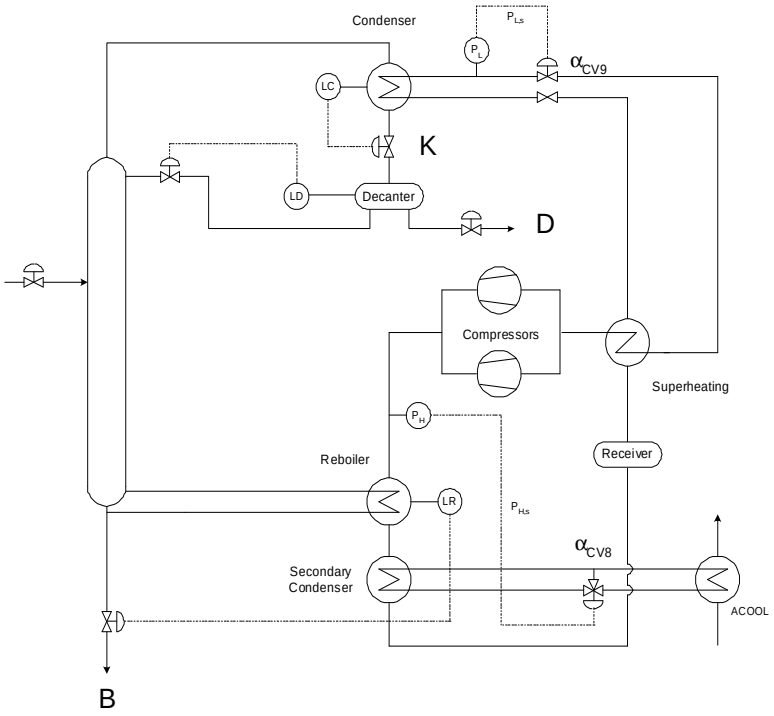

Figure 7.3: Flow sheet for the IVaRDiP with basic control loops

Figure 7.3 shows the flowsheet of the Indirect Vapor Recompression Distillation pilot Plant (IVaRDiP) suitable for separating a mixture of methanol and isopropanol with a little water impurity. The plant consists of a distillation column, a thermosiphoon reboiler, a total condenser and a reflux drum. The 0.45 m diameter column has 19 sieve trays with 8 mm holes. In order to reduce energy consumption, the reboiler and condenser are energy integrated through a heat pump. The heat pump transfers the energy released from the condenser to the reboiler. The experimental facility is located at the Department of Chemical Engineering at the Technical University of Denmark.

On trays 1, 5, 10, 15 and 19 PT100 temperature sensors are located in the gas-liquid spray. In combination with pressure measurements (located in the column bottom, on tray 10 and in the column top) the temperature measurements are suited for concentration estimates. All flows in and out of the system and the reflux flow rate are measured on a mass basis using Corioli flowmeters from experiment II and onwards. Feed, bottom product, and distillate are sampled manually at each steady state for later gas chromatographic analysis.

The heat pump has an expansion valve (Exp. Valve) which throttles high pressure liquid heat pump fluid to a lower pressure (P_L) suitable for evaporation in the condenser, which on the heat pump side works as a flooded boiler using the flow rate though the expansion valve as an actuator in a mechanical loop. After the condenser there is a control valve (CV9) by which the heat pump fluid vapour flowrate can be manipulated. After superheating the vapour the compressors elevates pressure to a higher value (P_H) suitable for condensation in the reboiler. A small part of the condensation takes place in a secondary condenser, which by a cooling water circuit is connected to a set of air coolers. The cooling rate can be manipulated by the control valve CV8, thus used to control P_H. Through storage tank (Rec) and the super heater heat exchanger the heat pump fluid circuit is closed at the expansion valve.

The additional basic control loops are: The accumulator level is controlled by reflux flow rate L and reboiler level is controlled by bottom product flow rate B. The column pressure and column vapour flow rate are controlled by a Multivariable Control (MIMOSC) which coordinates the two heat pump pressure control loop setpoints $P_{L,set}$ and $P_{H,set}$. The concentration profile is retained in the column by maintaining the estimated composition on tray 15 at x_{15}=0.75 by manipulating distillate flow rate D.

7.2.4 Pressure sensitivity

The pressure sensitivity of a distillation column may be analysed through simulation where different pressure profiles are induced using a particular operating policy, eg. through control. An investigation to illuminate this point is carried out for the IVaRDiP and illustrated in Figure 7.4 using the model of Li et al (2003), where different pressure profiles are imposed through the column operation policy. On the IVaRDiP this is achieved through selection of suitable combinations of P_L,set and $P_{H,set}$ with the level control loops closed. Thereby the reflux flow rate is varied as shown in Figure 7.4 while the top pressure is varied such that three cases result with different top pressure variations as shown in Figure 4b. Thus the top pressure is kept nearly constant, increases with 10 kPa and increases with 15 kPa as the reflux flow rate is increased from 10 to 28 L/min. Figure 4a clearly shows that, as the operating pressure is increased the separation factor for the simulated case develops a maximum around a reflux flow rate of 18-20 L/min thereby revealing the possibility for the occurrence an input multiplicity. The investigation also reveals that the selection of a control strategy for pressure may have significant impact upon the possible occurrence of input multiplicity of the separation factor.

The temperature profile in a distillation column is closely related to the pressure profile. For the IVaRDiP this relationship in the nearly binary distillation column may illustrated using the elastic mechanical analog shown in Figure 7.5 (Koggersbøl et al.[9]). Here the column is balanced between temperatures corresponding to the selected heat pump pressures $P_{L,set} = P_4^H$ and $P_{\mathrm{H,set}} = P_1^H$. The vertical location of the column in this analogy represents the column pressure in the reboiler P_B and the condenser P_C designated by their corresponding saturation temperatures for the nearly pure products. The vertical column length represents the pressure drop, which depends strongly upon the vapour flow rate V. The temperature differences over the reboiler and condenser multiplied by their effective heat transfer rates and areas must be balanced at steady state. This analogy clearly depicts that if both heat pump pressures are increased then the column pressure increases while if the difference between the two heat pump pressures is increased then the vapour flow rate is increased instead resulting in a higher pressure drop over the column. These relationships are explored further in the model analysis of Li et al. (2003). In the present context the mechanical anlogy illustrates that there may indeed be a difference between fixing the column pressure either in the reboiler or in the condenser.

Since the flow rates are measured accurately on a mass basis, it may be questioned which static relationship is being investigated when a zero of the separation factor (or top purity) transfer function to reflux flow rate is investigated. To elucidate this question further the relationship is derived below between the top purity transfer function from mass reflux flow rate dy_D/dL and the top purity from molar reflux flow rate dy_D/dL_M at steady state. During the derivation it is assumed that the bottoms and distillate flow rates remain constant as boilup reflux flow rates are changed. Thus:

$$\left(\frac{\partial y_D}{\partial L}\right)_p^0 = \left(\frac{\partial y_D}{\partial L_M}\right)_p^0 \frac{dL_M}{dL} = \left(\frac{\partial y_D}{\partial L_M}\right)_p^0 \left(\frac{1}{M_T - L_M(M_2 - M_1)\left(\frac{\partial y_D}{\partial L_M}\right)_p^0}\right) \tag{7.2}$$

Where the relation between molar and mass reflux flowrate $L = L_M M_T$ derives from the molar weight of the top composition: $M_T = y_D M_1 + (1 - y_D) M_2$. Note that superscript zero indicates static conditions while subscript p indicates constant pressure at a specified location in the column.

Hence a static zero of the mass based reflux flow rate is closely related to the location of a static zero of the molar based transfer. A similar result can be obtained for the bottom purity. Thus the separation factor sensitivity in Eq. 7.2 can be expressed for the static case with the mass flow rates:

$$\left(\frac{\partial y_D}{\partial L}\right)_p^0 = \left(\frac{\partial y_D}{\partial L_M}\right)_p^0 \frac{dL_M}{dL} = \left(\frac{\partial y_D}{\partial L_M}\right)_p^0 \left(M_T - L_M (M_2 - M_1) \left(\frac{\partial y_D}{\partial L_M}\right)_p^0 \right)^{-1} \tag{7.3}$$

Thus a static zero of the separation factor wrt. mass flow rate can only be due to a zero of the separation factor wrt. molar reflux flow rate since the input transformation does not possess a numerator zero. Thus it is reasonable even for this system with large difference in molecular weight of the two components to investigate the location of a zero using mass based flow rates.

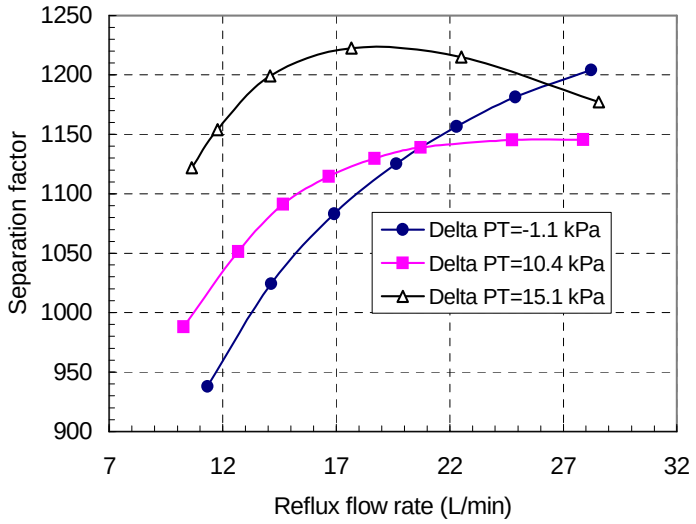

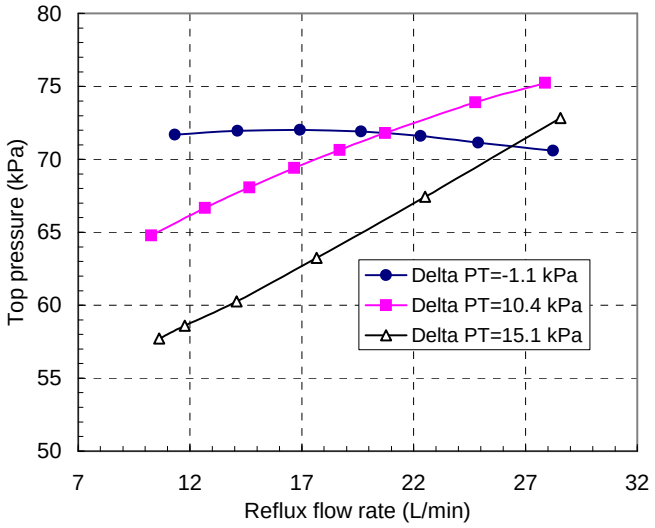

Figures 7.4 a & b: a): Separation factor dependence of the reflux flow rate for three imposed operating pressure dependences. Figure b) shows the top pressure as a function of the reflux flow rate for the three cases.

7.2.5 Control implications

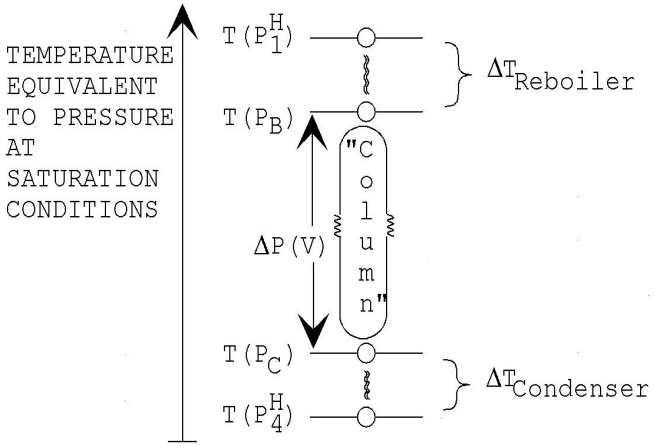

Figure 7.5: Illustration of the IVaRDiP pressure-temperature relationship on a mechanical analog.

From the analysis of operating pressure sensitivity in sections 7.2.2 and 7.2.4 above, input multiplicity may occur at high internal flow rates. Thus it is desirable to discuss how to control the system with a possible input multiplicity. Based on the discussion of potential problems related to operation with floating pressure one may decide that it would be reasonable to have column pressure under feedback control. However, as illustrated in section 7.2.4 above "column pressure" is an ambiguous phrase because the pressure is not the same on all the trays, and for conventionally equipped distillation columns it is not possible to keep the pressure constant on more than one tray when the internal flows change. It is therefore of interest to investigate on which tray it is most desirable to stabilize the column pressure. This issue is analysed in the following paragraphs.

Let us first assume that along with the two product purities the pressure on the top tray or in the condenser is under feedback control. Then it would traditionally be expected to be a good idea, if necessary, to use the cooling capacity (Q_C) for control of the pressure somewhere near the condenser (Shinskey (1985)). For the present example column this could be carried out by using the (D, P_H)--configuration to control the two purities while P_L is used for column pressure control. Now, if suddenly the bottom purity is decreased due to a disturbance, then the controllers would increase P_H and decrease P_L in order to increase the vapour flowrate while keeping the condenser pressure constant (Li et al (2003)). The increased internal flows enhance the separation and in this way the disturbance could be rejected. But in addition the increased internal flow rates result in larger pressure drop across the trays such that pressure on the lower trays is increased since pressure is controlled at the column top - thereby effectively controlling the top temperature, as illustrated in Figure 7.5. This increased pressure results for this negative pressure sensitive mixture in reduced separation capability on these trays. If the internal flow rates are relatively high then the variation of these will have relatively small direct impact upon the separation but large impact on the pressure drop across each tray. The combination of these effects may result in the dominating effect being that the pressures on the lower trays increase such that the relative volatility is reduced. Thus control of top column pressure for a negative pressure sensitive mixture is unfavourable for the separation.

Now, let us analyze the process in the same situation but with P_L used to control the pressure in the reboiler instead. If the bottom purity is decreased due to some disturbance then again P_H will be increased and P_L decreased such that the vapour flowrate is increased while now the reboiler pressure is kept nearly constant. As before the increased internal flows enhance the separation, however, if these flows are

relatively large this effect may be a relatively small. Due to the increased vapour flowrate the pressure drop across each tray is also increased as before, but since it is now the bottom pressure which is fixed, this increased vapour flowrate results in a reduction of the pressure on all the trays above the reboiler, and this reduction results in a higher relative volatility such that the separation capability is further improved. Thus through controlling pressure at the column bottom the two pressure sensitivity effects are now both improving the separation. Hence with control of bottom pressure the pressure drop over the trays is exploited to improve the separation for a negative pressure sensitive mixture.

The above analysis was performed on the example IVaRDiP with the actuators, which are specific for this column. However the analysis is valid for any column for which boil-up and column pressure are indirectly manipulated by heat input into the reboiler and the cooling rate in the condenser. Thus the observed properties are indeed valid for the majority of distillation columns. Even if the vapour flow is generated by blowing vapour directly into the column base, i.e. no reboiler, the column pressure will still depend on this vapour flowrate, because with constant conditions of the cooling medium a changed requirement for cooling rate (due to changed vapour rate) can only be met by changing column pressure and thereby condensation temperature. Hence for any real distillation column separating pressure sensitive mixtures the conflict between internal flows and column pressure potentially exists. The above analysis shows firstly that for such systems operated at higher purities it is desirable to control column pressure. Secondly the analysis further shows that pressure should be controlled at the proper column end such that column pressure drop increases will enhance the separation when internal flow rates increase. That means for negative pressure sensitive mixtures column pressure should be controlled at the column bottom, while for positive pressure sensitive mixtures then pressure should be controlled at the column top. The above analysis also implies that switching to the desirable control structure from controlling pressure at the wrong end of the column also will improve the capacity of the distillation column, without seriously affecting the energy expenditure. Alternatively part of the increased capacity may be traded for a lower energy expenditure to produce to the same specification due to the improved separation factor.

Finally the qualitative analysis indicates that synergistically exploiting the effect of the increased pressure drop to improve the separation factor for part of the column when the internal flow rates increase may have a more pronounced effect on low

pressure separations, where the relative effect of pressure drop variations will constitute a larger fraction of the total column pressure.

7.3 Experiment

7.3.1 Experimental design

Four input multiplicity experiments have been carried out with increasing feed flow rates as shown in Table 7.1. Column top pressure was controlled in part of all experiments. The set point for this loop was 100kPa. For the fourth experiment at the end of the top pressure control phase, the pressure control was changed such that the bottom pressure was controlled instead. The composition profiles were fixed at an interior point within the column for all four experiments such that the estimated methanol mole fraction at tray 15, XPTT15, is controlled by manipulating the distillate flow rate D. To eliminate the influence of profile shape the separation factors were compared for the different experiments.

Table 7.1: The feed flow rates set point for the four experiments

Name	I	II	III	IV
Feed flow rate set point [tons/hr]	0.066±0.0004	0.070±0.0009	0.110±0.0002	0.12±0.0004

In all experiments the on-line data for each operating point were collected. The steady state measurement means and standard deviations, time range specification of the individual steady states obtained at these operating points. The data of experiments I, II and III which only had top pressure control structure are shown in the Appendix. These initial experiments are used to compare with the results from experiment IV on which the discussion in this paper is focused. The steady state flow rates and the power consumption obtained during experiment IV are given in Table 7.2.

Table 7.2: Static flow rates and power consumption in experiment IV with F=0.12±0.0004

Name	Steady state time(hr)	P_T(Top) (kPa)	P_B(Bot)	V (m^3/hr)	F (ton/hr)	D (ton/hr)	B (ton/hr)	L (ton/hr)	P_COW (%)
SS1	1.5	100		1.09	0.12	0.035	0.085	0.827	40.9
SS2	1.5	100		0.981	0.12	0.035	0.085	0.742	40.0
SS3	1.5	100		0.868	0.12	0.035	0.085	0.647	38.1
SS4	1.5	100		0.739	0.12	0.035	0.085	0.552	35.1
SS5	1.5	100		0.661	0.12	0.034	0.086	0.484	35.2
SS6	1.5	100		0.538	0.12	0.034	0.086	0.392	33.0
SS7	1.5		103	0.536	0.12	0.034	0.086	0.390	33.7
SS8	1.5		103	0.660	0.12	0.034	0.086	0.483	35.2
SS9	1.5		103	0.738	0.12	0.034	0.086	0.553	35.0
SS10	1.5		103	0.860	0.12	0.034	0.086	0.646	35.9
SS11	1.5		103	0.979	0.12	0.034	0.086	0.744	38.9
SS12	1.5		103	1.083	0.12	0.034	0.086	0.823	39.5

The details of four experiments are given below. After start-up of the IVaRDiP operation entered phase B and phase C which are distinguished by column top and bottom pressure control respectively. For both phases, the liquid levels of the reboiler and accumulator were controlled at constant values. The below described Phase B was executed in all fours experiments while phase C only was executed in experiment IV.

Phase B:

B.1 Phase A is to start-up the system, and to bring the system to steady state. Then the multivariable receding horizon controller (MIMOSC) is activated with set points equal to process values (P_B, V_{EST}). Set point to column top pressure is 100 kPa. One-point composition control is activated with the set point for the mole fraction on tray 15 (XPTT15) equal to 0.75 mol/mol

B.2 Initial set point for the boil up is 1.12 m^3/hr

B.3 When steady state conditions have been reached, the column operation is maintained for one to two hours in order to collect reliable data for each steady state.

Subsequently samples of the feed and products are collected for subsequent gaschromatographic analysis. The boil up flow rate is decreased according to Table 2 (from steady state 1 to 6) above, and steady state conditions are obtained as described above for each boil up flow rate

Phase C:

C.1 When all steady states in phase B have been obtained, the pressure control scheme is changed, such that MIMOSC controls the column bottom pressure. The set-point for the column bottom pressure is set equal to the actual measurement of the column bottom pressure at the last obtained steady state (where V_{SET} = 0.52 m^3/hr), i.e, 103 kPa

C.2 The boil up flow rate is then increased stepwise again as shown in Table 3 (Steady state 7 to 12) , and steady state conditions are obtained for each boil up flow rate. After each set of steady state conditions has been reached samples of the feed and products are collected and analysed as above.

7.3.2 Data reconciliation

In order to obtain consistent data sets, the results from the GC – analysis and the on – line external flow measurements from the experiments were reconciled. This is done to ensure that the overall mass and component balances are achieved at a steady state. The objective function for the measurements for the data reconciliation is:

$$F_{Obj} = \sum_i \left(\frac{y_i^m - y_i^f}{\sigma_i}\right)^2 \tag{7.4}$$

Where y_i^m is the measured valued, y_i^f is the calculated fitted value and σ_i is the standard deviation of measurement i. The measured variables y_i^m are feed, top, bottom compositions and external flow rates as follows:

$$y^m = [\ x_{F,H2O}\ \ x_{F,MeOH}\ x_{F,\mathrm{Pr}OH}\ x_{D,H2O}\ x_{D,MeOH}\ x_{D,\mathrm{Pr}OH}\ \ x_{B,H2O}\ x_{B,MeOH}\ x_{B,\mathrm{Pr}OH}\ \mathrm{F\ D\ B}]^{\mathrm{T}} \tag{7.5}$$

The static balances and constraints are:

$$0 = F - D - B \tag{7.6}$$

$$0 = F_M x_{F,MeOH} - D_M x_{D,MeOH} - B_M x_{B,MeOH} \tag{7.7}$$

$$0 = F_M x_{F,\mathrm{Pr}OH} - D_M x_{D,\mathrm{Pr}OH} - B_M x_{B,\mathrm{Pr}OH} \tag{7.8}$$

$$0 \le x_{k,j} \le 1 \tag{7.9}$$

$$\sum_{j}^{3} x_{k,j} = 1 \tag{7.10}$$

$$0 \le F \le F_{Feed} \tag{7.11}$$

$$0 \le D \le F_{Feed} \tag{7.12}$$

$$0 \le B \le F_{Feed} \tag{7.13}$$

The above objective function equation (1) was minimized to determine y_i^f .

The standard deviation for each composition measurement is found from the measured GC results:

$\sigma = [\sigma_{F,xH2O}\ \sigma_{F,xMeOH}\ \sigma_{F,x\mathrm{Pr}OH}\ \sigma_{D,xH2O}\ \sigma_{D,xMeOH}\ \sigma_{D,x\mathrm{Pr}OH}\ \sigma_{B,xH2O}\ \sigma_{B,xH2O}\ \sigma_{B,xH2O}\ \sigma_F\ \sigma_D\ \sigma_B\ ]$

=[0.0018 0.006924 0.005825 0.001869 0.002225 0.001338

0.001857 0.005209 0.005068 0.000614 0.00068 0.004578] (7.14)

The reconciled composition data for each state are listed in Table 7.3. With the reconciled composition data, the inherent separation factors are calculated for each steady state.

Table 7.3:Compositions

	SS1	SS2	SS3	SS4	SS5	SS6
$x_{F,H2O}$	0.0841	0.034	0.0364	0.0322	0.0358	0.0251
$x_{F,MeOH}$	0.4505	0.4245	0.4257	0.4277	0.4186	0.4247
$x_{F,\mathrm{Pr}OH}$	0.4654	0.5415	0.5379	0.5401	0.5455	0.5501
$x_{D,H2O}$	0	0.0017	0.0024	0	0	0.0024
$x_{D,MeOH}$	0.9731	0.9721	0.9698	0.9736	0.9752	0.9741
$x_{D,\mathrm{Pr}OH}$	0.0269	0.0262	0.0277	0.0264	0.0248	0.0236
$x_{B,H2O}$	0.0116	0.0316	0.0357	0.0307	0.0368	0.0297
$x_{B,MeOH}$	0.0563	0.0342	0.0323	0.0298	0.0292	0.0417
$x_{B,\mathrm{Pr}OH}$	0.9321	0.9342	0.932	0.9395	0.934	0.9287
	SS7	SS8	SS9	SS10	SS11	SS12
$x_{F,H2O}$	0.0318	0.0321	0.0329	0.0331	0.0296	0.0284
$x_{,\ OH}$	0.4227	0.4184	0.4176	0.4184	0.4196	0.4177
$x_{F,\mathrm{Pr}OH}$	0.5455	0.5495	0.5496	0.5485	0.5508	0.5539

$x_{,H2O}$	0	0.0021	0.0024	0.002	0.0012	0.0025
$x_{D,MeOH}$	0.9766	0.9728	0.9709	0.971	0.973	0.9716
$x_{D,\mathrm{Pr}OH}$	0.0234	0.0251	0.0267	0.0269	0.0259	0.0259
$x_{B,H2O}$	0.0264	0.033	0.0372	0.0318	0.0673	0.0379
$x_{B,MeOH}$	0.0414	0.0284	0.029	0.031	0.0372	0.0365
$x_{B,\mathrm{Pr}OH}$	0.9322	0.9386	0.9338	0.9372	0.8955	0.9257

Figure 7.6 shows the vapor flow rate in the column during the whole experiment IV. The state steady number, top pressure and bottom pressure controlled and the set of vapor flow rates are listed in Table 7.2. It can be seen that from steady 1 to steady 6 the column was top pressure controlled from 6 to 56 hours and from steady state 7 to 12 the column was switched to bottom pressure control from time 56 to 120 hours.

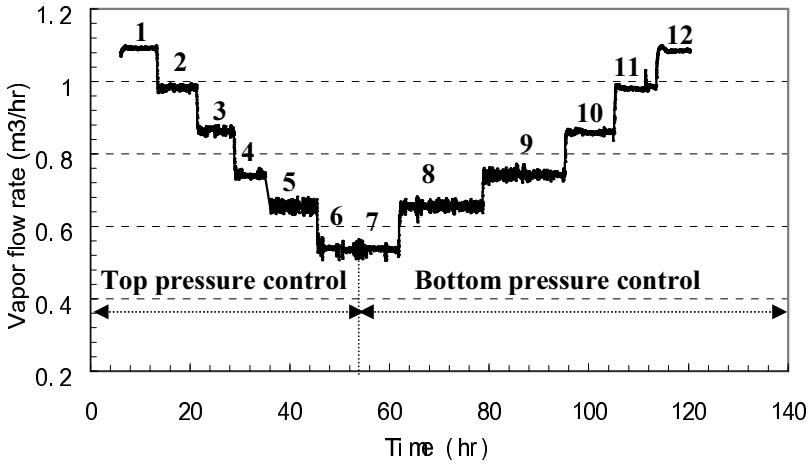

Figure 7.6: Vapour flow rate during experiment IV

7.4 Experimental results and discussion

The column pressure drop, the top and bottom pressures during the experiment IV are shown in Figures 7.7 and 7.8 respectively. Figure 7.9 shows the pressure drop versus the reflux flow rate. With the selected pressure set-points the mean column pressure

during top pressure control was around 102 kPa while around 100.5 kPa during bottom pressure control.

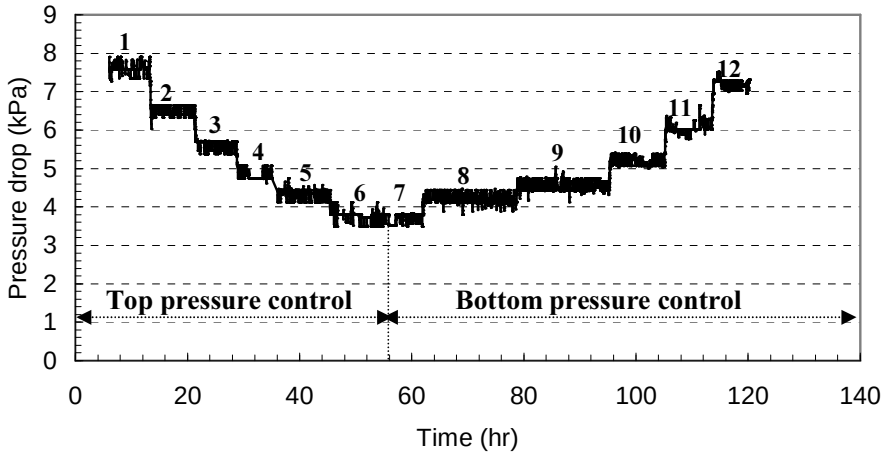

Figure 7.7: Pressure drop over the column during experiment IV

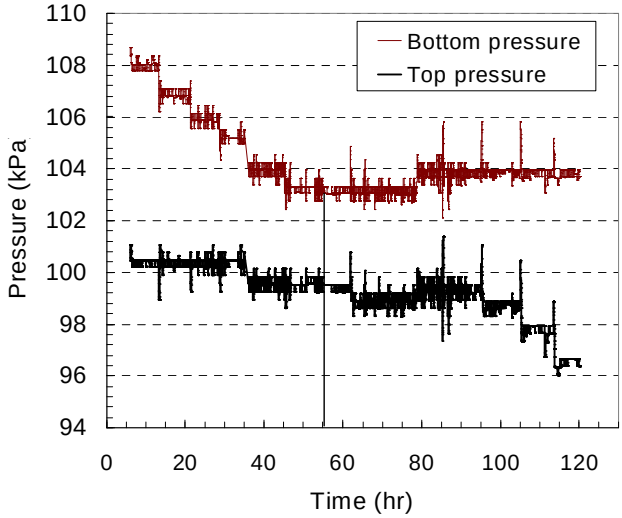

Figure 7.8: Unfiltered values of distillation column bottom and top pressure during experiment IV

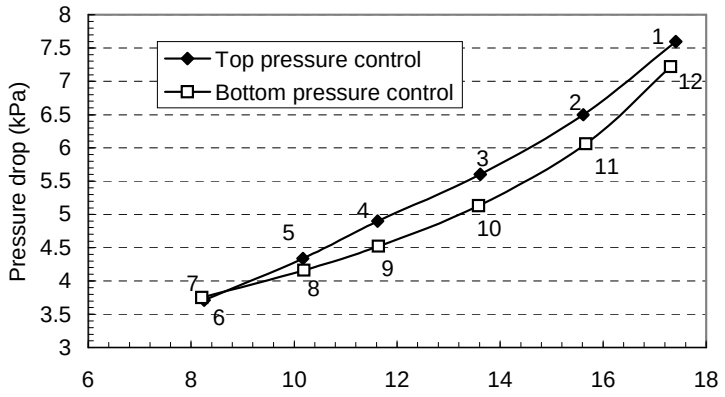

Figure 7.9: The pressure drop vs. reflux flow rate at the steady state experiment IV

7.4.1 Inherent separation factor

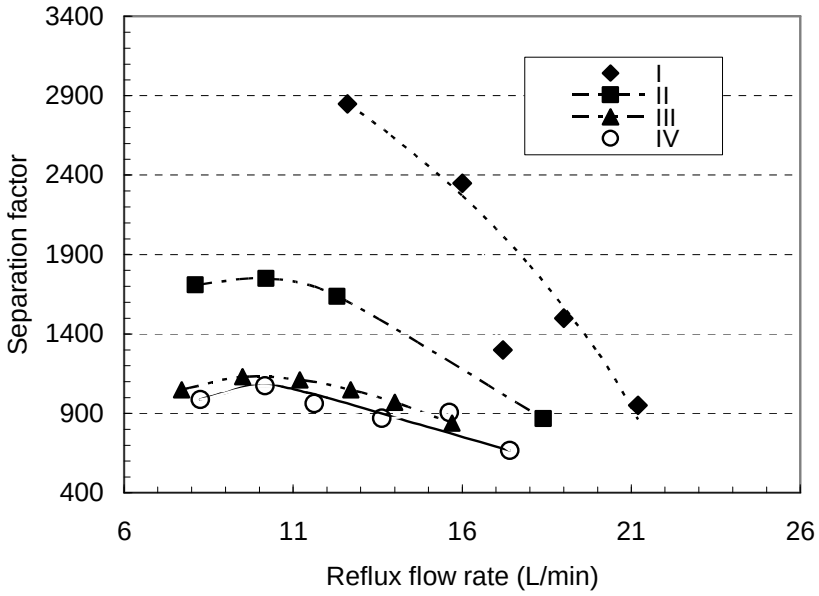

Figure 7.10: Inherent separation factor vs. reflux flow rate with top pressure control for the four input multiplicity experiments

Control of column top pressure:

The separation factors for column top pressure control are shown in Figure 7.10. From Figure 7.10 an input multiplicity becomes more and clearer as the feed flow increased from 0.066 to 0.12 (ton/hr). This result validates the theoretical analysis, i.e., the separation factor can be viewed as consisting of two contributions of different sign; the first one comes from the well understood effect of changing the slope of the operating lines, while the second is due to the effect of pressure on the equilibrium curve. The contribution from the equilibrium curve sensitivity will in most cases be insignificant at low internal flow rate. Thus at low internal flow rate the operating lines sensitivity is dominating effect, i.e. when reflux flow rate increases, the separation factor increases. But the increased internal flow rate will increase the column pressure and thus reduce the separation capability for the negative pressure sensitivity of the present separation mixture. When the internal flow rates increase the column pressure reaches such a value that it may bring the plant to a situation where the two contributions are of equal magnitude, i.e. where maximum separation is achieved. After the maximum separation both the pressure effect, with control of column pressure at the column top but also entrainment may play a significant role in reducing the separation factor. Thus increasing the internal flow rate further will decrease the separation factor, as clearly seen at high internal flow rates in Figure 7.10.

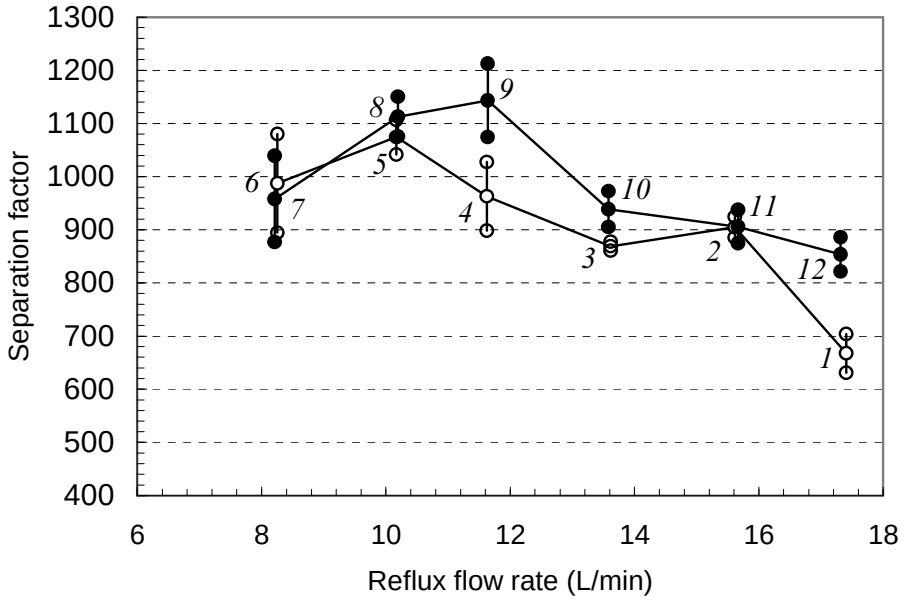

Figure 7.11: Inherent separation factor with standard deviation vs. reflux flow rate with both top pressure and bottom pressure control for experiments IV. Steady states 1-6 have top pressure control, while steady states 7-12 have bottom pressure control.

Control of column bottom pressure:

An approximately 5% higher maximal separation factor is obtained with bottom pressure control shown in Figure 7.11 when compared to top pressure control at about the same mean column pressure. Furthermore the maximal separation factor is obtained at about 20% higher internal flow rate than with column top pressure control. From Table 7.2 it is noted that the energy expenditure for operation at steady state 9 versus steady state 4 are about the same, as also seen in Figure 7.12. Thus this finding validates that the column is more efficiently utilized with control of column bottom pressure when separating a negative pressure sensitive mixture.

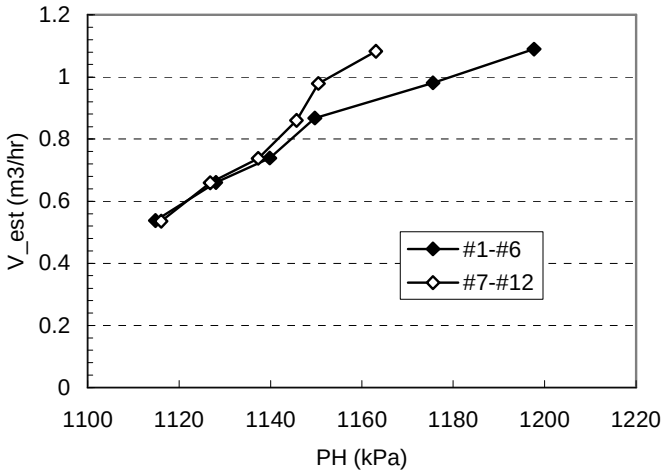

Figure 7.12: Vapor flow rate versus heat pump high pressure
1-6: top pressure control
7-12: bottom pressure control

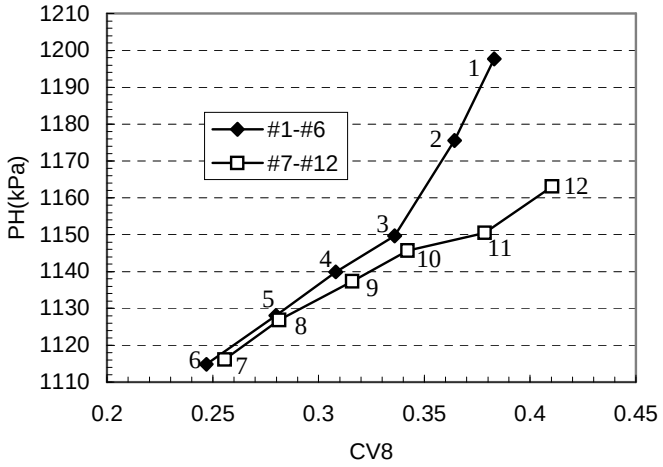

Figure 7.13: Heat pump high pressure versus control valve CV8
1-6: top pressure control
7-12: bottom pressure control

However it is also clear that both control structures display a maximal separation factor thereby indicating that also entrainment plays a role at high reflux flow rates.

It can been seen clearly from Figure 7.12 & 7.13 that for the same boil-up flow rate a lower heat pump high pressure is needed with the bottom pressure control than with top pressure control, which means less energy is needed to achieve the same boil-up

rate. Further more around the maximal separation that also means for an improved separation with control of bottom pressure.

7.5 Conclusions

Distillation column pressure dynamics is investigated to reveal its influence upon distillation column control configuration and upon column operation efficiency. Phenomenological analysis results reveal a possibility for input multiplicity in a distillation plant. Experiments were carried out on an IVaRDiP separating a negative pressure sensitive mixture with both top pressure and bottom pressure control structures. The results from these experiments verify the existence of the proposed input multiplicity for a top pressure control structure. For bottom pressure control, a 5% higher maximal separation factor is obtained at a 20 % higher internal flow rate at a slightly lower energy expenditure. The experimental results thereby confirm that the efficiency of a distillation column separating a mixture with a pressure sensitive equilibrium relation can benefit significantly from using a proper pressure control configuration.

The experiment with bottom pressure control also reveals that an input multiplicity exists, even with this most suitable sensor location; this multiplicity is presumably due to entrainment. Controlling column pressure at the proper end of the column also may be crucial to column operating stability when both product purities are controlled in a decentralized control structure since the occurrence of input multiplicity can destabilize a decentralized control structure. For such cases a centralized multivariable control structure with a pressure sensor suitably located according to the mixture pressure sensitivity should be considered.

Symbols:

B: flow rate of bottom product, ton/hr and B_M in kmol/hr

CV8 (α_{CV8}): control valve 8

CV9 (α_{CV9}): control valve 9

D: flow rate of top product, ton/hr and D_M in kmol/hr

F: feed flow rate, ton/hr and F_M in kmol/hr

F_{Obj} : object function for data reconciliation

L: reflux flow rate, L/min or ton/hr

L_M : Reflux flow rate mol/min or kmol/hr

M: Molecular weight. Subscript T indicates column top, while 1 or 2 indicate component number.

P: column pressure, kPa

P_T: column top pressure, kPa

P_B: column bottom pressure, kPa

P_L (PL): low pressure on the heat pump section, kPa

P_H (PH): high pressure on the heat pump section, kPa

Q_C: heat duty of the condenser, kJ/hr

Q_B: heat duty of the reboiler, kJ/hr

S: separation factor

V_SET: setpoint of vapour flow rate, m^3/hr

X15: methanol mole fraction on tray 15

x_{MeOH} : methanol mole fraction in the liquid phase

XPTT15: estimated methanol mole fraction on tray 15

$x_{B,MeOH} = x_B$: methanol mole fraction in the bottom product

$x_{B,\mathrm{Pr}OH}$: isopropanol mole fraction in the bottom product

$x_{D,MeOH}$: methanol mole fraction in the top product

$x_{D,\mathrm{Pr}OH}$: isopropanol mole fraction in the top product

$x_{F,MeOH}$: methanol mole fraction in the feed product

$x_{F,\mathrm{Pr}OH}$: isopropanol mole fraction in the feed product

x_{F,H_2O} : water mole fraction in the feed product

y_D : methanol mole fraction in the top product

y_{MeOH} : methanol mole fraction in the vapor phase

y_i^m : measured value

y_i^f : fitted value

y^m : vector of measurement

σ_i : standard deviation of measurement i

References:

Chin, T.G.(1979), Guide to distillation pressure control methods. Hydrocarbon Processing 59, pp. 145-153

Tolliver, T. L.; Waggoner, R.C. (1980), Distillation Column Control: A review and perspective from the CPI. ISA,,35, 83-106.

Skogestad, S.(1992) Dynamics and Control of Distillation Columns – a Critical Survey. IFAC-Symposium DYCORD+92, Maryland, Apr. 27-29.

Buckly, P.S.; Luyben, W.L.; Shunta, J.P.(1985), Design of Distillation Column Control System, Instru. Socie. America.

Shinskey, F. G.(1984), Distillation Control. McGraw-hill Book Company.

Desphande, P. B.(1985), Distillation Dynamics and Column, Instru. Socie. of Ameri..

Andersen,.T. R. (2002), Optimal Design and Operation of Process Integrated Distillation. Ph.D thesis, Technical University of Denmark, Lyngby, Denmark.

Li, H., W.; Gani, R. And Jørgensen, S., B.(2003), Process Insights-Based Control Structuring of an Integrated Distillation Pilot Plant, Ind. Eng. Chem. Res., 42, 4620-4627

Koggersbøl, A.; Andersen, B.R.; Nielsen, J.S.; Jørgensen, S.B. (1996), Control Configurations for an Energy Integrated Distillation Column, Computers, chem. Engng. 20S, S853-S858.

Appendix

Tables 7A.1-3 contain the experimental flow rates for the steady states obtained during experiment I-III.

Table 7A.1: Experiment I with F=0.066±0.0004

Name	Steady state time(hr)	P_T (kPa)	V (m^3/hr)	F (ton/hr)	D (ton/hr)	B (ton/hr)	L (ton/hr)
SS1	1.0	100	1.378	0.066	0.02	0.046	1.089
SS2	1.0	100	1.28	0.066	0.02	0.046	1.011
SS3	1.0	100	1.13	0.066	0.02	0.046	0.893
SS4	1.0	100	1.029	0.066	0.02	0.046	0.813
SS5	1.0	100	0.9612	0.066	0.02	0.046	0.759
SS6	1.0	100	0.7601	0.066	0.02	0.046	0.601
SS7	1.0	100	0.4627	0.066	0.02	0.046	0.366

Table 7A.2: Experiment II with F=0.070±0.0009

Name	Steady state time(hr)	P_T (kPa)	V (m^3/hr)	F (ton/hr)	D (ton/hr)	B (ton/hr)	L (ton/hr)
SS1	2.0	100	0.5191	0.070	0.0242	0.0434	0.386
SS2	2.0	100	0.766	0.070	0.0245	0.0438	0.581
SS3	2.0	100	0.9825	0.070	0.0242	0.0434	0.752
SS4	2.0	100	101331	0.070	0.0233	0.0456	0.872
SS5	2.0	100	0.6409	0.070	0.0237	0.0445	0.483
SS6	2.0	100	0.416	0.070	0.0235	0.0448	0.306
SS7	2.0	100	0.5152	0.070	0.0236	0.0449	0.385

Table 7A.3: Experiment III with F=0.110±0.0002

Name	Steady state time(hr)	P_T (kPa)	V (m^3/hr)	F (ton/hr)	D (ton/hr)	B (ton/hr)	L (ton/hr)
SS1	2.0	100	0.5152	0.11	0.035	0.075	0.373
SS2	2.0	100	0.6159	0.11	0.035	0.075	0.452
SS3	2.0	100	0.714	0.11	0.035	0.075	0.529
SS4	2.0	100	0.816	0.11	0.037	0.073	0.607
SS5	2.0	100	0.8844	0.11	0.037	0.073	0.662
SS6	2.0	100	0.9841	0.11	0.037	0.073	0.741
SS7	2.0	100	0.812	0.11	0.037	0.073	0.604
SS8	2.0	100	0.5152	0.11	0.037	0.073	0.660

8

Conclusions and Future Work

This project has demonstrated development of systematic methodology for optimal operation. The methodology has been developed through model analysis and the results are validated through simulation and experiment demonstrated in practice on the IVaRDiP at the Department of Chemical Engineering at DTU. The model analysis results provide insight for development of control structures. These control structures are demonstrated to be suitable for handling operational consequences from heat integrating distillation column. Thereby the operation of the distillation column can resemble that of a conventional distillation column. At the optimizing level control of distillation column operating pressure is investigated. It is shown through model analysis and demonstrated experimentally that the point where pressure should be controlled in a distillation column depends upon the pressure sensitivity of the mixture being separated. The experimental demonstration reveals that a 5% higher maximal separation factor is achieved at a 20% higher internal flow rate.

8. 1. The conclusions from a methodological point of view:

Operability analysis of integrated processes: Methodology development to investigate process dynamics of integrated processes

Synthesis of model based control: Methodology development of control hierarchy for model based control to circumvent performance limiting behaviours which have arisen as a consequence of process integration.

Demonstration of model based control: The developed methodologies have been validated experimentally on the IVaRDiP at the Department of Chemical Engineering at DTU through the usage of model based control.

8.2. The results are summarized relative to the above point:

8.2.1 Operability analysis of integrated processes: a general model based analysis methodology for control structure has been developed. This methodology has been investigated on the IVaRDiP with the purpose of rendering the operation of the IVaRDiP resemble that of a conventional distillation column separating a binary mixture:

A model based analysis method investigates how the degrees of freedom after process (i.e. heat) integration affect the plant operation within the operating.

A model based nonlinear analysis is used to investigate possible nonlinear behaviours around optimal plant operation. This has been exemplified on the IVaRDiP and shown to give rise to two fold bifurcations, where the feasible operation by control will be forced to occur on an open loop unstable branch.

8.2.2 Synthesis of model based control: the results from the above operability analysis give rise to a control structure as follows:

The model analysis based upon the available degrees of freedom decides how the basic control loops of the heat pump may be combined to enable movement of the distillation plant operation within the operating window. This has been exemplified on the IVaRDiP and shown to give rise to a relatively simple multivariable decoupling control structure. This control structure has been implemented at the multivariable control level in the control hierarchy on the plant and shown experimentally to give rise to reliable operation over a large part of the operating window.

The nonlinear analysis gives rise to control structures at the single variable controller level to ensure plant stability. In particular the unstable state variable has to be measured and controlled using a suitable actuator. In the case of the IVaRDiP such a loop is implemented from the high pressure measurement in the heat pump to control the air-cooler bypass valve position. This loop will determine the heat removal rate from the plant to maintain heat pump high pressure at its setpoint thus ensuring stability of the plant assuming the two level controllers in the accumulator and the reboiler to be in operation. Together these three control loops ensure stability at the basic control level. The results of the analysis and the control structure synthesis imply that operation of the IVaRDiP indeed may resemble operation of a conventional distillation plant if the heat pump is operated at high capacity. The closer the heat pump capacity is operated to the actual plant load, the slower the heat pump can respond to disturbances, but the closer the operation will be to minimal energy expenditure.

8.2.3 Demonstration of model based control: validation of the above findings has been undertaken experimentally on the IVaRDiP.

In the case of the IVaRDiP a multivariable controller with rectangular structure, where as many as six measurements are used to determine the manipulation of two actuators, i.e. the two heat pump pressures: high pressure P_H and low pressure P_L such that the distillation column behaviour may follow the intuition developed for operation of standard distillation columns. The experiments verify that the IVaRDiP indeed behaves as expected over a large part of the operating window and thereby the rectangular controller implements the relatively simple decoupling control structure.

The stabilization by the single loop controller – i.e. from the heat pump high pressure to the position of the air-cooler bypass valve position – is verified experimentally. It is shown that indeed the IVaRDiP operates on the unstable branch through the action of the single loop controller and that this enables operation over a large part of the operating window.

The IVaRDiP with the developed control structure is used to investigate operating pressure control for enabling optimal operation pressure. The pressure control structure is experimentally verified through a carefully planned experiment on the IVaRDiP where model based control is utilized to enable the multivariable control and a single loop controller is used to stabilize the nonlinear plant behaviour as described above. Furthermore at the optimizing level for this distillation it is shown that it is possible to obtain approximately 5% higher separation factor at 20 % higher internal flow rates by using the optimal pressure control configuration when operating the column close to maximal separation performance, which will be close to conditions where entrainment starts reducing the achievable separation. Thereby the column capital investment can be utilized more efficiently by enabling higher production rates to be achieved at maximal separation performance through using the optimal pressure control loop.

8.3. Future work:

The developed methodology can be further developed to be incorporated during process design thereby enabling integration of process and control design even during development of process integration.

It is desirable to further investigate how the cascade controller coupling can manage to move across the infinite gain point A1 in Figure 6.4.

Two parameter bifurcation analyses should be carried out to improve understanding of the dynamic behavior of the system. The suggested bifurcation parameters are the control valves α_{CV8} and α_{CV9}.

An experiment can be carried out to validate the bifurcation results, i.e., Figure 6.4. First it is the start up phase to bring the column in to steady state. After that, MIMOSC is actuated and the vapor flow is controlled for each steady state. Then it is to set the control valve α_{CV9} into 0.4 and bring the system into steady state again. With this experiment the vapor flow rate in the column vs. control valve α_{CV8} can be drawn, which may be used to compare to the theoretical Figure 6.4.

A quantitative analysis is desirable to explain why fold bifurcation happens and where the bifurcation happens. This may be done from a model analysis. One possible method may investigate the heat transfer into and out from the heat pump side at constant column status. Then these two curves may intersect to each other at more than one point.

An optimal control using MPC may be implemented on the IVaRDiP at the optimizing level of the control hierarchy.

A: Parameter Estimation

A.1 Introduction

This part presents the parameter estimation using the experimental data during this study. The details of this experiment are described in Appendix D. In this part data from that experiment is used for parameter estimation. The heat integration consists of an indirect heat pump, which transfers energy from the column condenser to the column reboiler. In this way the primary energy consumption is reduced. The column separates a mixture of methanol and isopropanol with a small impurity of water.

A.2. Indirect vapor recompression distillation pilot plant (IVaRDiP)

Mass and energy integration of chemical plants can improve the plant efficiency significantly with respect to energy consumption and environmental impact as well as financially. But, process integration often results in a more complex behavior of the plant, such as multiple steady states, limit cycles and other complicating behaviors including chaos. This complex behavior is the reason why the chemical industry often chooses to use only limited process integration. To reduce the negative effect of process integration on operability then careful control structure may be employed. In order to investigate the influence of process integration a simplified model of the plant is needed. Such a simplified model is developed in this part based upon the more comprehensive model developed by Koggersbøl (1995). The ICAS implementation of the simplified model is shown in Appendix C.

A.2.1. Description of the IVaRDiP

This part presents our case study of this report related to the IVaRDiP at the Department of Chemical Engineering. The IVaRDiP contains mainly three parts: column section, heat pump section and tank park which are shown schematically in Figure A.1 to Figure A.3 and discussed separately below.

The column section is constructed in stainless steel (18-8) to reduce corrosion problems when the system contains water. During binary operation feed is pumped

from two of the tanks WA, MET, ISOP, BOT and TOP by means of the pumps PF1 and PF2, through the pre-heater (HEFS) and into the column. The re-boiler produces a vapour and some liquid that may be removed as bottom product through the bottom product tank (BOT),

The vapour is condensed at the top of the column in HECOND, pumped to the accumulator (DEC) by PC. The pump PT then returns reflux to the column and top product through the water cooled HETW and HEBW to the top product tank (TOP). A small fraction of the top vapour flows to the effluent condenser (EFFCOND) where inert are removed to the venting system. The column separates methanol and iso-propanol with a small water impurity.

A.2.2 Column section

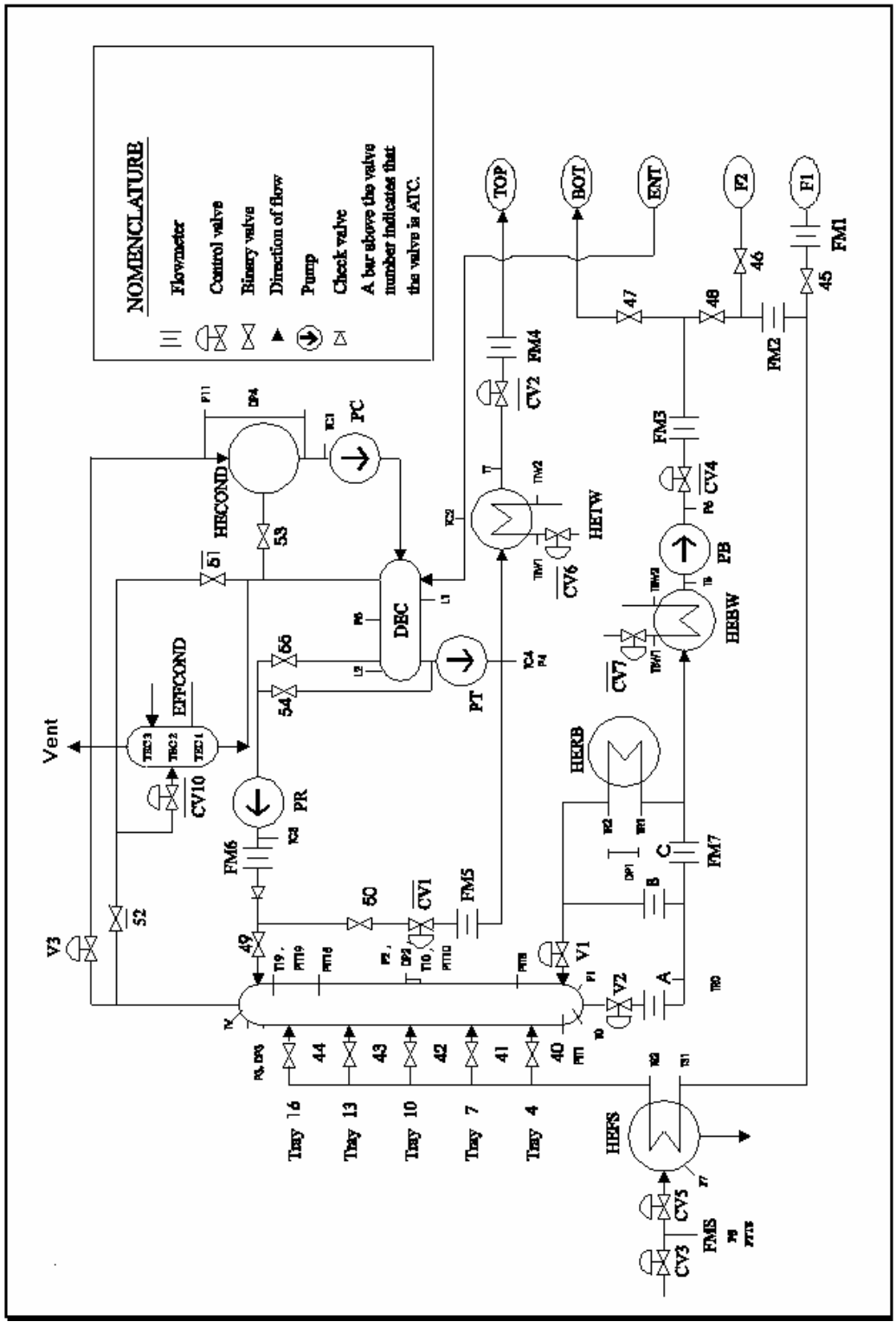

Figure A.1: Flow sheet of distillation column section

A.2.3 Heat pump section:

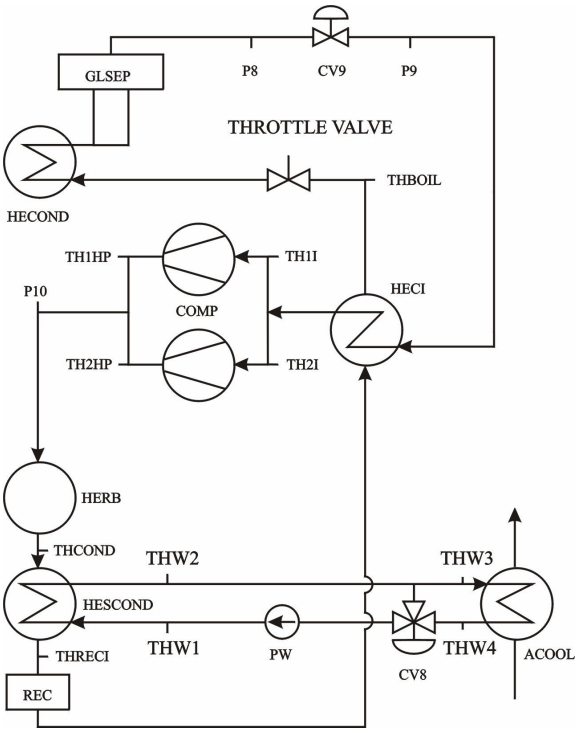

Figure A.2: Flow sheet of heat pump section.

This section is physically connected to the distillation column through heat transfer in the condenser (HECOND) and the reboiler (HERB). Two 8 cylinders piston flow compressors are installed. The heat pump is presently Freon 114. The equipment is designed to run between approximately 55 and 105 ^{o}C corresponding to approximate 5.5 and 16 bar abs. The compressors (COMP) compress the heat pump fluid vapour. Most of the vapour is condensed in the re-boiler (HERB). The extra condenser (HESCOND) condenses an amount corresponding to the heat introduced by the compressors. The liquid passes on to the receiver (REC) and through a heat Exchanger (HECI) to the freon evaporator (HECOND). GLSEP acts as a demister, preventing liquid to pass on to the compressors and also enabling HECOND to operate as a thermo siphon re-boiler to improve heat transfer. In HECI the vapour is superheated before it enters the compressors in order to prevent condensation during the compression cycle. ACOOL is an air-cooled heat exchanger, which at steady state transfers an amount of heat equivalent to the compressor power to the surroundings.

A.2.4. Tank park

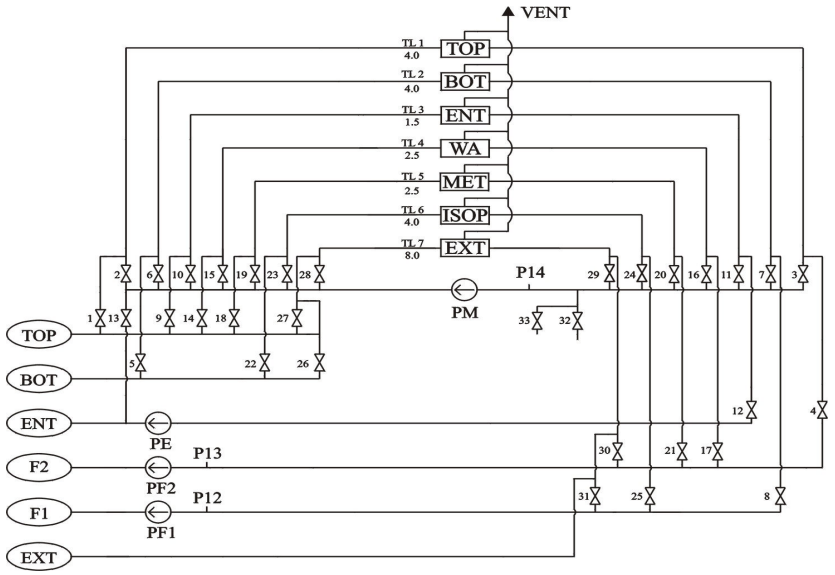

Figure A.3: Flow sheet of the tank park. This is connected to the distillation column as indicated.

The tank park contains seven tanks buried 1.5m below the ground level. Two of these reservoirs serve as bottom and top product tanks (BOT and TOP), four contain the raw materials for the distillations (ISOP, MET, ENT and WA), and one serves as an extra tank (EXT), provide a general dump facility connected to the security system. The pumps associated with the tanks are surrounded by a battery of on/off valves (BV1 – BV31) by which it is possible to connect the tanks to the feed pumps and thereby feed tubes, and to the product tubes. There are three feed-pumps: a small metering pump for the entrainer (PE), and two regular feed-pumps (PF1, PF2) for the 'heavy' and 'light' component respectively. A fourth pump (PM) is connected to all of the tanks, and is used to transport the contents from one arbitrary tank to another. The above pumps are contained in a semi open outdoors pump grave.

A.3 The mathematical model

A comprehensive model of the IVaRDiP was developed by Koggersbøl (1995) with the purpose to perform dynamic simulation. In recent years the work has concentrated on model analysis, its relation with optimal operation and control structure design. Therefore a simplified model is desirable to enable continuation of bifurcation analysis to be performed into ICAS. This simplified model should catch the main dynamic behavior of the system. During to recent changes in the IVaRDiP an

experiment was carried out. The experiment is reported in Appendix D and results are used for estimating essential parameters in the model.

A.3.1 The main assumptions of the model

The model is developed for this IVaRDiP. The number of assumptions is made to reduce the number of states in the model without losing the most important dynamics of the system. The mail assumptions are stated below:

A.-1 Water impurity is neglected; hence the system is assumed binary
A.-2 Constant molar vapor and liquid overflow
A.-3 Saturated liquid as feed
A.-4 No vapor holdup
A.-5 Constant liquid molar holdup on the trays
A.-6 Vapor-liquid equilibrium and perfect mixing on all trays
A.-7 Quasi-stationary energy balances around column ends
A.-8 Quasi-stationary and ideal vapor phase
A.-9 Negligible heat loss
A.-10 Expansions over the expansion and the throttling valves are assumed isenthalpic
A.-11 Constant heat transfer coefficient in the reboiler and condenser
A.-12 Constant delivery temperature from the aircooler

A.3.2 The simplified model developed for bifurcation analysis

Clausen (2002) was simplified the model based on the Arne's model the heat exchanger HECI was omitted. Alonso and Diaz (2002) added the HECI into the Clause's model. But this simple model suffers somewhat from usage of too simple correlation between heat transfer coefficient in the reboiler and condenser, heat pump flow rate on the heat pump section and its relationship between the transfer coefficient and air fan temperature.

A.3.3 The work should be done for obtaining a more actuate simplified model

As stated above, some equipment have been changed through the years and the fluid of cooling system on the heat pump side has been refilled, it is necessary to fit some corresponding parameters with a recent experiment. The dynamic behavior of the reboiler in the bottom and the condenser in the top of the column are very much

related to the H-P diagram of the heat pump fluid, on the heat pump side, which is shown in Figure 3.4.

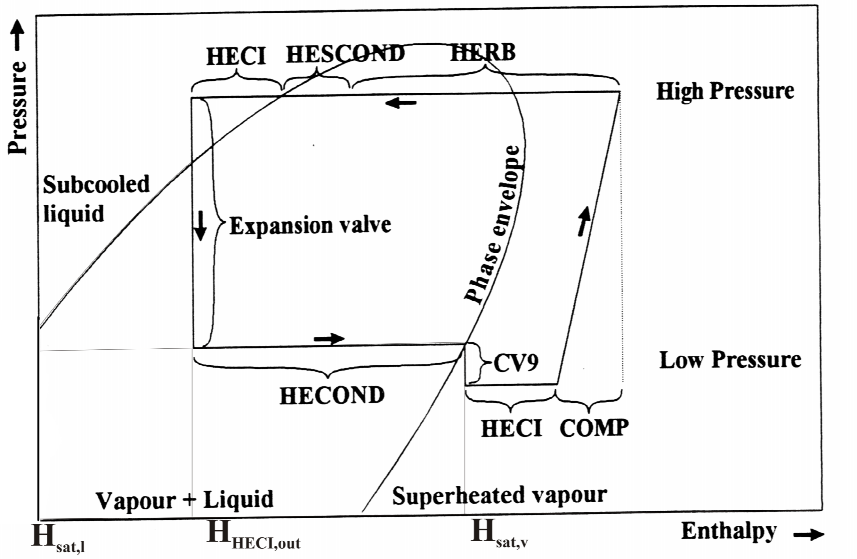

Figure A. 4: Principal H-P Diagram for the Heat Pump cycle

A.4 Model parameters estimation from experimental data

A.4.1 Short description of the experiment

The experiment carried out had three purposes, i.e., to estimate model parameters; to validate the control structures and to validate the multiplicity. i.e. pressure sensitivity of the IVaRDiP. More details of this experiment will be described in Appendix D. The heat transfer coefficients in the reboiler and condenser will be first estimated with the experimental data since the reboiler and the condenser play a very important part in the pilot plant, which related to the distillation column and heat pump side. Later, the temperature in the air fan cooler is calculated from the experimental results.

A.4.2 The calculation of the Freon flow rate

According to Koggersbøl (1995), the heat pump molar flow rate through the compressors can be calculated:

$$L_{COMP} = V^{\sec} N^{cyl} \left(\frac{1}{1-\alpha}\frac{1}{V_{inlet}} - \frac{\alpha}{1-\alpha}\frac{1}{V_{outlet}}\right) \quad \text{(A.1)}$$

where:

L_{COMP} : the Freon molar flow rate through the compressors on the heat pump side

The ratio α and the coefficient $V^{\sec}$ are the parameters of the compressors, where 0.071 and 0.01739 m^3/sec from Koggersbøl (1995), respectively

N^{cyl} : the number of the cylinders that can be switched from 4 to 16

V_{inlet} : molar gas volume before compressors

V_{outlet} : molar gas volume after compressors

A.4.3 The heat transfer coefficient in the reboiler (UA_HERB)

For closer inspections into the heat transfer in the reboiler and condenser during the experimental period, 12 steady states were recorded. More details about this experiment are given in Appendix D. For evaluating the results of the experiment it is necessary to extract the generated data. MODAC creates a series of files containing all the recorded data from the experiment. The commands from the operator to the operating system are listed in Appendix D4. Hence to calculate the heat transfer coefficient in the reboiler, the temperatures on both side the reboiler are shown in Figure A.5 to Figure A.7.

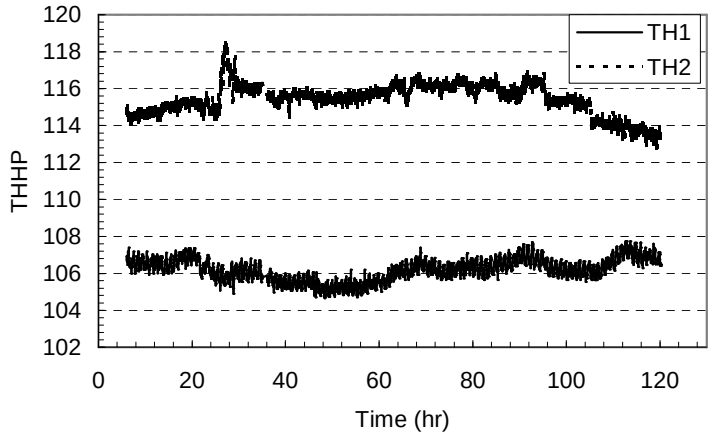

Figure A.5: The inlet temperatures of the reboiler on the heat pump side

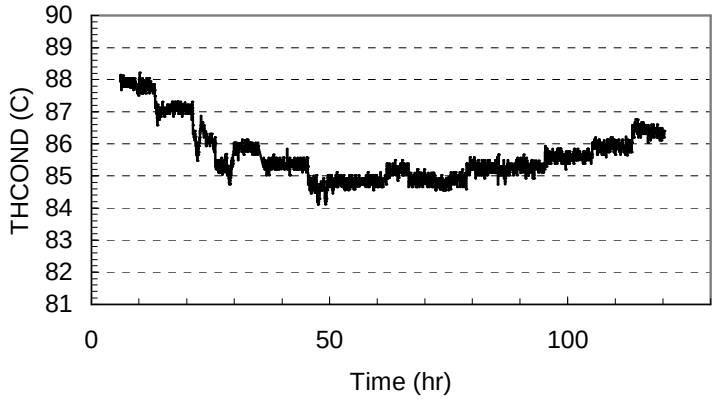

Figure A.6: The outlet temperature of the reboiler on the heat pump side

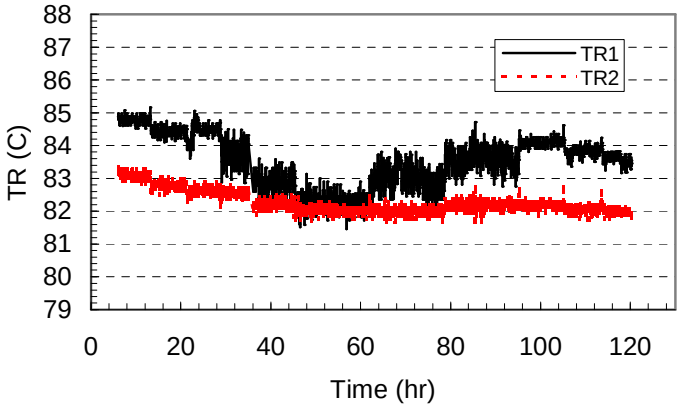

Figure A.7: The outlet (TR2) and inlet (TR1) temperature of the reboiler on the column side

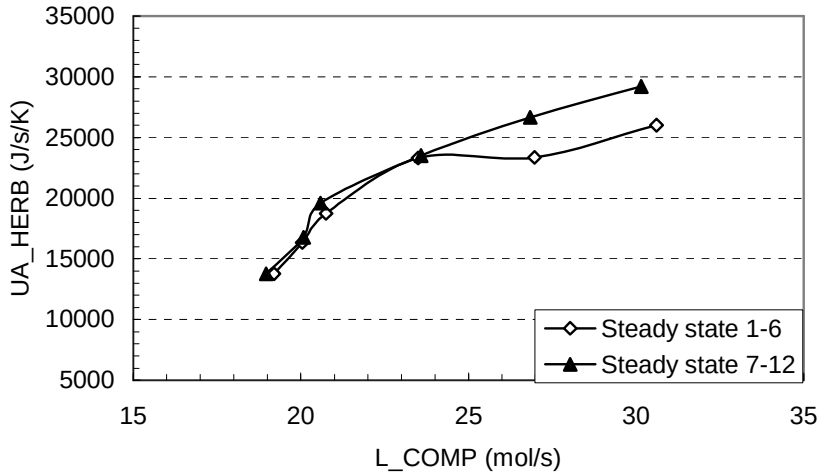

Figure A.8 Calculated heat transfer coefficient of the reboiler as function heat pump flow rate based upon experiment IV

From the Figure A.8 it can be seen that the heat transfer coefficient of the reboiler depends mainly on the experimental heat pump flow rate.

A.4.4 The heat transfer coefficient in the condenser (UA_HECOND)

To calculate the heat transfer coefficient in the condenser, the temperatures of the condenser on the column side are shown from Figure A.9 and10. The heat pump temperature is calculated from the low pressure on the heat pump side. The heat transfer coefficient in condenser is shown in Figure A.11.

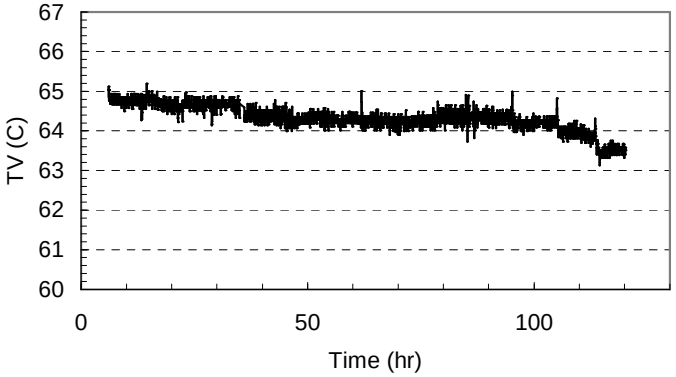

Figure A.9: Inlet temperature of the condenser on the column side

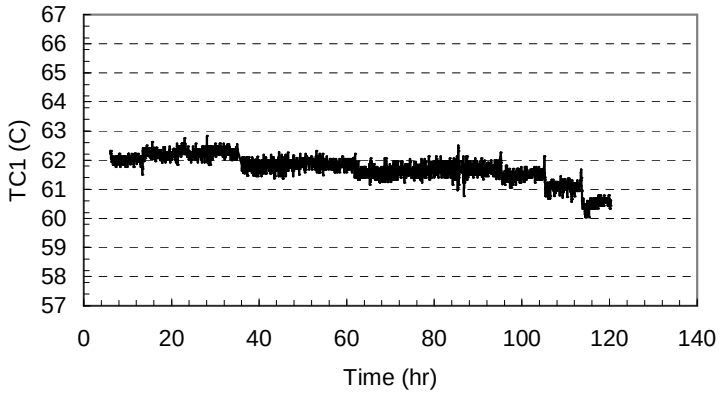

Figure A.10: The outlet temperature of the condenser on the column side

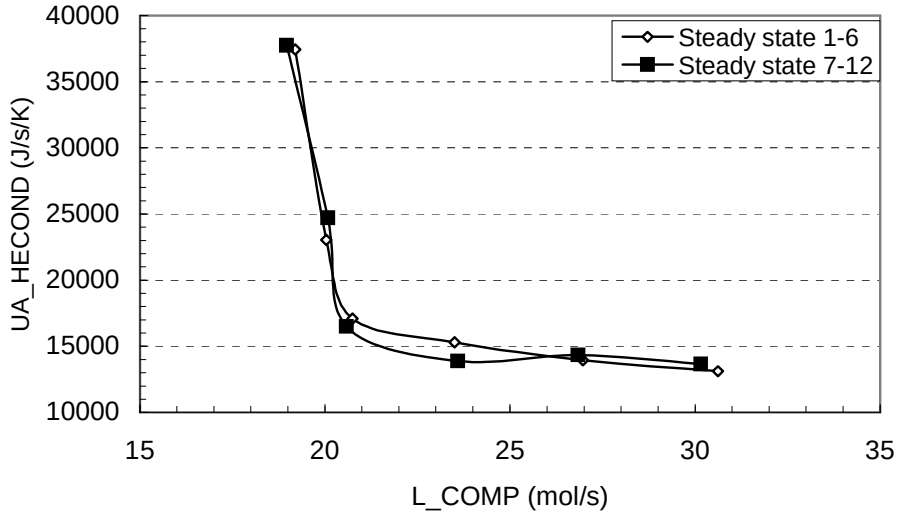

Figure A.11 Calculated heat transfer coefficient of the condenser as function Freon
flow rate on the heat pump side based upon experiment IV

From Figure A.11 it can be seen that the heat transfer coefficient of the condenser constant at high heat pump fluid flow rate. While at low flow rate, the heat transfer coefficient is function of heat pump fluid flow rate.

A.4.5 The air fan cooler temperature T_0

The air fan cooler temperature T_0 is needed to be estimated because of refilling the cooling system. The schematic of air fan is shown in Figure A.12.

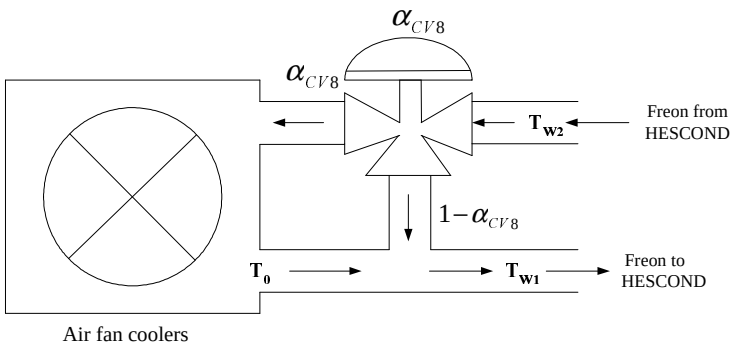

Figure A.12: Schematic of air fan and HECOND

The equation around the control valve α_{CV8} and air fan coolers

$$T_{W1} = \alpha_{CV8}.T_0 + (1-\alpha_{CV8}).T_{W2} \tag{A.2}$$

From (A.2) T_0 can be calculated:

$$T_0 = \frac{1}{\alpha_{CV8}}(T_{W1} - (1-\alpha_{CV8})T_{W2}) \tag{A.3}$$

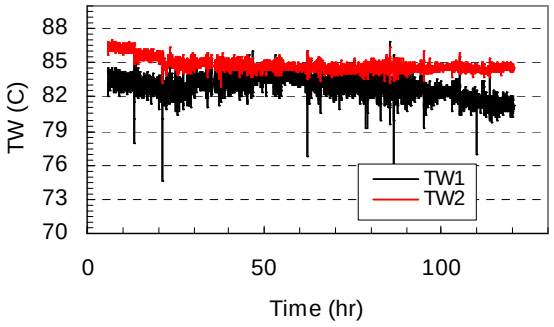

Figure A.13: The inlet and outlet temperature of the HESCOND

The cooling water inlet and outlet temperature of the air fan coolers is shown in Figure A.13, where T_{W2} is the inlet temperature and T_{W1} is the outlet temperature of

the air fan cooler. The temperature of the outlet of the air fan cooler is the mixture temperature of the inlet of the air fan coolers and the temperature in the air coolers shown in equation (A.2). The average temperature of each state of this experiment is calculated and shown at the Appendix D2.1. With each average value of the inlet and outlet temperature of the air fan coolers, the Freon temperature in the air fan coolers obtained as the function of α_{CV8} as drawn in Figure A.14.

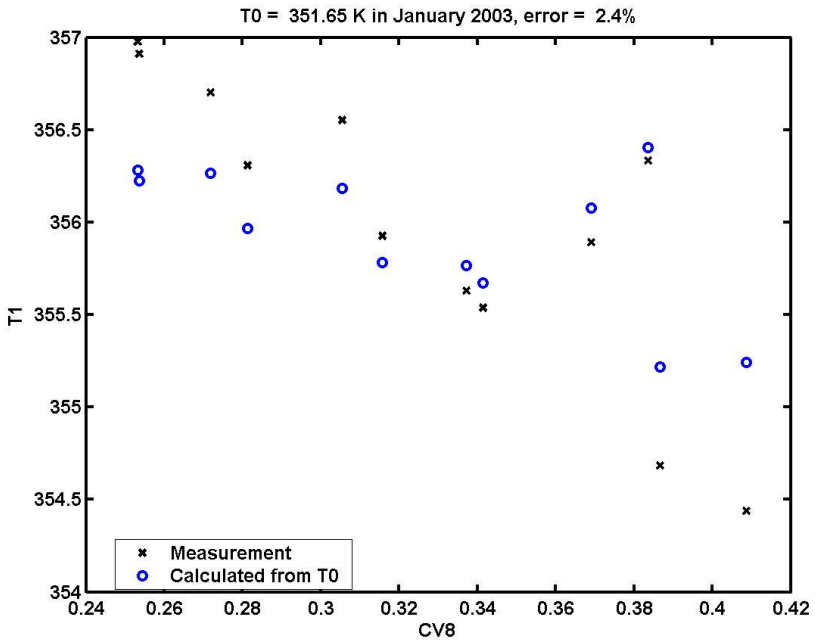

Figure A.14: Temperature out from the air fan coolers (T_0)

From Figure A.14 it can be seen that the maximum error between the measured temperature and the calculated value from Equation (A.2) is 2.4%.

Symbols:

α: constant, 0.071
$\alpha_{CV8:}$ the value of control valve
CV8: the same as α_{CV8}
L_{comp}: Freon molar flow rate through the compressors, mol/s
N^{cyl}: number of cylinder
T_0: outlet temperature of air fan cooler, K
T1: the calculated outlet temperature of air fan cooler, K
THHP: inlet temperature of reboiler on the heat pump side, K
THCOND: outlet temperature of reboiler on the heat pump side
TR1, TR2: the inlet and outlet temperature of the reboiler on the column side, K
TV, TC1: the inlet and outlet temperature of the condenser on the column side, K
TW1,TW2: inlet and outlet temperature of HECOND
UA_HERB: heat transfer coefficient of the reboiler, J/s.K
UA_HECOND: heat transfer coeffcient of the condenser, J/s.K
V_{inlet}: molar gas volume before compressors, m^3/mol
V_{outlet}: molar gas volume after compressors, m^3/mol
V^{set}: constant, 0.01739

B: User guide to using CONT for one parameter bifurcation

The purpose of this guide is to help the new users to use CONT to do bifurcation analysis because there is no graphical user interface of CONT.

B.1 Following files are needed for bifurcation analysis

B.1.1. Mot file: 40.mot

B1.2 Data file: Dynsim

B1.3 Text file: Contінp

B1.4 Matlab file: landsc, SplitMup_13Tay

B1.5 Application file: Parser

B1.6 Copy all the files above in one directory (40.mot file should reach steady state).

B.2 The steps to do bifurcation

B.2.1 Start ICAS simulation program and select the MoTUnitDS and bring the following screen:

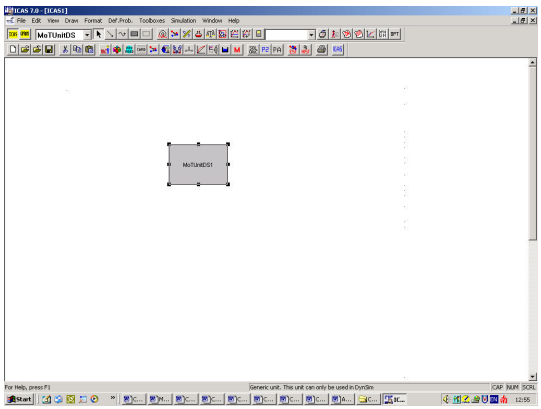

B 2.2 Select the components and thermodynamic property from ICAS the main toolbox

buttons

B 2.3 Double click the MoTUnitDS unit. From the Unit Specific Specification button,

choose the directory that the Mot file saved. Then Click the Dynamic Balances button, select mass balances and energy balance, press OK button back the above

screen

B 2.4 Copy the steady state value of the differential variables in Mot file to Continp and Dynsimb files. The Continp file should also add the values of two bifurcation parameters at the end of state value and finally add 1.00 and 1.00 in the column

The Dynsimb file should add 0.00D+0000 at the end of the column

B 2.5 Press DYNSIM button at the ICAS main toolbox, bring the follow window:

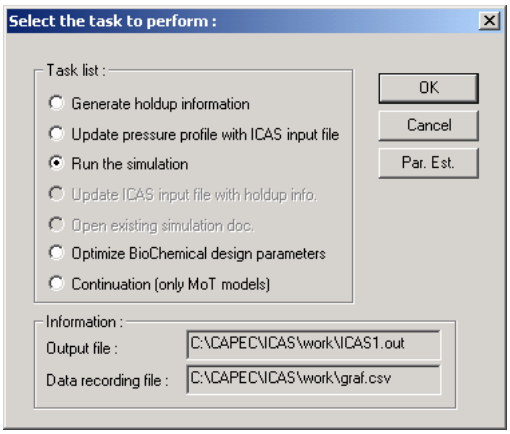

B 2.6 The first time select Run the simulation, when the simulation is finished. Select the Continuation [only MoT model]

B.2.7 The bifurcation results are saved at the same directory with all the files saved, the name of the results is given by the program named Contout.

C: Program of the Simplified ICAS Model

```
---Bifurcation parameters---
V_set= cont_alpha
alphacv9 = cont_beta

--- Correlations---:
#UA_B=1707.1*L_COMP+571.69
#UA_Cv=407700-12810*L_COMP-583*(P4)^2
UA_HECI=40.624*L_COMP+4000

---Condenser pressure---
P4 = 10^(Af - Bf/(Cf+T4-273.15))*133.3225*1e-5

---Expansion valve---
f2 = c_plf/Hvapfr*(T3-T4)

---Reboiler---
0 = Cps*(T7-T1)*L_COMP + f1*L_COMP*Hvapfr - UA_B*HB*(T1-TB)

---Control valve---
0 = L_COMP - Kcv9*alphacv9^acv9*(P5*(P4-P5)*1e10)^bcv9
0 = P5*1e5 - R*T4/(V5-bf) + af/(T4^0.5*V5*(V5+bf))

---Compressors---
epsilon=((1/(1-alfa))*(1/V6))-((alfa/(1-alfa))*(1/V7))
0 = L_COMP - Vsec*Ncyl*epsilon
0=38.78*ln(T7/T6)+0.344*(T7-T6)-0.0002995/2*(T7^2-T6^2)+8.508*1e-8*(T7^3-
T6^3)/3+R*ln((V7-bf)/(V6-bf))+R*ln(T6/T7)+af/(2*bf)*(T6^(-3/2)*ln(1-(bf/V6))-T7^(-
3/2)*ln(1-(bf/V7)))
0=P1*1e5-R*T7/(V7-bf)+af/(T7^0.5*V7*(V7+bf))

---Reboiler pressure---
0 = P1*1e5 - 10^(Af - Bf/(Cf + T1 - 273.15))*133.3225

---Secondary heat exchanger---
0 = (1-f1)*L_COMP*Hvapfr - UA_HESC*(T1-Tw)

---Expansion valve---
0 = L_EXP - K0*((1-  ( dFr/Vcell*W4 - Tubevol/Vcell + V4*LBOB/Vcell*(  f2*L_EXP +
(UA_Cl*HC*(TC-T4) + UA_Cv*(1-HC)*(TNT-T4) )/Hvapfr) )  ))*(((P1-P4)*1e5)^0.5)
0 = P4*1e5 - R*T4/(V4-bf) + af/(T4^0.5*V4*(V4+bf))
0 = P5*1e5 - R*T5/(V5-bf) + af/(T5^0.5*V4*(V5+bf))


---Parameters for HECI---
a=UA_HECI/(L_EXP*c_plf*Ltubes)
b=UA_HECI/(L_COMP*Ltubes)*(Cps-(T6-T2)*(0.334-
0.000295*(T6+T5)/2*2+0.00000008508*3*((T6+T5)/2)^2))/Cps^2
c=UA_HECI/(L_COMP*Ltubes*Cps)
```

```
r1=0.5*(b-a+(a*(a+2*b-4*c)+b^2)^0.5)
r2=0.5*(b-a-(a*(a+2*b-4*c)+b^2)^0.5)

---Column (algebraic and explicit equations)---

---Perfect level control of reboiler and condenser---
L = V - D
B = L + F - V

--- VLE---
yB = alpha*xB/(1 + (alpha-1)*xB)
y1 = alpha*x1/(1 + (alpha-1)*x1)
y2 = alpha*x2/(1 + (alpha-1)*x2)
y3 = alpha*x3/(1 + (alpha-1)*x3)
y4 = alpha*x4/(1 + (alpha-1)*x4)
y5 = alpha*x5/(1 + (alpha-1)*x5)
y6 = alpha*x6/(1 + (alpha-1)*x6)
y7 = alpha*x7/(1 + (alpha-1)*x7)
y8 = alpha*x8/(1 + (alpha-1)*x8)
y9 = alpha*x9/(1 + (alpha-1)*x9)
y10 = alpha*x10/(1 + (alpha-1)*x10)
y11 = alpha*x11/(1 + (alpha-1)*x11)
y12 = alpha*x12/(1 + (alpha-1)*x12)
y13 = alpha*x13/(1 + (alpha-1)*x13)

---Column pressure---
PB = ( xB*10^(Ac1-Bc1/(Cc1+TB-273.15)) + (1-xB)*10^(Ac2-Bc2/(Cc2+TB-273.15))
)*133.3224*1e-5
PC = ( x13*10^(Ac1-Bc1/(Cc1+TNT-273.15)) + (1-x13)*10^(Ac2-Bc2/(Cc2+TNT-273.15))
)*133.3224*1e-5

---Liquid height in reboiler and condenser---
HB = WB/WBmax
HC = WC/(WCmax-WD)

---Pressure drop---
DeltaP = (KDP1*V^2 + KDP2)*1e-5

---Top tray temperature---
0 = (x13*10^(Ac1-Bc1/(Cc1+TNT-273.15)) + (1-x13)*10^(Ac2-Bc2/(Cc2+TNT-273.15))  -
xB*10^(Ac1-Bc1/(Cc1+TB-273.15)) - (1-xB)*10^(Ac2-Bc2/(Cc2+TB-273.15)) +
DeltaP/133.3224*1e5 )

---Boiltup---
0 = V - UA_Cv*(1-HC)*(TNT - T4)/DHvap

---Heat balance for HECI---
DiffT6=((((r1*r2*(r1-r2))/((r1+c-b)*(r1+a)*r2*exp(r1)-(r2+c-b)*(r2+a)*r1*exp(r2)+a*(r1-
r2)*(c-b))*c)*T4)+((r1*r2*(exp(r1)-exp(r2))*c/((r1+c-b)*(r1+a)*(r2*exp(r1))-(r2+c-
b)*(r2+a)*r1*exp(r2)+(a*(r1-r2)*(c-b)))-1)*c)*T2)
0=Cps*L_COMP*Ltubes*DiffT6+UA_HECI*(T2-T6)

---Ordinary Differential equations---

---Freon holdup in condenser---
```

```
dW4 = (1-f2)*L_EXP - (UA_Cl*HC*(TC-T4) + UA_Cv*(1-HC)*(TNT-T4) )/Hvapfr

---Freon temperature in condenser---
dT4 = ( L_EXP*(c_plf*T4+f2*Hvapfr) - L_COMP*(c_plf*T4 + Hvapfr) + UA_Cl*HC*(TC-
T4) + UA_Cv*(1-HC)*(TNT-T4) - c_plf*T4*(L_EXP-L_COMP) )/c_plf/W4

---Freon temperature in condenser---
dT2 = L_COMP/(Wtot-W4)*(T1-T2)

---Air cooler---
Twin=alphacv8*T0+(1-alphacv8)*Tw

---Water temperature in secondary heat exchanger---
dTw = (Lw*cpw*(Twin-Tw) + UA_HESC*(T1-Tw))/Ww/cpw

---Column composition---
---Reboiler---
dxB = ( (L+F)*x1 - V*yB - B*xB )/WB

---Stripper---
dx1 = ( (L+F)*(x2-x1) + V*(yB-y1) )/Wtray
dx2 = ( (L+F)*(x3-x2) + V*(y1-y2) )/Wtray
dx3 = ( (L+F)*(x4-x3) + V*(y2-y3) )/Wtray
dx4 = ( (L+F)*(x5-x4) + V*(y3-y4) )/Wtray
dx5 = ( (L+F)*(x6-x5) + V*(y4-y5) )/Wtray
dx6 = ( (L+F)*(x7-x6) + V*(y5-y6) )/Wtray

---Feed tray---
dx7 = ( L*x8 + F*xF - (L+F)*x7 + V*(y6-y7) )/Wtray

---Rectifier---
dx8 = ( L*(x9-x8) + V*(y7-y8) )/Wtray
dx9 = ( L*(x10-x9) + V*(y8-y9) )/Wtray
dx10 = ( L*(x11-x10) + V*(y9-y10) )/Wtray
dx11 = ( L*(x12-x11) + V*(y10-y11) )/Wtray
dx12 = ( L*(x13-x12) + V*(y11-y12) )/Wtray
dx13 = ( L*(xC-x13) + V*(y12-y13) )/Wtray

---Condenser---
dxC = (V*y13 - (L+D)*xC)/WC

---Column-side temperature in reboiler---
dTB = ( UA_B*HB*(T1-TB) - V*DHvap )/(c_pl*WB)

---Column-side temperature in condenser---
dTC = (c_pl*V*(TNT-TC)  - UA_Cl*HC*(TC-T4))/(c_pl*WC)

---HECI-Liquid Side---
DiffT3=((a*(r1+c-b)*exp(r1)-a*(r2+c-b)*exp(r2))/(r1-r2)*(r1*r2*(r1-r2))/((r1+c-
b)*(r1+a)*r2*exp(r1)-(r2+c-b)*(r2+a)*r1*exp(r2)+a*(r1-r2)*(c-b)))*T4+((a*(r1+c-
b)*exp(r1)-a*(r2+c-b)*exp(r2))/(r1-r2)*(r1*r2*(exp(r1)-exp(r2))*c/((r1+c-
b)*(r1+a)*(r2*exp(r1))-(r2+c-b)*(r2+a)*r1*exp(r2)+(a*(r1-r2)*(c-b))))+((r1-b)*r1*exp(r1)-
(r2-b)*r2*exp(r2))/(r1-r2))*T2
dT3=-(L_EXP*Ltubes/W_HECI)*DiffT3+UA_HECI/(W_HECI*c_plf)*(T5-T3)
```

---HECI-Vapour Side---
0=P5*1e5-R*T6/(V6-bf)+af/ (T6^0.5*V6*(V6+bf))

---Cascade control loop---

---Primary control loop---

P1_set = P1_r +KP1*(V_set-V)

---Secondary control loop---

alphacv8=alphacv8_r+Kcv8*(P1_set-P1)

Values of parameters in the above model:

Af	6.95085	dFr	0.00013	WC	212	Ncyl	16
Bf	996.919	Vcell	0.005	WCmax	6000	UA_HESC	110000
Cf	241.156	Tubevol	0.234	WD	1000	UA_CI	4000
c_plf	183	LBOB	0.5	KPD1	77.4	UA_Cv	14000
Hvapfr	18600	Ltubes	2.8	KDP2	3051	D	0.363357
Cps	125	alpha	2.25	Dhvap	39900	F	0.72462
Kcv9	1.07E-05	Ac1	8.09058	Wtot	5000	T0	330
acv9	4	Bc1	1583.726	cpw	75.284	Lw	185
bcv9	0.742	Cc1	239.162	Ww	1000	xF	0.495
R	8.314	Ac2	8.11205	Wtray	244		
bf	9.26E-05	Bc2	1619.835	c_pl	120		
af	32.56758	Cc2	225.709	W_HECI	917		
Vsec	0.01739	WB	4654	UA_B	17000		
KD	0.024	WBmax	6000	alfa	0.071		

D: Program for Calculating the Temperature in the Air Fan Coolers

```
% Estimate T0 from January 2003 experiments
% Twin = cv8 * T0 + (1-cv8) * Tw

% Twin, Tw and cv8 are the average steady state values
% From SS1 to SS12


Twin=[83.1833 82.7424 82.48 83.4038 83.5519 83.8264 83.7602
      83.1584 82.7776 82.3887 81.5341 81.2887]';
Tw=[86.216 85.521 84.714 85.03 84.841 84.705 84.632 84.509 84.539 84.612
      84.32 84.576]';
cv8=[0.3836 0.369 0.3372 0.3054 0.2719 0.2532 0.2536 0.2812 0.3157 0.3415
      0.3866 0.4086]';

% Twin=cv8*T0+(1-cv8)*Tw
%
y=Twin-(1-cv8).*Tw;
% Calculate the T0 from Experimental data
T0=cv8\y;
mean(T0)+273.15
%
% Calculate the difference
dif=y-cv8*T0;
error=sum(dif.^2)
%
% Calculate the T0 from the experimental data
calc=cv8*T0+(1-cv8).*Tw
figure(1)
% plot(Tw+273.15,Twin+273.15,'rx',Tw+273.15,calc+273.15,'bo')
plot(Tw+273.15,Twin+273.15,'kx','LineWidth',2.0)
hold on
plot(Tw+273.15,calc+273.15,'bo','LineWidth',2.0)
legend('Measurement','Calculated from T0',1)

txt=sprintf('T0 = %7.2f K in %s, error = %4.1f',T0+273.15,md,error);
%txt=sprintf('T0 = %7.2f K in %s data',T0,md);
title(txt)
xlabel('T2')
ylabel('T1')

figure(2)
% plot(cv8,Twin+273.15,'rx',cv8,calc+273.15,'bo')
plot(cv8,Twin+273.15,'kx','LineWidth',2.0)
hold on
```

```
plot(cv8,calc+273.15,'bo','LineWidth',2.0)
legend('Measurement','Calculated from T0',1)

title(txt)
xlabel('CV8')
ylabel('T1')
```

E: Experiment IV

E1. Experimental plan

DISTILLATION COLUMN EXPERIMENT
VALIDATION OF INPUT MULTIPLICITY
FINAL PLAN

Participants

Torben Ravn Andersen (TRA), Dennis Bonné (DB), Carsten Aarosiin Hansen (CAHA), Sten Bay Jørgensen (SBJ), Hong Wen Li (LHW), Erik Bek-Pedersen (EBP), José Manuel Roman Marin (JOMA), Niels Rode Kristensen (NRK)

Purpose of experiment

Validation of boil up - separation input multiplicity

Operating conditions

Constant conditions

Feed flow rate (FM1):	0.120	ton/hr
Reboiler level (DP1):	19.4	kPa
Decanter level (L1):	12	mA
Compressor cylinders (C_CYL):	16	cylinders

Initial conditions (before MIMOSC and composition control):

Distillate flow rate (FM4):	0.040	ton/hr (initially)
Low pressure (P8):	400	kPa (initially)
High pressure (P10):	1180	kPa (initially)

MIMOSC control:

Column top pressure (P3):	100	kPa (**Phase B and D**)
Column bottom pressure (P1):	~104	kPa (**Phase C and D**)

Composition control (DV-configuration):

Methanol mole fraction on tray 15 (XPTT15):	0.75	

Varying conditions

Boil up flow rate (VSET): [0,52;0,64;0,76;0,88;1,0;1,12]	0.52-1,12	m^3/hr

Tank strategy

Feed from EXT tank (TL7).

Products to TOP tank (TL1) and BOT tank (TL2).

Strategy of investigations

Phase A: Start up

1. Start up is made as described in the start up manual (case A) and the system is brought to a "steady" operation at high pressure 1180 kPa and low pressure 400 kPa.

Phase B: Steady state experiment

2. MIMOSC (MIM.CNF) is activated with setpoints equal to process values (P3, V_EST). Setpoint to column top pressure is changed to 100 kPa. 1-point composition control (see procedure on the board in control room) is activated with setpoint for the molefraction on tray 15 (XPTT15) equal to 0.75 mol/mol.
3. Initial setpoint for the boil up (VSET) is 1.12 m^3/hr.
4. When steady state conditions have been reached samples of the feed and products are collected. The boil up flow rate is decreased according to the plan above, and steady state conditions are obtained for each boil up flow rate.

Phase C: Steady state experiment

5. When all steady states in phase B have been obtained, the pressure control scheme is changed, such that MIMOSC controls the column bottom pressure (MIM2.CNF). The setpoint for the column bottom pressure is set equal to the actual measurement of the column bottom pressure at the last obtained steady state (where VSET = 0.52 m^3/hr).
6. The boil up flow rate is then increased again according to the plan above, and steady state conditions are obtained for each boil up flow rate. After each set of steady state conditions has been reached samples of the feed and products are collected.

Phase D: Dynamic experiment

7. When all steady states in phase B and C have been obtained, a dynamic experiment is carried out with both top and bottom compositions controlled. Deactivate 1-point control.
8. At high boil up flow rate (i.e. VSET = 1.12 m^3/hr), with bottom tray pressure controlled, switch to 2-point control (i.e. control of both top and bottoms compositions with setpoints equal to actual composition estimates).
9. Validate stability (if time permits make a small setpoint change in the composition control).
10. Deactivate 2-point control.
11. Change pressure control configuration, such that MIMOSC now controls the column top pressure (P3). The setpoint for the column top pressure is set equal to the actual measurement of the column top pressure.
12. At high boil up flow rate (same VSET as in point B above), with top tray pressure controlled, switch to 2-point control (with setpoints equal to actual composition estimates).
13. Validate instability (if apparent stable operation, make a small setpoint change in the composition control – validate instability…).

Phase E: Shut down

Shut down of the plant is made according to the start up manual

The experimental file of this experiment is shown in the following table

Phase	Steady state	MODAC file	MODAC time(hr)		Real time(hr)		Steady state Time(hr)
			Start	End	Start	End	
B	1	D220103E.DAT	11.60	13.10	20.92	22.42	1.5
	2	D220103E.DAT	19.50	21.00	28.82	30.32	1.5
	3	D220103E.DAT	26.50	28.00	35.82	37.32	1.5
	4	D220103E.DAT	33.60	35.10	42.92	44.42	1.5
	5	D240103A.DAT	8.60	10.10	54.53	56.03	1.5
	6	D240103A.DAT	19.58	21.08	65.51	67.01	1.5
C	7	D250103A.DAT	3.92	5.42	71.06	72.56	1.5
	8	D250103A.DAT	19.87	21.37	87.01	88.51	1.5
	9	D250103A.DAT	37.00	38.50	104.14	105.64	1.5
	10	D250103A.DAT	47.08	48.58	114.23	115.73	1.5
	11	D250103A.DAT	55.55	57.05	122.69	124.19	1.5
	12	D250103A.DAT	62.58	64.08	129.73	131.23	1.5

E 2. Experimental data:

E 2.1 Steady State Data

Name	SS1	SS2	SS3	SS4	SS5	SS6
P1	108	106.8	105.9	105.2	103.9	103.2
P2	103.7	103.3	102.9	102.6	101.6	101.1
P3	100.4	100.3	100.3	100.3	99.56	99.49
P8	374.8	409.4	449.3	488.1	531.9	579
P9	363.4	330.8	298.2	273.5	266.3	257.8
P10	1197	1175	1149	1139	1127	1116
FM1	0.12	0.12	0.12	0.1199	0.1199	0.1199
FM2	0.12	0.12	0.12	0.1199	0.1199	0.1199
FM3	0.08405	0.08392	0.0831	0.08283	0.08406	0.08494
FM4	0.03489	0.03493	0.03526	0.03531	0.03425	0.03415
FM6	0.8274	0.7422	0.6469	0.5522	0.4835	0.3921
V_EST	1.092	0.9839	0.8634	0.7434	0.6547	0.539
DP1	19.39	19.39	19.39	19.37	19.39	19.39
DP2	0.4638	0.4179	0.3817	0.3663	0.3462	0.3191
DP3	0.3728	0.3283	0.3031	0.2519	0.2359	0.2126
DP4	0.679	0.7212	0.7694	0.7935	0.8418	0.8659
L1	12	12	12	12	12	12
L2	3.86	3.849	3.868	3.861	3.839	3.845
XPTT1	0.08482	0.07853	0.06558	0.06286	0.0646	0.06528
XPTT5	0.1512	0.1344	0.1299	0.1308	0.1344	0.1383
XPTT10	0.3452	0.3416	0.3404	0.3439	0.3467	0.3537
XPTT15	0.749	0.7503	0.7497	0.7498	0.75	0.7498
XPTT19	0.9576	0.9629	0.9673	0.9693	0.9727	0.9775
PTT1	81.94	81.8	81.87	81.75	81.42	81.22
PTT5	79.99	80.16	80.1	79.95	79.59	79.36
PTT10	75.56	75.54	75.47	75.32	75.01	74.77
PTT15	68.29	68.22	68.18	68.14	67.91	67.85
PTT19	64.87	64.79	64.73	64.69	64.45	64.37
TV	64.77	64.65	64.66	64.65	64.38	64.3
TC1	62.02	62.22	62.25	62.22	61.81	61.85
TC2	25.25	26.49	25.98	25.89	25.81	24.83
TC3	60.71	60.81	60.73	60.45	59.86	59.51
TC4	51.46	51.86	51.67	51.74	51.2	51.01
TT	17.27	18.32	17.14	17.69	16	15.41
TR0	82.23	82.08	81.65	81.66	81.31	81.04
TR1	84.79	84.44	84.48	83.87	83.01	82.24
TR2	83.07	82.81	82.62	82.54	82.21	82.03
TB	21.77	22.33	21.73	22.27	22.06	21.57
THP8	43.4	46.53	49.89	52.97	56.22	59.5
THP10	90.85	89.97	88.9	88.51	88	87.52
THBOILI	83.93	83.4	82.75	82.92	82.9	82.93
TH1I	77.13	76.75	75.36	75.11	74.96	74.59
TH2I	73.85	73.51	73.25	71.7	71.42	71.45
TH1HP	106.5	106.9	105.8	106.1	105.6	105.3
TH2HP	114.7	115.3	117.6	116.1	115.7	115.5
THCOND	87.79	87.08	85.33	85.86	85.34	84.8
THRECI	88.64	87.72	86.51	86.62	86.16	85.88
THW1	83.1833	82.7424	82.48	88.4038	83.5519	83.8264
THW2	86.216	85.521	84.714	85.03	84.841	84.705
C_CYL	16	16	16	16	16	16

C_POW	40.91	40.04	38.12	35.08	35.23	33.03
CV8	0.3836	0.369	0.3372	0.3054	0.2719	0.2532
CV9	0.7031	0.4817	0.4213	0.3925	0.3753	0.3594
CV2	0.3462	0.348	0.3497	0.3381	0.3553	0.3487

Name	SS7	SS8	SS9	SS10	SS11	SS12
P1	103.1	103.1	103.8	103.8	103.7	103.8
P2	101.1	100.8	101.2	100.8	100.3	99.55
P3	99.35	98.94	99.28	98.67	97.64	96.58
P8	579.3	535.9	477.4	426.1	403.5	371.8
P9	256.7	266.2	271.4	297.6	326.2	355.7
P10	1115	1127	1137	1145	1150	1160
FM1	0.12	0.1199	0.1199	0.12	0.1199	0.1199
FM2	0.1199	0.1199	0.1199	0.12	0.1199	0.1199
FM3	0.08408	0.08412	0.0845	0.08413	0.08806	0.08589
FM4	0.03393	0.0344	0.03437	0.0344	0.03402	0.03398
FM6	0.3902	0.4843	0.5529	0.6456	0.7444	0.8228
V_EST	0.5359	0.6563	0.743	0.8609	0.9853	1.085
DP1	19.38	19.39	19.38	19.39	19.39	19.39
DP2	0.3146	0.3399	0.3466	0.3951	0.4169	0.4699
DP3	0.2043	0.2418	0.2508	0.3038	0.3339	0.3849
DP4	0.89	0.8478	0.7935	0.7272	0.7212	0.7031
L1	12	12	12	12	12	12
L2	3.85	3.854	3.863	3.858	3.865	3.859
XPTT1	0.06526	0.06406	0.06389	0.06412	0.07552	0.08348
XPTT5	0.1381	0.1334	0.1309	0.1278	0.1287	0.1476
XPTT10	0.3545	0.3452	0.3412	0.336	0.3371	0.3423
XPTT15	0.7501	0.7489	0.7503	0.7492	0.7521	0.7497
XPTT19	0.9755	0.9745	0.9757	0.9747	0.97	0.9662
PTT1	81.2	81.23	81.4	81.41	81.13	80.95
PTT5	79.36	79.42	79.61	79.64	79.54	79.04
PTT10	74.75	74.85	75.02	75.03	74.87	74.58
PTT15	67.82	67.75	67.82	67.71	67.47	67.27
PTT19	64.36	64.27	64.34	64.2	64	63.77
TV	64.28	64.27	64.31	64.19	63.84	63.52
TC1	61.87	61.65	61.68	61.51	61.06	60.57
TC2	25.06	24.88	25.51	24.98	26.55	26.68
TC3	59.53	59.71	59.86	59.85	59.7	59.24
TC4	50.99	51.06	51.31	51.09	51.54	50.92
TT	16	15.44	16.01	15.88	15.94	16.06
TR0	81.01	81.05	81.18	81.23	81.1	81.01
TR1	82.21	82.78	83.38	84.14	83.82	83.49
TR2	82.01	82.01	82.18	82.15	82.06	81.96
TB	21.72	21.6	21.94	21.66	22.5	22.49
THP8	59.53	56.51	52.14	47.96	46	43.11
THP10	87.51	88.01	88.4	88.75	88.95	89.36
THBOILI	82.94	82.91	82.8	82.47	82.21	82.32
TH1I	74.74	75.24	75.21	75.39	76.44	76.69
TH2I	71.65	71.84	71.93	72.1	72.95	73.47
TH1HP	105.5	106.2	106.7	106.2	107.2	106.8
TH2HP	115.8	116.4	116.4	115.1	113.9	113.5
THCOND	84.84	84.92	85.29	85.63	85.91	86.31
THRECI	85.84	85.86	86.16	86.47	86.6	87.07
THW1	83.7602	83.1584	82.7776	82.3887	81.5341	81.2887
THW2	84.632	84.509	84.539	84.612	84.32	84.576
C_CYL	16	16	16	16	16	16

C_POW	33.66	35.24	34.98	35.85	38.9	39.47
CV8	0.2536	0.2812	0.3157	0.3415	0.3866	0.4086
CV9	0.3563	0.3795	0.4035	0.4427	0.489	0.6546
CV2	0.3499	0.3619	0.3453	0.333	0.3423	0.3351

E 2.2 Steady standard deviation

Name	SS1	SS2	SS3	SS4	SS5	SS6
P1	0.177	0.171	0.201	0.206	0.296	0.175
P2	0.186	0.235	0.253	0.286	0.379	0.231
P3	0.0956	0.114	0.229	0.231	0.277	0.112
P8	0.177	1.29	1.36	1.76	1.76	1
P9	0.359	1.4	1.43	2.22	6.28	3.28
P10	0.999	1.32	1.79	2.16	2.46	1.31
FM1	0.000432	0.000645	0.000656	0.00092	0.00098	0.000575
FM2	0.000435	0.000644	0.000658	0.000919	0.00098	0.000576
FM3	0.00333	0.00413	0.00559	0.00315	0.00515	0.00531
FM4	0.000147	0.00103	0.00117	0.00127	0.000891	0.00076
FM6	0.0012	0.00354	0.00327	0.00392	0.00639	0.00464
V_EST	0.00192	0.00493	0.00465	0.00571	0.00864	0.00566
DP1	0.0265	0.0332	0.03	0.0219	0.0265	0.0307
DP2	0.00178	0.00205	0.00273	0.00198	0.00177	0.000691
DP3	0.00161	0.0019	0.00157	0.00175	0.00207	0.000724
DP4	0.00000	0.00000	0.00000	0.00000	0.00000	0.00000
L1	0.00731	0.0175	0.0132	0.017	0.0315	0.0228
L2	0.00506	0.0137	0.00868	0.00685	0.00969	0.00674
XPTT1	0.000793	0.00182	0.00172	0.00149	0.00154	0.00105
XPTT5	0.00229	0.00324	0.0037	0.00338	0.00392	0.00288
XPTT10	0.00365	0.00476	0.00604	0.00434	0.00482	0.00388
XPTT15	0.00385	0.00724	0.00853	0.00741	0.0076	0.00566
XPTT19	0.00288	0.00414	0.00345	0.00346	0.00355	0.00322
PTT1	0.0441	0.0533	0.058	0.0625	0.0902	0.0513
PTT5	0.061	0.0826	0.09	0.106	0.136	0.0856
PTT10	0.0836	0.114	0.122	0.131	0.163	0.104
PTT15	0.0659	0.125	0.127	0.147	0.167	0.105
PTT19	0.0439	0.0637	0.066	0.0783	0.0975	0.0557
TV	0.096	0.101	0.12	0.141	0.142	0.0977
TC1	0.113	0.118	0.138	0.14	0.189	0.118
TC2	0.0786	0.077	0.103	0.0636	0.0854	0.0779
TC3	0.0964	0.104	0.103	0.0968	0.132	0.101
TC4	0.117	0.0995	0.109	0.0808	0.102	0.0789
TT	0.102	0.0974	0.0879	0.111	0.13	0.0761
TR0	0.0995	0.0945	0.109	0.103	0.122	0.0966
TR1	0.113	0.124	0.103	0.376	0.275	0.222
TR2	0.105	0.1	0.101	0.112	0.143	0.0794
TB	0.138	0.131	0.144	0.145	0.137	0.146
THP8	0.0166	0.113	0.111	0.135	0.126	0.0678
THP10	0.0397	0.0531	0.0732	0.089	0.102	0.0549
THBOILI	0.125	0.146	0.162	0.179	0.218	0.129
TH1I	0.0762	0.099	0.132	0.0922	0.104	0.11
TH2I	0.136	0.104	0.275	0.105	0.141	0.156
TH1HP	0.262	0.249	0.249	0.327	0.257	0.267
TH2HP	0.158	0.131	0.578	0.166	0.154	0.181
THCOND	0.1	0.0914	0.122	0.0987	0.121	0.106
THRECI	0.0995	0.108	0.163	0.141	0.155	0.113
THW1	0.47616	0.75195	0.74601	0.98346	0.96438	0.52702
THW2	0.21933	0.33254	0.34658	0.46303	0.41826	0.227055
C_CYL	0.00000	0.00000	0.00000	0.00000	0.00000	0.00000
C_POW	0.995	1.17	0.652	0.424	0.664	0.894
CV8	0.0139	0.0263	0.0324	0.0442	0.0507	0.0282
CV9	0.00000	0.00415	0.00251	0.00275	0.00335	0.00152
CV2	0.0279	0.0305	0.0314	0.0302	0.0242	0.022

Name	SS7	SS8	SS9	SS10	SS11	SS12
P1	0.0987	0.23	0.125	0.106	0.135	0.0931
P2	0.156	0.286	0.232	0.212	0.169	0.123
P3	0.114	0.214	0.137	0.158	0.132	0.102
P8	0.292	2.29	0.462	0.301	0.767	0.0567
P9	0.939	6.29	0.468	0.3	0.734	0.268
P10	0.996	1.78	1.05	0.995	0.954	1.11
FM1	0.000559	0.000627	0.000541	0.000526	0.000464	0.00044
FM2	0.000562	0.000628	0.000539	0.000525	0.000462	0.000441
FM3	0.00564	0.00379	0.00571	0.000915	0.00736	0.00486
FM4	0.000366	0.000338	0.000834	0.000423	0.0000833	0.000847
FM6	0.00238	0.00591	0.0029	0.00167	0.00251	0.00159
V_EST	0.00259	0.00764	0.00364	0.00259	0.00345	0.00204
DP1	0.0335	0.0286	0.0345	0.0000	0.0665	0.0269
DP2	0.000341	0.00236	0.0013	0.00163	0.00191	0.00238
DP3	0.00108	0.00243	0.00131	0.00127	0.00161	0.00198
DP4	0.00000	0.00000	0.00000	0.00000	0.00000	0.00000
L1	0.0126	0.0233	0.0114	0.01	0.011	0.00848
L2	0.008	0.0118	0.00821	0.00849	0.00957	0.00868
XPTT1	0.00145	0.00102	0.00152	0.0016	0.00116	0.00151
XPTT5	0.00306	0.00295	0.0034	0.0033	0.00295	0.00259
XPTT10	0.00369	0.00401	0.00484	0.00454	0.00367	0.00402
XPTT15	0.00554	0.00695	0.00746	0.00633	0.00498	0.00566
XPTT19	0.00271	0.00324	0.00374	0.00293	0.00252	0.00263
PTT1	0.0319	0.0571	0.0478	0.0488	0.0376	0.0317
PTT5	0.0743	0.099	0.0876	0.0835	0.0709	0.0587
PTT10	0.083	0.12	0.107	0.0981	0.086	0.0842
PTT15	0.0928	0.138	0.116	0.0999	0.085	0.0908
PTT19	0.0405	0.0807	0.0598	0.0586	0.0444	0.0403
TV	0.084	0.11	0.115	0.0985	0.0939	0.0821
TC1	0.113	0.178	0.152	0.114	0.121	0.105
TC2	0.0765	0.0754	0.0887	0.0647	0.0924	0.0616
TC3	0.0983	0.126	0.111	0.106	0.0931	0.102
TC4	0.0778	0.066	0.0895	0.0835	0.11	0.0832
TT	0.133	0.0901	0.149	0.112	0.124	0.0928
TR0	0.0871	0.109	0.1	0.0729	0.104	0.072
TR1	0.245	0.329	0.263	0.108	0.138	0.137
TR2	0.0965	0.0907	0.121	0.0826	0.0891	0.0681
TB	0.156	0.155	0.14	0.144	0.159	0.144
THP8	0.0197	0.164	0.036	0.0256	0.0678	0.00534
THP10	0.0416	0.0742	0.0432	0.0408	0.039	0.0451
THBOILI	0.129	0.135	0.117	0.102	0.142	0.0998
TH1I	0.083	0.121	0.119	0.0848	0.0926	0.0982
TH2I	0.116	0.1	0.128	0.133	0.127	0.105
TH1HP	0.193	0.238	0.292	0.274	0.28	0.276
TH2HP	0.138	0.186	0.141	0.155	0.261	0.226
THCOND	0.0952	0.106	0.0905	0.099	0.12	0.0996
THRECI	0.114	0.0992	0.121	0.107	0.117	0.0952
THW1	0.39154	0.70289	0.511812	0.60837	0.66605	0.48271
THW2	0.18715	0.279615	0.22823	0.24588	0.26300	0.21527
C_CYL	0.00000	0.00000	0.00000	0.00000	0.00000	0.00000
C_POW	0.814	1.31	0.648	0.782	0.637	0.595
CV8	0.0219	0.0399	0.025	0.0215	0.0174	0.0133
CV9	0.00000	0.00298	0.000821	0.00000	0.00198	0.00000
CV2	0.022	0.0253	0.0317	0.023	0.016	0.034

E 2.3 GC results and data reconciliation

E 2.3.1 Mole fraction from the GC results

	SS1	SS2	SS3	SS4	SS5	SS6
$x_{F,H2O}$	0.0016065	0.001851	0.002851	0.002424	0.002155	0.000831
$x_{F,MeOH}$	0.0093697	0.0053	0.002907	0.002147	0.0073	0.003933
$x_{F,\mathrm{Pr}OH}$	0.0078793	0.003608	0.002623	0.000342	0.005198	0.003163
$x_{D,H2O}$	0.0015311	0.000806	0.000649	0.002112	0.004043	0.00022
$x_{D,MeOH}$	0.0020859	0.000791	0.000535	0.0021	0.004049	0.000129
$x_{D,\mathrm{Pr}OH}$	0.0006841	3.96E-05	0.000142	6.99E-05	0.00013	9.42E-05
$x_{B,H2O}$	0.0024983	0.002976	0.002716	0.00123	0.001858	0.002238
$x_{B,MeOH}$	0.001157	0.001634	0.000263	0.000744	0.000344	0.005222
$x_{B,\mathrm{Pr}OH}$	0.0013719	0.004548	0.00279	0.001942	0.001601	0.007248

	SS7	SS8	SS9	SS10	SS11	SS12
$x_{F,H2O}$	0.000293	0.002175	0.002956	0.001844	0.002757	0.00168
$x_{F,MeOH}$	0.003561	0.004099	0.005168	0.004182	0.003402	0.003371
$x_{F,\mathrm{Pr}OH}$	0.003284	0.001924	0.002615	0.002371	0.000663	0.001784
$x_{D,H2O}$	0.003707	0.001235	0.000724	0.001886	0.002216	0.001721
$x_{D,MeOH}$	0.003807	0.001388	0.000835	0.002028	0.002507	0.001256
$x_{D,\mathrm{Pr}OH}$	0.000103	0.000186	0.000112	0.000156	0.000291	0.000589
$x_{B,H2O}$	0.000461	0.003847	0.002375	0.00285	0.004221	0.003872
$x_{B,MeOH}$	0.003622	0.000252	0.000341	0.000118	0.000776	0.000157
$x_{B,\mathrm{Pr}OH}$	0.004043	0.00366	0.002245	0.002867	0.003849	0.003833

E 2.3.2 Deviation of the mole fraction of each steady state

Deviation	SS1	SS2	SS3	SS4	SS5	SS6
$x_{F,H2O}$	0.0016065	0.001851	0.002851	0.002424	0.002155	0.000831
$x_{F,MeOH}$	0.0093697	0.0053	0.002907	0.002147	0.0073	0.003933
$x_{F,\mathrm{Pr}OH}$	0.0078793	0.003608	0.002623	0.000342	0.005198	0.003163
$x_{D,H2O}$	0.0015311	0.000806	0.000649	0.002112	0.004043	0.00022
$x_{D,MeOH}$	0.0020859	0.000791	0.000535	0.0021	0.004049	0.000129
$x_{D,\mathrm{Pr}OH}$	0.0006841	3.96E-05	0.000142	6.99E-05	0.00013	9.42E-05
$x_{B,H2O}$	0.0024983	0.002976	0.002716	0.00123	0.001858	0.002238
$x_{B,MeOH}$	0.001157	0.001634	0.000263	0.000744	0.000344	0.005222
$x_{B,\mathrm{Pr}OH}$	0.0013719	0.004548	0.00279	0.001942	0.001601	0.007248

Deviation	SS7	SS8	SS9	SS10	SS11	SS12
$x_{F,H2O}$	0.000293	0.002175	0.002956	0.001844	0.002757	0.00168
$x_{F,MeOH}$	0.003561	0.004099	0.005168	0.004182	0.003402	0.003371
$x_{F,\mathrm{Pr}OH}$	0.003284	0.001924	0.002615	0.002371	0.000663	0.001784
$x_{D,H2O}$	0.003707	0.001235	0.000724	0.001886	0.002216	0.001721
$x_{D,MeOH}$	0.003807	0.001388	0.000835	0.002028	0.002507	0.001256
$x_{D,\mathrm{Pr}OH}$	0.000103	0.000186	0.000112	0.000156	0.000291	0.000589
$x_{B,H2O}$	0.000461	0.003847	0.002375	0.00285	0.004221	0.003872
$x_{B,MeOH}$	0.003622	0.000252	0.000341	0.000118	0.000776	0.000157
$x_{B,\mathrm{Pr}OH}$	0.004043	0.00366	0.002245	0.002867	0.003849	0.003833

E 2.3.3 The σ used for the data reconciliation

	σ
$x_{F,H2O}$	0.0018
$x_{F,MeOH}$	0.006924
$x_{F,\mathrm{Pr}OH}$	0.005825
$x_{D,H2O}$	0.001869
$x_{D,MeOH}$	0.002225
$x_{D,\mathrm{Pr}OH}$	0.001338
$x_{B,H2O}$	0.001857
$x_{B,MeOH}$	0.005209
$x_{B,\mathrm{Pr}OH}$	0.005068
F	0.000614
D	0.00068
B	0.004578

E2.4 Reconciliation results of the component mole fraction and mole flow rate (kmol/hr)

	SS1	SS2	SS3	SS4	SS5	SS6
$x_{F,H2O}$	0.0841	0.034	0.0364	0.0322	0.0358	0.0251
$x_{F,MeOH}$	0.4505	0.4245	0.4257	0.4277	0.4186	0.4247
$x_{F,\mathrm{Pr}OH}$	0.4654	0.5415	0.5379	0.5401	0.5455	0.5501
$x_{D,H2O}$	0	0.0017	0.0024	0	0	0.0024
$x_{D,MeOH}$	0.9731	0.9721	0.9698	0.9736	0.9752	0.9741
$x_{D,\mathrm{Pr}OH}$	0.0269	0.0262	0.0277	0.0264	0.0248	0.0236
$x_{B,H2O}$	0.0116	0.0316	0.0357	0.0307	0.0368	0.0297
$x_{B,MeOH}$	0.0563	0.0342	0.0323	0.0298	0.0292	0.0417
$x_{B,\mathrm{Pr}OH}$	0.9321	0.9342	0.932	0.9395	0.934	0.9287
F	2.5649	2.5628	2.5592	2.5522	2.5438	2.5423
D	1.0662	1.0682	1.0772	1.0833	1.0499	1.0457
B	1.4987	1.4946	1.482	1.4689	1.4939	1.4966

	SS7	SS8	SS9	SS10	SS11	SS12
$x_{F,H2O}$	0.0318	0.0321	0.0329	0.0331	0.0296	0.0284
$x_{F,MeOH}$	0.4227	0.4184	0.4176	0.4184	0.4196	0.4177
$x_{F,\mathrm{Pr}OH}$	0.5455	0.5495	0.5496	0.5485	0.5508	0.5539
$x_{D,H2O}$	0	0.0021	0.0024	0.002	0.0012	0.0025
$x_{D,MeOH}$	0.9766	0.9728	0.9709	0.971	0.973	0.9716
$x_{D,\mathrm{Pr}OH}$	0.0234	0.0251	0.0267	0.0269	0.0259	0.0259
$x_{B,H2O}$	0.0264	0.033	0.0372	0.0318	0.0673	0.0379
$x_{B,MeOH}$	0.0414	0.0284	0.029	0.031	0.0372	0.0365
$x_{B,\mathrm{Pr}OH}$	0.9322	0.9386	0.9338	0.9372	0.8955	0.9257
F	2.5452	2.5439	2.5415	2.5399	2.5463	2.5458
D	1.0398	1.0521	1.0498	1.056	1.0393	1.0388
B	1.5053	1.4918	1.4916	1.484	1.5071	1.5069

The method used for data reconciliation can be seen in the references, Toben (2002).

E 2.5 The program of data reconciliation

E2.5.1. Main program

```
 % Li Hongwen
% 2005 - 4 - 27
% Programe to reconciliate the experimental data

% x0 is the initial value of x for iteration

%

% Function 'fun' return back the sum
% fminunc use the least-square method
% to minumus fun, which return the x value
% that makes the sum minumum

% Results below are the last three constrains added
x0=[1 1 1 1 1 1 1 1 1 1 1];
%x=[0.0314 0.4315 0.5371 0.0016 0.9719 0.0265 0.0327 0.0481 0.9192 2.5649
1.0662 1.4987]

% Constrain, kmol/hr
F1=2.545886976
D1=1.038458315
B1=1.494451268


Aeq=[0 F1 0 0 -D1 0 0 -B1 0 0 0 0;
    0 0 F1 0 0 -D1 0 0 -B1 0 0 0;
    0 0 0 0 0 0 0 0 0 1 -1 -1;
    1 1 1 0 0 0 0 0 0 0 0 0;
    0 0 0 1 1 1 0 0 0 0 0 0;
    0 0 0 0 0 0 1 1 1 0 0 0];


Beq=[0; 0; 0; 1; 1; 1];

% Upper and lower bounds for all the components
LB=[0 0 0 0 0 0 0 0 0 0 0 0];
UB=[1 1 1 1 1 1 1 1 1 2.6 2.6 2.6];

Options=optimset('GradObj','off','LargeScale','off','TolFun',1E-20,'TolX',1E-
20,'TolCon',1E-20)

x=fmincon('fun',x0,[],[],Aeq,Beq,LB,UB,[],Options)
```

E2.5.2. Function

```
function [F]=fun(x)
% w is the deviation
% LHW'S DATA
w=[0.00167975      0.00337114   0.001783503  0.00172073   0.001256081
      0.000588675  0.00387196   0.000157359  0.003833136  0.000441
      0.000847     0.00486];


% The weight of each component, H20, MeOH, PrOH
% Feed, top, bottom
% The last three are the F (feed flow rate),
% D (distillate flow rate),
% B (bottom product flow rate


% y is the experimental data matrix


% F is the sum of the object

F=((x(1)-y(1))/w(1))^2+((x(2)-y(2))/w(2))^2+((x(3)-y(3))/w(3))^2+((x(4)-
y(4))/w(4))^2+((x(5)-y(5))/w(5))^2+((x(6)-y(6))/w(6))^2+((x(7)-
y(7))/w(7))^2+((x(8)-y(8))/w(8))^2+((x(9)-y(9))/w(9))^2+((x(10)-
y(10))/w(10))^2+((x(11)-y(11))/w(11))^2+((x(12)-y(12))/w(12))^2;
```

E 3. Some commands executed on experiment IV

Time (hr) Command that the users input
0.128: USR: CMD: EXEC MIM2.CNF
0.133: USR: CMD: MIMOSC:SHOW OLD CONTROL STRUCTURE
0.144: USR: CMD: MIMOSC:ACCEPT CHANGES
0.165: USR: CMD: MIMOSC:SET FILTER CONSTANT FOR ID TO 0.98
0.172: USR: CMD: MIMOSC:ACCEPT CHANGES
0.177: USR: CMD: SET_APD=1
0.201: USR: CMD: MIMOSC:SET ESTIMATION ON
0.205: USR: MIMOSC:SET ESTIMATION ON
0.205: USR: CMD: EST_ON
0.334: USR: CMD: MIMOSC:SET ESTIMATION OFF
0.338: USR: MIMOSC:SET ESTIMATION OFF
0.338: USR: CMD: EST_OFF
0.345: USR: CMD: MIMOSC:SET NR TO 20
0.349: USR: MIMOSC:SET NR TO 20
0.349: USR: CMD: RICC_ON
0.397: USR: CMD: MIMOSC:SET NR TO 0
0.400: USR: MIMOSC:SET NR TO 0
0.400: USR: CMD: RICC_OFF
0.406: USR: CMD: MIMOSC:SET CONTROL ON
0.413: USR: MIMOSC:SET CONTROL ON
0.413: USR: CMD: CON_ON
0.443: USR: CMD: P3SET=100
0.451: USR: CMD: VSET=1.12
0.456: USR: CMD: OUT_APD=1
1.998: USR: CMD: EXEC PIDINIT2
2.009: USR: CMD: XSET=0.75
5.409: USR: CMD: BV5A=1
5.411: USR: CMD: BV1A=1
5.442: USR: CMD: BV18A=0
5.445: USR: CMD: BV22A=0
5.555: USR: CMD: VSET=1.1
5.814: USR: CMD: VSET=1.11
10.104: USR: CMD: QTYP3 L3KP L3TI L3TD
10.118: USR: CMD: QTYP3 L6KP L6TI L6TD
10.123: USR: CMD: QTYP3 L19KP L19TI L19TD
13.237: USR: CMD: VSET=1.0
21.249: USR: CMD: VSET=0.88
22.894: USR: CMD: LOOP18_AUTO=0
22.920: USR: CMD: LOOP3_SET=0.01
23.329: USR: CMD: LOOP3_SET=0.055
24.228: USR: CMD: LOOP3_SET=0.09
24.254: USR: CMD: LOOP18_AUTO=1
28.751: USR: CMD: VSET=0.76
29.885: USR: CMD: BV23A=1
29.896: USR: CMD: PMIXA=1
29.922: USR: CMD: BV20A=1
30.456: USR: CMD: BV20A=0
30.477: USR: CMD: BV24A=1
30.554: USR: CMD: BV10A=1
30.596: USR: CMD: BV23A=0
31.191: USR: CMD: BV23A=1

31.231: USR: CMD: BV10A=0
31.244: USR: CMD: BV24A=0
31.267: USR: CMD: BV10A=1
31.280: USR: CMD: PMIXA=1
31.286: USR: CMD: BV24A=1
31.333: USR: CMD: BV23A=0
34.424: USR: CMD: BV24A=0
34.435: USR: CMD: PMIXA=0
34.454: USR: CMD: BV10A=0
35.260: USR: CMD: VSET=0.64
35.298: USR: CMD: BV23A=1
35.311: USR: CMD: PMIXA=1
35.324: USR: CMD: BV19A=1
35.333: USR: CMD: BV23A=0
35.349: USR: CMD: BV29A=1
35.509: USR: CMD: BV21A=1
35.520: USR: CMD: BV30A=0
35.596: USR: CMD: BV28A=1
35.609: USR: CMD: BV19A=0
35.620: USR: CMD: BV29A=0
35.635: USR: CMD: BV7A=1
35.638: USR: CMD: BV3A=1
36.618: ERR: CMD: BV3A=1

0.147: USR: CMD: EXEC MIM2.CNF
0.158: USR: CMD: MIMOSC:SHOW OLD CONTROL STRUCTURE
0.172: USR: CMD: MIMOSC:ACCEPT CHANGES
0.186: USR: CMD: MIMOSC:SET FILTER CONSTANT FOR ID TO 0.98
0.190: USR: CMD: MIMOSC:ACCEPT CHANGES
0.196: USR: CMD: SET_APD=1
0.226: USR: CMD: MIMOSC:SET ESTIMATION ON
0.228: USR: MIMOSC:SET ESTIMATION ON
0.228: USR: CMD: EST_ON
0.448: USR: CMD: MIMOSC:SET ESTIMATION OFF
0.453: USR: MIMOSC:SET ESTIMATION OFF
0.453: USR: CMD: EST_OFF
0.461: USR: CMD: MIMOSC:SET NR TO 20
0.465: USR: MIMOSC:SET NR TO 20
0.465: USR: CMD: RICC_ON
0.516: USR: CMD: MIMOSC:SET NR TO 0
0.521: USR: MIMOSC:SET NR TO 0
0.521: USR: CMD: RICC_OFF
0.527: USR: CMD: MIMOSC:SET CONTROL ON
0.530: USR: MIMOSC:SET CONTROL ON
0.530: USR: CMD: CON_ON
0.546: USR: CMD: VSET=0.64
0.552: USR: CMD: P3SET=100
0.563: USR: CMD: OUT_APD=1
0.576: USR: CMD: EXEC PIDINIT2
0.583: USR: CMD: XSET=0.75
0.995: USR: CMD: BV3A=0
1.003: USR: CMD: BV3A=1

1.075: USR: CMD: BV7A=0

1.097: USR: CMD: BV3A=0
1.126: USR: CMD: PMIXA=0
1.141: USR: CMD: BV28A=0
1.202: USR: CMD: BV30A=1
1.220: USR: CMD: BV21A=0
3.375: USR: CMD: QTYP3 L8KP L8TI L8TD
3.495: USR: CMD: LOOP8_TI=100
3.504: USR: CMD: LOOP8_EVAL=0
3.915: USR: CMD: QTYP3 L9KP L9TI L9TD
4.419: USR: CMD: QTYP3 L8KP L8TI L8TD
4.801: USR: CMD: LOOP9_TI=300
4.803: USR: CMD: LOOP9_EVAL=0
5.240: USR: CMD: QTYP3 L9KP L9TI L9TD
5.364: USR: CMD: LOOP9_TI=400
5.368: USR: CMD: LOOP9_KP=175
5.370: USR: CMD: LOOP9_EVAL=0
5.375: USR: CMD: QTYP3 L9KP L9TI L9TD
5.626: USR: CMD: LOOP9_KP=150
5.627: USR: CMD: LOOP9_EVAL=0
5.650: USR: CMD: QTYP3 L9KP L9TI L9TD
5.782: USR: CMD: LOOP9_KP=125
5.783: USR: CMD: LOOP9_EVAL=0
5.788: USR: CMD: QTYP3 L9KP L9TI L9TD
6.042: USR: CMD: QTYP3 L8KP L8TI L8TD
6.937: USR: CMD: OUT_APD=0
6.943: USR: MIMOSC:SET CONTROL OFF
6.943: USR: CMD: CON_OFF
6.949: USR: CMD: MIMOSC:SET CONTROL OFF
6.967: USR: CMD: MIMOSC:SET ESTIMATION ON
6.969: USR: MIMOSC:SET ESTIMATION ON
6.969: USR: CMD: EST_ON
7.081: USR: CMD: LOOP9_TI=300
7.086: USR: CMD: LOOP9_EVAL=0
7.095: USR: CMD: MIMOSC:SET ESTIMATION OFF
7.097: USR: MIMOSC:SET ESTIMATION OFF
7.097: USR: CMD: EST_OFF
7.103: USR: CMD: MIMOSC:SET NR TO 20
7.106: USR: MIMOSC:SET NR TO 20
7.106: USR: CMD: RICC_ON
7.142: USR: CMD: MIMOSC:SET NR TO 0
7.144: USR: MIMOSC:SET NR TO 0
7.144: USR: CMD: RICC_OFF
7.149: USR: CMD: MIMOSC:SET CONTROL ON
7.151: USR: MIMOSC:SET CONTROL ON
7.151: USR: CMD: CON_ON
7.166: USR: CMD: OUT_APD=1
7.180: USR: CMD: LOOP9_TI=200
7.183: USR: CMD: LOOP9_EVAL=0
7.207: USR: CMD: QTYP3 L9KP L9TI L9TD
7.349: USR: CMD: LOOP9_KP=150
7.351: USR: CMD: LOOP9_EVAL=0
7.353: USR: CMD: QTYP3 L9KP L9TI L9TD
7.364: USR: CMD: QTYP3 L8KP L8TI L8TD
7.390: USR: CMD: LOOP8_TI=60
7.393: USR: CMD: LOOP8_EVAL=0

7.402: USR: CMD: QTYP3 L8KP L8TI L8TD
7.683: USR: CMD: LOOP8_EVAL=0
7.690: USR: CMD: LOOP9_KP=125
7.691: USR: CMD: LOOP9_EVAL=0
8.284: USR: CMD: OUT_APD=0
8.425: USR: CMD: OUT_APD=1
9.592: USR: CMD: LOOP9_TI=400
9.594: USR: CMD: LOOP9_EVAL=0
10.347: USR: CMD: VSET=0.52
12.689: USR: CMD: QTYP3 L8KP L8TI L8TD
12.757: USR: CMD: LOOP8_TD=12
12.763: USR: CMD: LOOP8_EVAL=0
16.017: USR: CMD: QTYP3 L9KP L9TI L9TD
19.009: USR: CMD: QTYP3 L8KP L8TI L8TD
21.223: CMD: SUSPEND SAMPLE LEVEL

E.4 Dynamic data

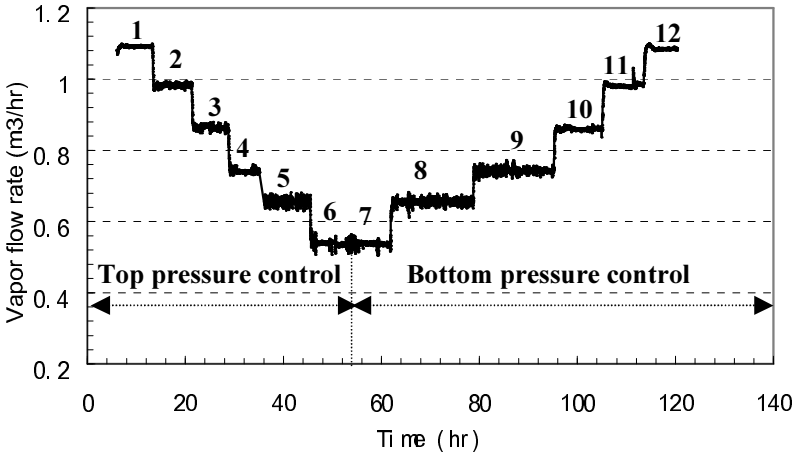

Figure E 4.1 Column vapor flow rate

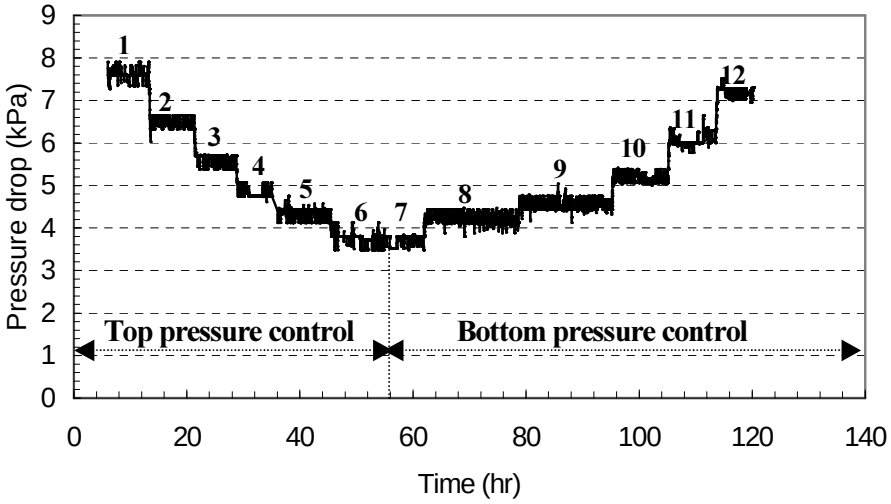

Figure E 4.2 Column pressure drop

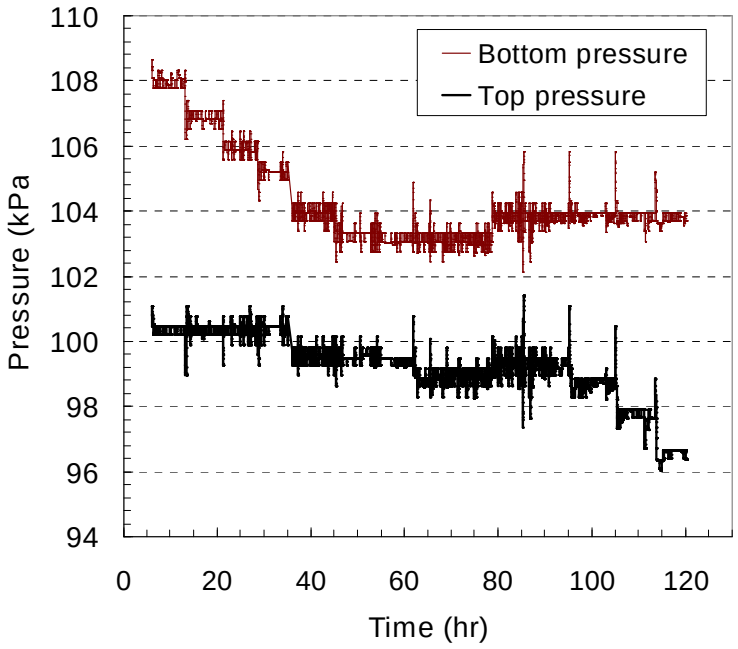

Figure E4.3 Top and bottom pressure

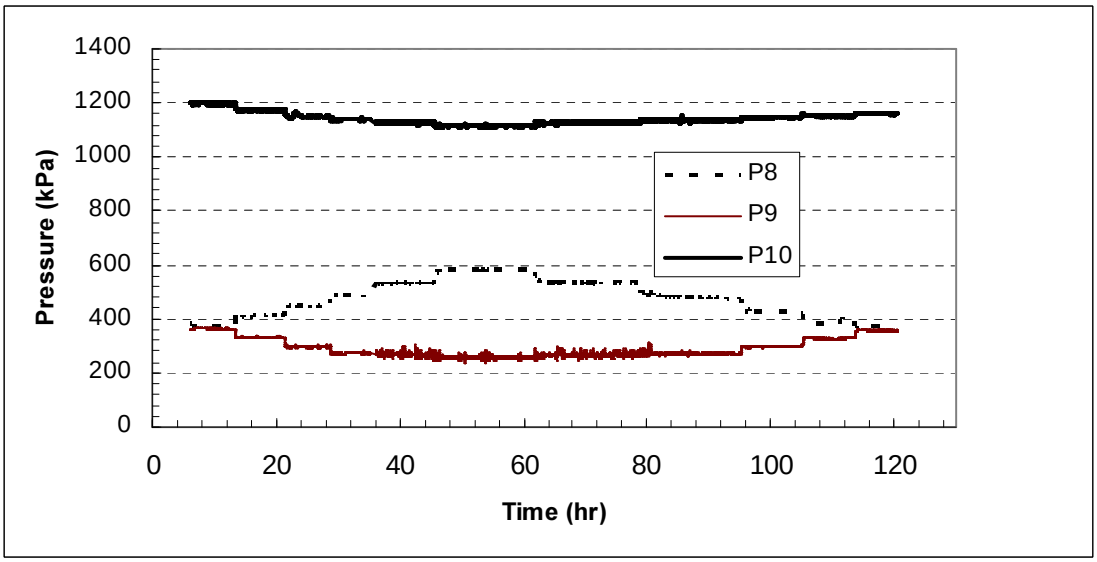

Figure E4.4: Heat pump pressure
P8 (PL)- low pressure
P9- pressure after CV9
P10 (PH) –High pressure

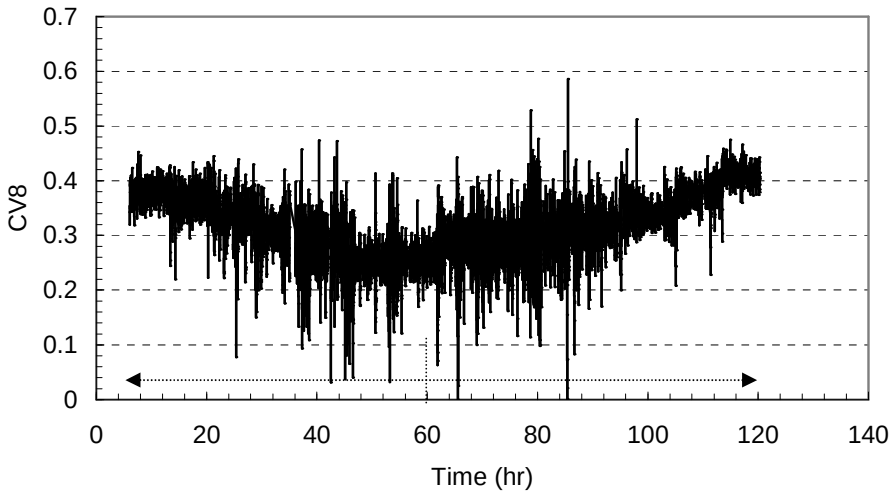

Figure E4.5 Control valve CV8

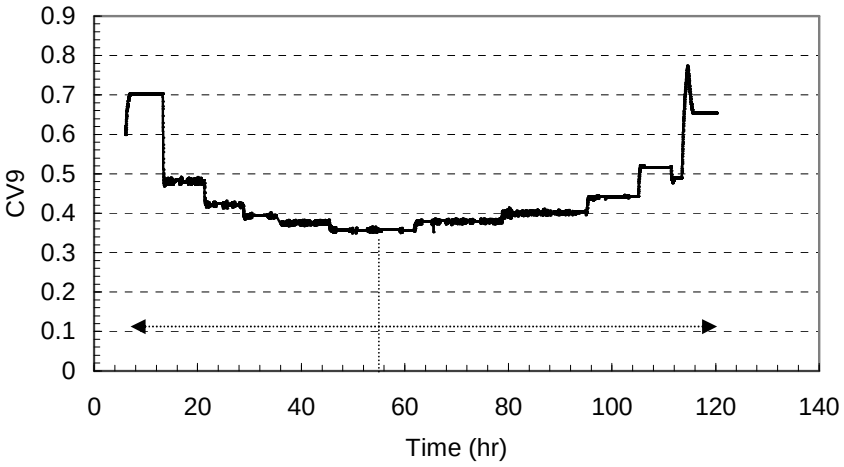

Figure E4.6: Control valve CV9

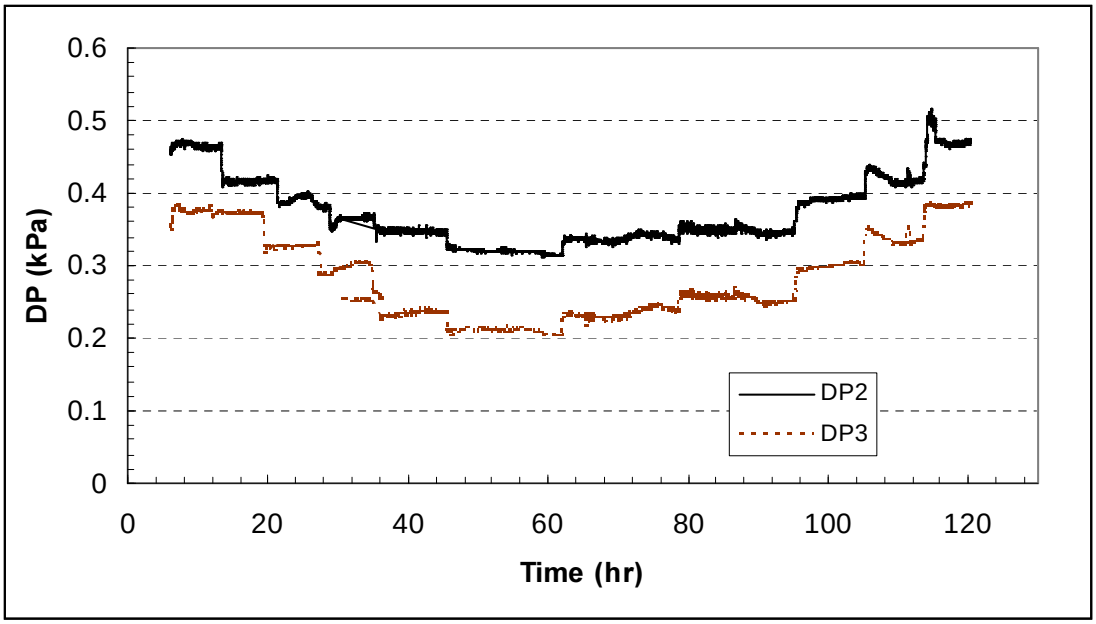

Figure E4.7: Differential Pressures
DP2-Tray 10
DP3 – tray 19

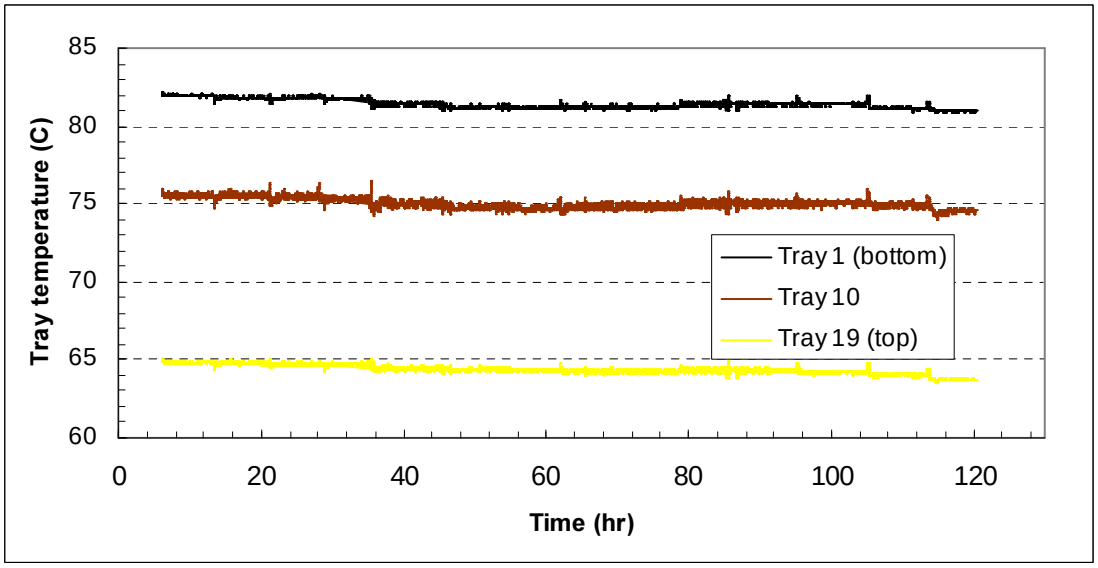

Figure E4.8: Tray temperature
PTT1 – tray1 (bottom)
PTT10 – tray10
PTT19 – tray 19 (top)

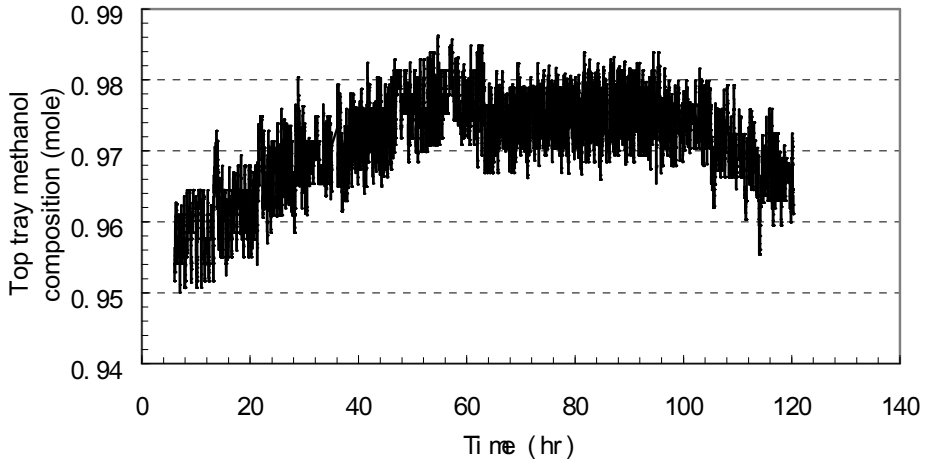

Figure E 4.9: Estimated product purities ($X_{MeOH, Top}$)

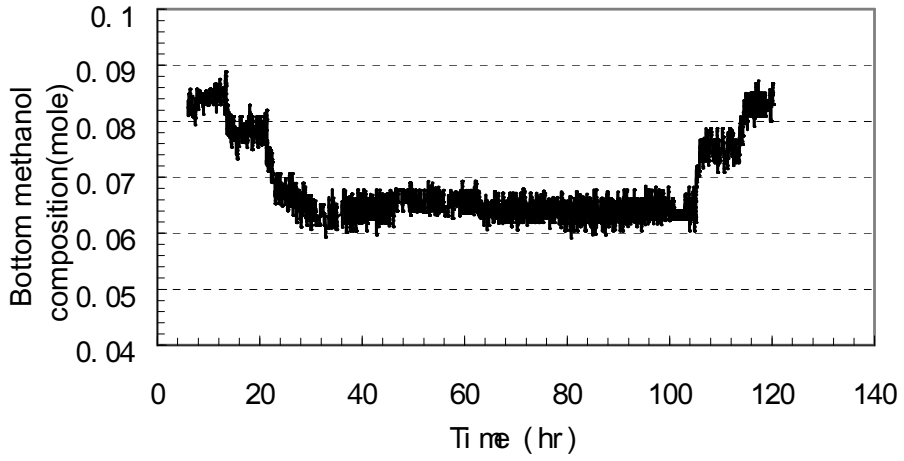

Figure E 4.10: Estimated product purities ($X_{MeOH, Bot}$)

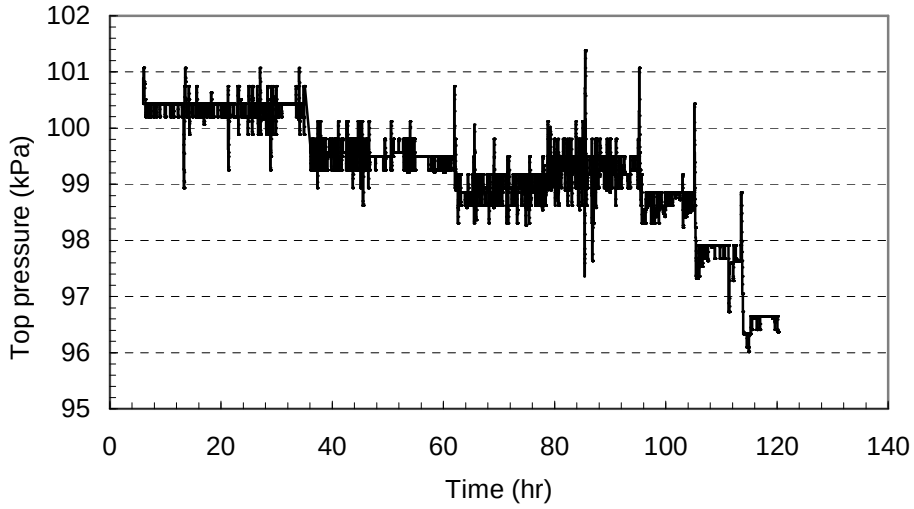

Figure E 4.11: Column top pressure

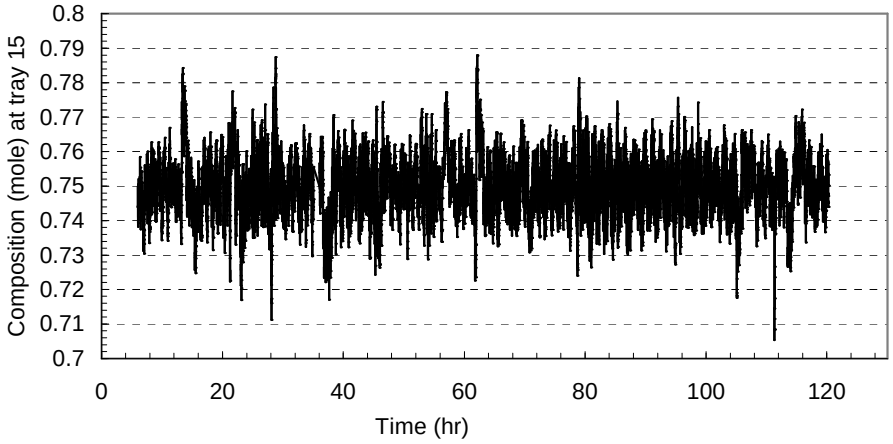

Figure E 4.12: Tray 15 composition controller ($X_{MeOH,\ tray15,set}$)

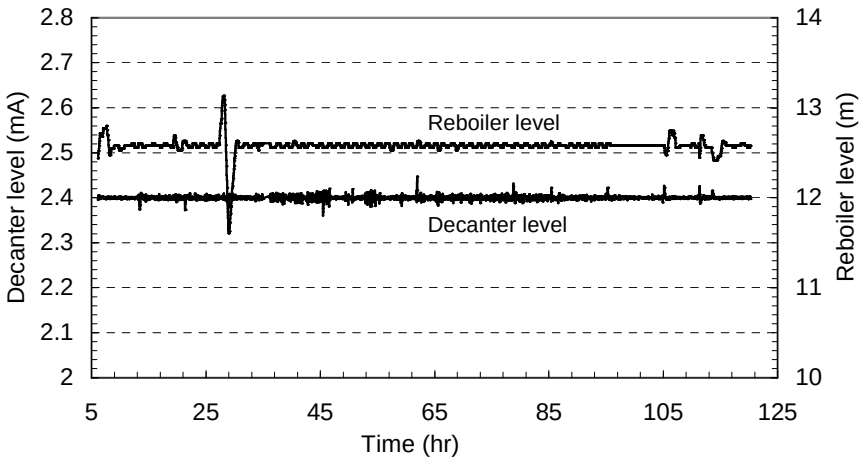

Figure E 4.13 Decanter and reboiler controlled level ($h_{Dcanter}$)

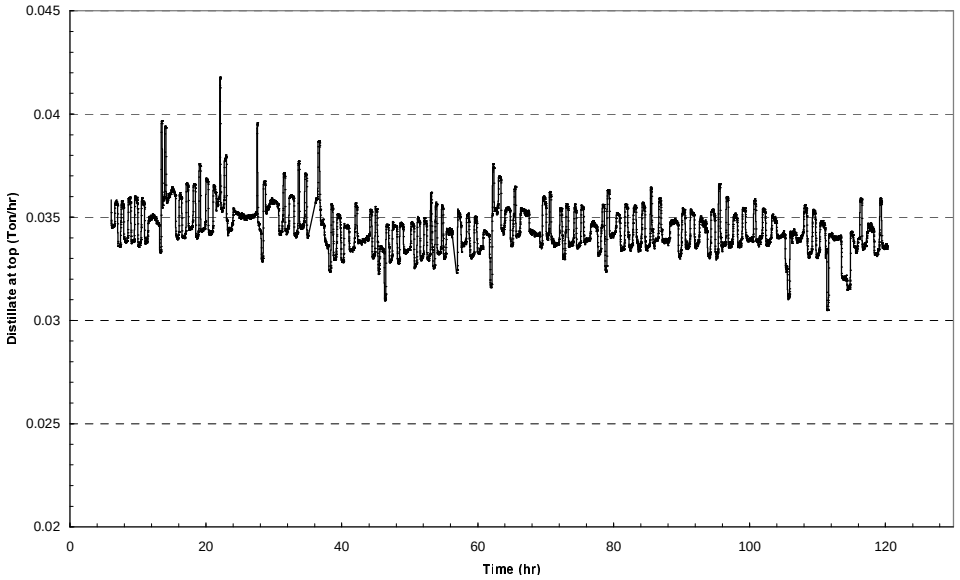

Figure E4.14: Distillate flow rate (D_{mass})

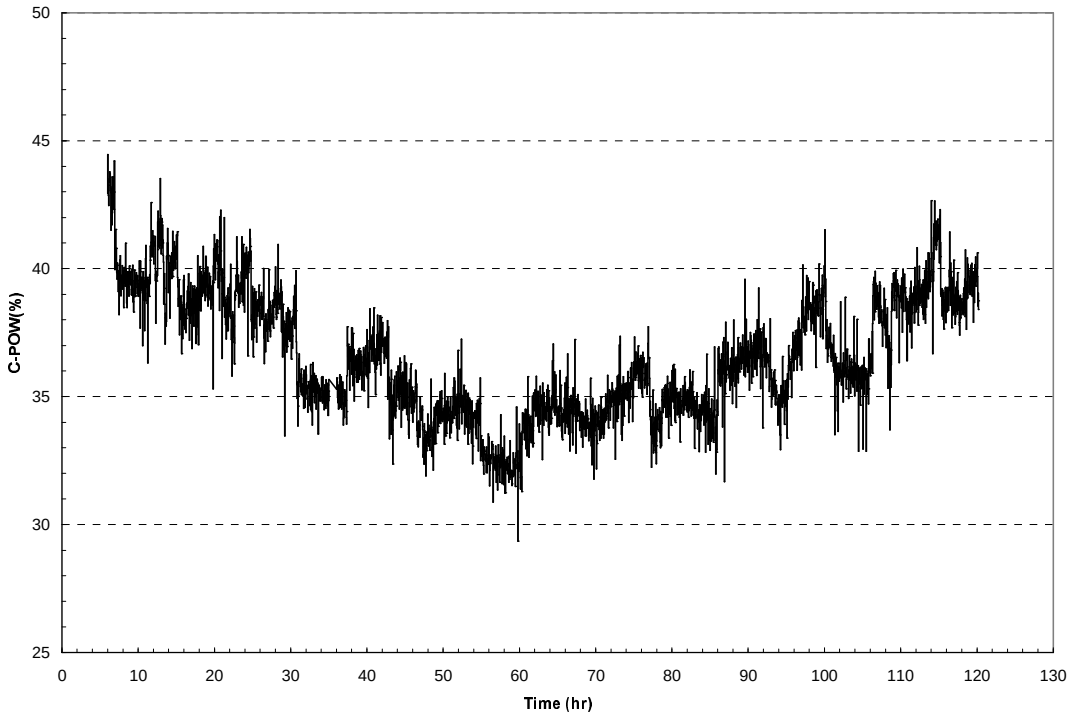

Figure E4.15: Power consumed by two compressors

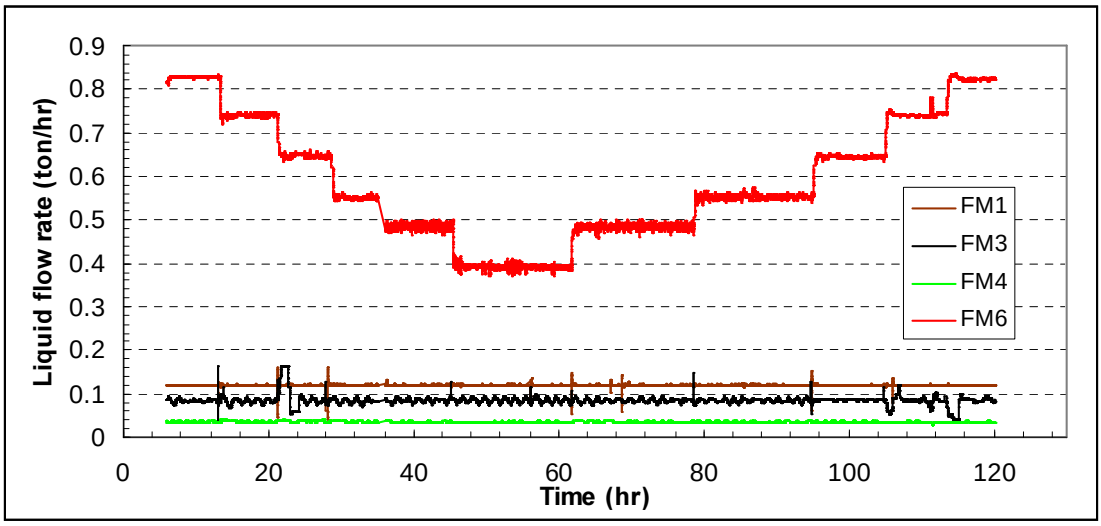

Figure E4.16: Liquid flow rates in the column
FM1 - Feed flow rate
FM3 - Bottom product flow rate
FM4 - Top product flow rate
FM6 - Reflux flow rate

E.5 Start up data

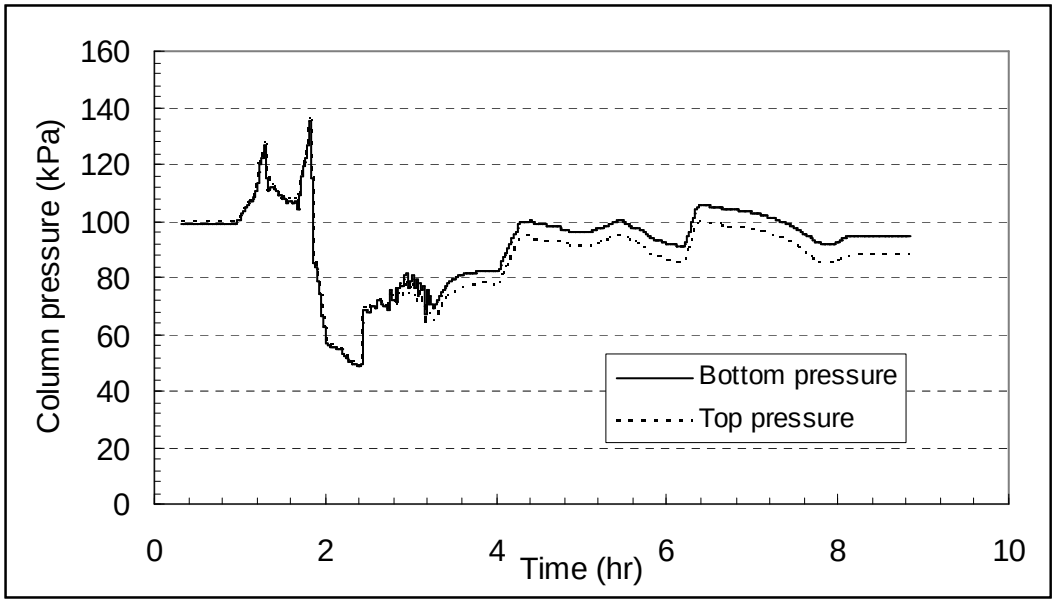

Figure E5.1 Column pressure

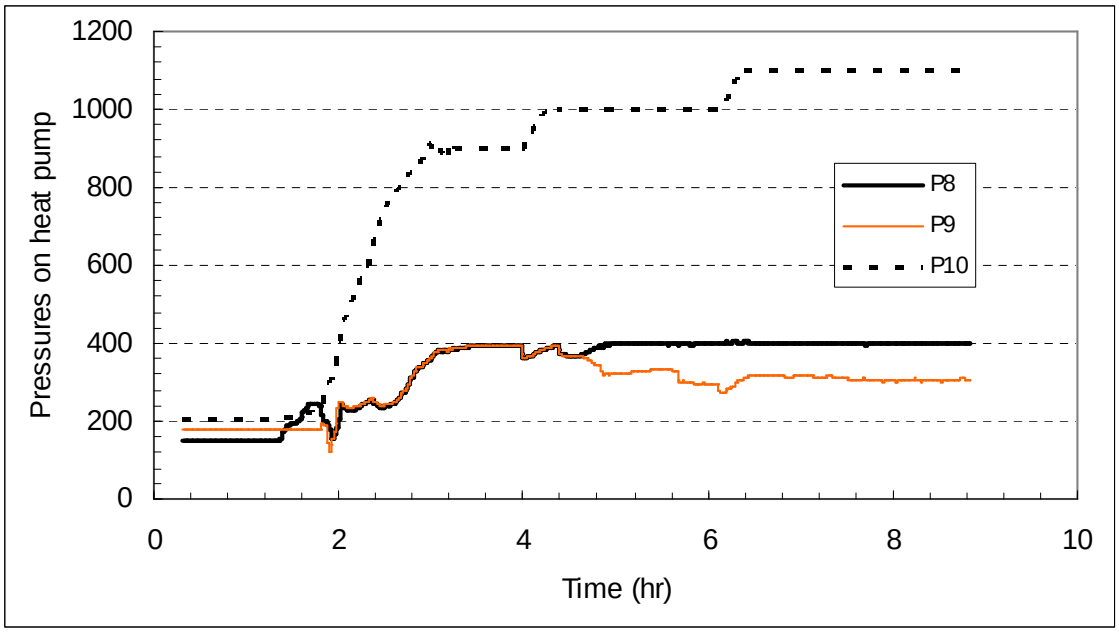

Figure E5.2: Heat pump pressure

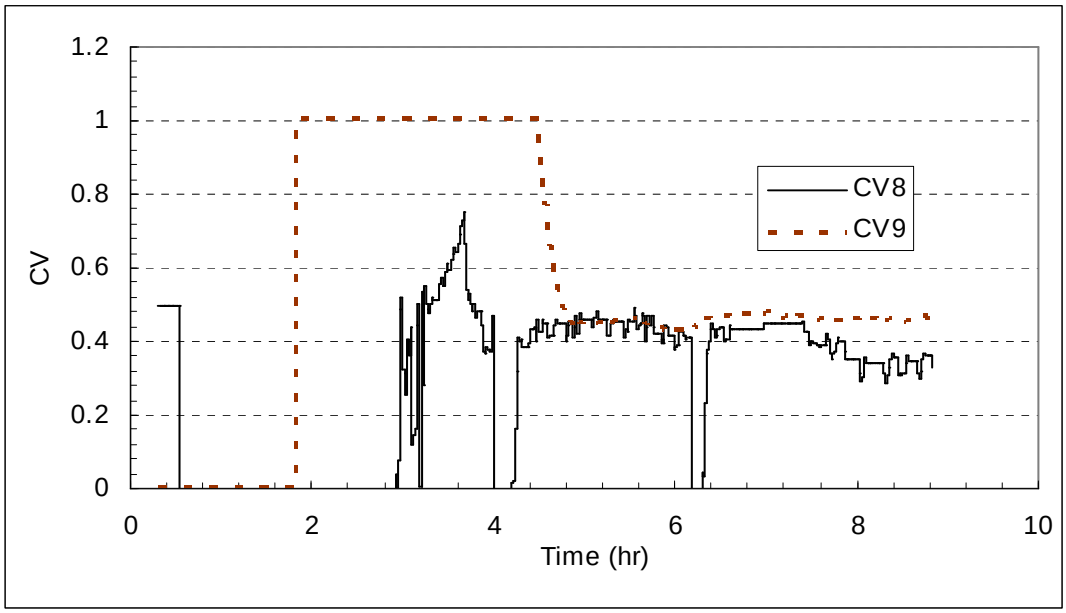

Figure E5.3: Control valves

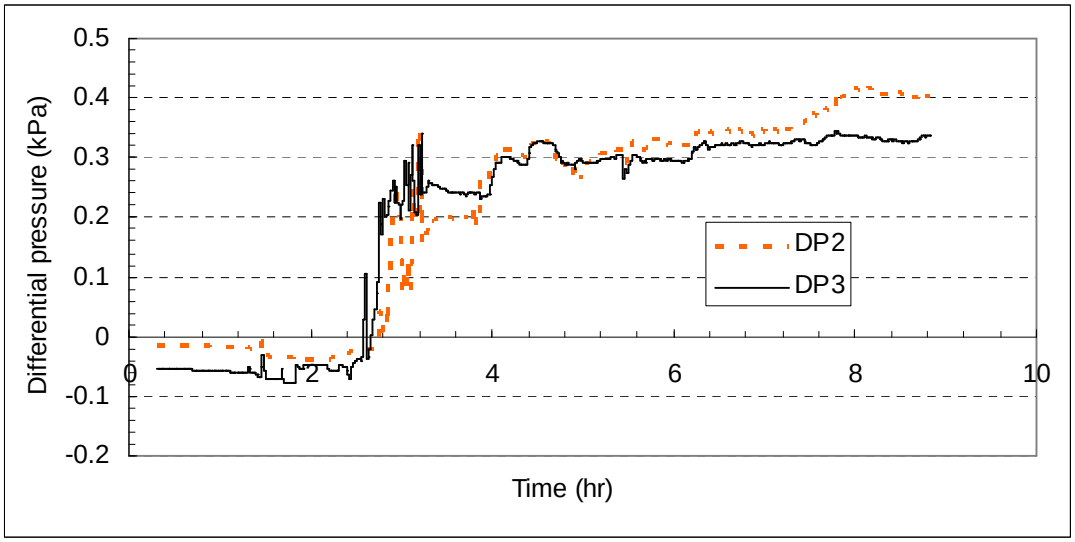

Figure E5.4: Differential Pressure
DP2 - tray 10 (in the middle)
DP3 - tray 19 (top tray)

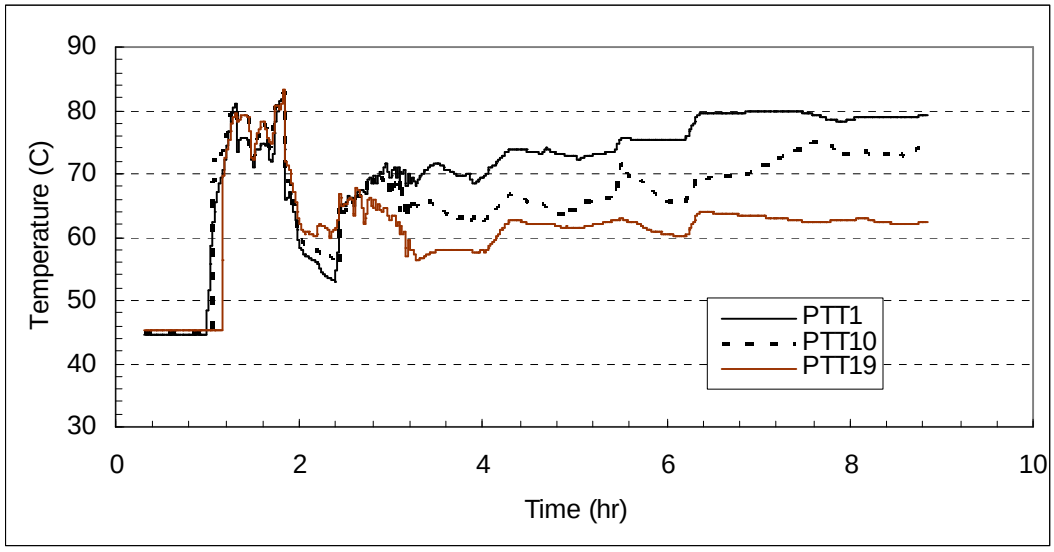

Figure E5.5: Temperature on trays
PTT1 - tray 1 (bottom)
PTT10 - tray 10
PTT19 - tray 19 (top)

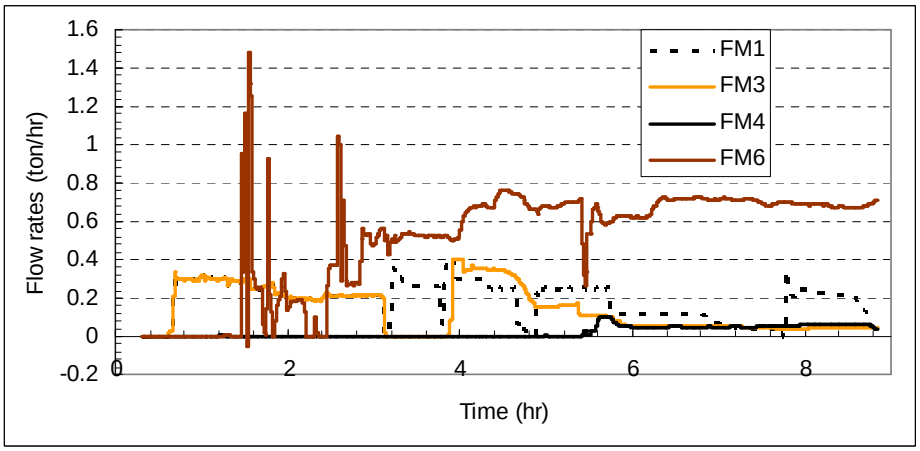

Figure E5.6: Liquid flow rates
FM1 - feed flow rate
FM3 - bottom product flow rate
FM4 - top product flow rate
FM6 - reflux flow rate

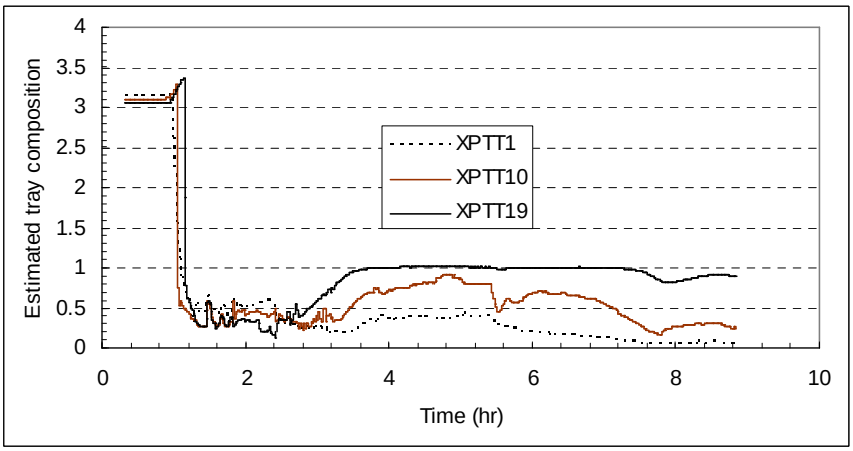

Figure E5.7: Composition on trays
XPTT1 - tray 1 (bottom tray)
XPTT10 - tray 10
XPTT19 - tray 19 (top tray)

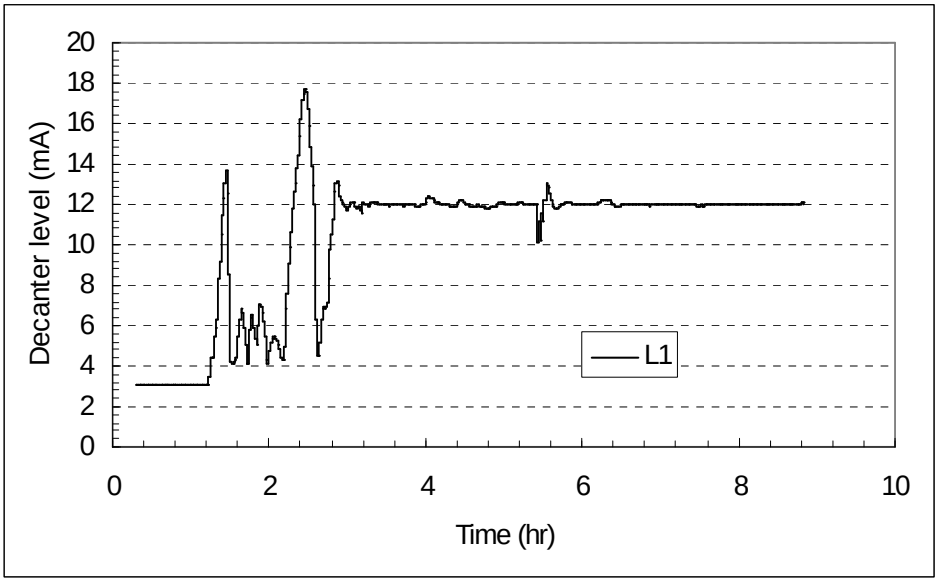

Figure E5.8:: Decanter level

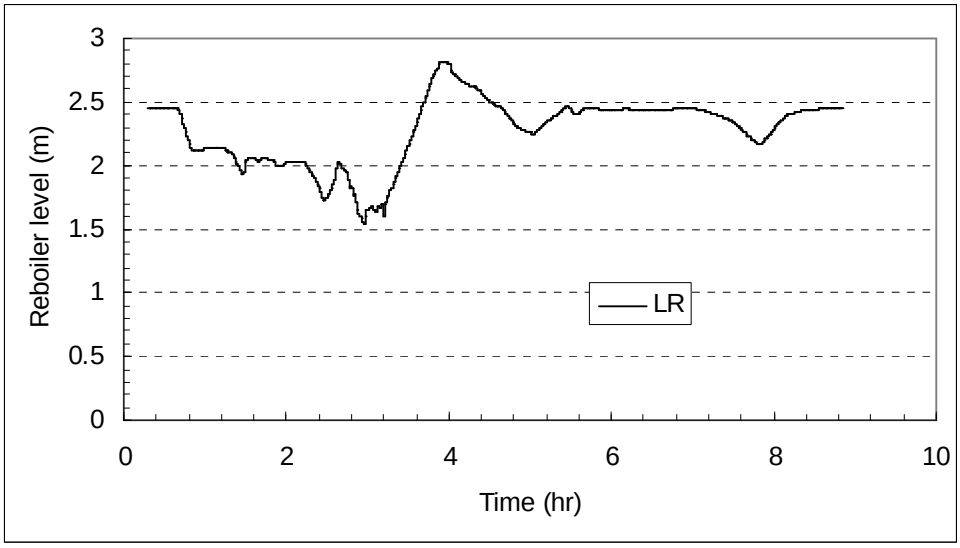

Figure E5.9: Boiler up level

F: Calculation of Separation Factor

F1. The separation factor calculated from the GC results

	Feed (w/w%)								
Steady state	1			2			3		
	H2O	MeOH	PrOH	H2O	MeOH	PrOH	H2O	MeOH	PrOH
SS1	0.8797	29.6355	69.3748	0.9052	29.90332	69.0786	0.7932	31.0867	68.01246
SS2	0.8894	29.76133	69.23816	0.9079	29.9734	69.00639	0.7782	30.55746	68.55844
SS3	0.8409	29.70645	69.34542	0.9423	30.00466	68.93796	0.7209	30.12498	69.0558
SS4	0.8162	29.83137	69.24575	0.9335	29.65442	69.29796	0.7482	29.88912	69.26189
SS5	0.9088	28.77992	70.20197	0.9414	28.78652	70.15372	0.7888	29.7708	69.33688
SS6	0.8682	28.84404	70.18211	0.8955	28.795	70.20103	0.8347	29.36417	69.69634
SS7	0.8832	28.90534	70.10357	0.8788	28.81575	70.19819	0.8647	29.36795	69.65937
SS8	0.9070	28.99214	69.99093	0.9379	28.87987	70.07045	0.7818	29.43694	69.67927
SS9	1.0640	28.24307	70.57442	1.1848	28.14712	70.54136	0.9599	28.83178	70.09505
SS10	0.9176	28.91006	70.06098	0.9176	29.01384	69.9578	0.7968	29.49271	69.60723
SS11	0.9458	29.04121	69.90003	0.9793	28.94213	69.96348	0.7818	29.36417	69.75225
SS12	0.8682	29.12333	69.90003	0.9520	28.9176	70.01744	0.8267	29.40858	69.65937
	Top (w/w%)								
Steady state	1			2			3		
	H2O	MeOH	PrOH	H2O	MeOH	PrOH	H2O	MeOH	PrOH
SS1	0.291366	94.61556	4.966915	0.234036	94.92089	4.748196	0.12555	95.05513	4.757457
SS2	0.256968	94.89081	4.749354	0.309888	94.81215	4.757457	0.219042	93.82558	4.707679
SS3	0.133488	94.72887	5.072181	0.186408	94.67106	5.060615	0.118494	94.71268	5.108034
SS4	0.237564	94.80983	4.855835	0.188172	94.89775	4.831532	0.016182	95.01925	4.843105
SS5	0.43866	94.86304	4.538621	0.470412	94.77282	4.586104	0.069102	95.32952	4.555994
SS6	0.119376	95.47317	4.346316	0.137898	95.4778	4.317347	0.142308	95.47201	4.317347
SS7	0.15201	95.48591	4.290693	0.475704	95.03082	4.320823	0.096444	95.57166	4.276786
SS8	0.237564	95.03776	4.627791	0.150246	95.15699	4.622001	0.1035	95.27509	4.565258
SS9	0.127314	94.92668	4.882451	0.099972	94.96949	4.875508	0.17847	94.82718	4.91485
SS10	0.175824	94.8214	4.924107	0.242856	94.73813	4.919479	0.379566	94.50459	4.973857
SS11	0.26667	94.79711	4.829217	0.174942	94.95444	4.792181	0.025002	95.13499	4.716941
SS12	0.245502	94.86304	4.791024	0.26226	94.96602	4.666	0.09027	94.98569	4.872036
	Bottom (w/w%)								
Steady state	1			2			3		
	H2O	MeOH	PrOH	H2O	MeOH	PrOH	H2O	MeOH	PrOH
SS1	1.152198	2.612435	96.22845	1.251864	2.519706	96.22676	1.093104	2.636046	96.2615
SS2	1.152198	1.722252	97.12298	1.264212	1.877633	96.85874	1.071936	1.702103	97.21998
SS3	1.224522	1.775153	97.00061	1.361232	1.804548	96.84015	1.19718	1.801188	96.9871
SS4	1.257156	1.802028	96.94235	1.185714	1.715536	97.1002	1.190124	1.74996	97.05885
SS5	1.213056	1.634954	97.1525	1.2942	1.599709	97.11032	1.177776	1.619848	97.20143
SS6	1.264212	1.965875	96.77086	1.302138	2.375636	96.32248	1.15749	1.79111	97.04872
SS7	1.230696	1.986049	96.78354	1.23687	2.209783	96.55187	1.205118	1.797829	96.99639
SS8	1.233342	1.567826	97.20058	1.387692	1.574538	97.04619	1.142496	1.58964	97.26551
SS9	1.213056	1.634954	97.1525	1.2942	1.599709	97.11032	1.141614	1.609778	97.24696
SS10	1.209528	1.717215	97.07404	1.308312	1.733167	96.96346	1.124856	1.724771	97.1466
SS11	1.434438	2.017156	96.5561	1.363878	1.954947	96.68634	1.17072	2.03229	96.79368
SS12	1.198062	2.02136	96.77847	1.31625	2.039858	96.6466	1.066644	2.03229	96.89337

Steady state	Feed (m/m%)								
	1			2			3		
SS1	0.02293	0.434543	0.542527	0.023544	0.437474	0.538983	0.020506	0.452037	0.527457
SS2	0.02316	0.435939	0.540901	0.0236	0.438266	0.538134	0.020196	0.446059	0.533746
SS3	0.021923	0.435671	0.542406	0.024474	0.438365	0.537161	0.018782	0.44148	0.539738
SS4	0.021271	0.437324	0.541405	0.024307	0.434352	0.541342	0.019516	0.438521	0.541963
SS5	0.023816	0.424254	0.55193	0.024657	0.424108	0.551235	0.020576	0.436824	0.542599
SS6	0.022759	0.425316	0.551926	0.023472	0.424532	0.551996	0.021815	0.431703	0.546482
SS7	0.023136	0.42593	0.550934	0.023037	0.424904	0.552059	0.022587	0.431521	0.545892
SS8	0.023736	0.426775	0.549489	0.024549	0.425216	0.550235	0.020441	0.432966	0.546592
SS9	0.02791	0.416722	0.555368	0.031033	0.414687	0.55428	0.025125	0.424482	0.550394
SS10	0.024022	0.425729	0.550249	0.024005	0.426951	0.549044	0.02082	0.433506	0.545674
SS11	0.024726	0.42706	0.548214	0.025604	0.425638	0.548757	0.020452	0.432111	0.547437
SS12	0.022716	0.42862	0.548665	0.024906	0.425555	0.549539	0.021605	0.432288	0.546107
Steady state	Top (m/m%)								
	1			2			3		
SS1	0.005297	0.967612	0.027091	0.004251	0.969874	0.025875	0.002282	0.971778	0.02594
SS2	0.004667	0.969454	0.025878	0.005627	0.968455	0.025917	0.004026	0.970017	0.025958
SS3	0.00243	0.969874	0.027697	0.003392	0.968983	0.027625	0.002157	0.969944	0.027899
SS4	0.004317	0.969208	0.026474	0.00342	0.970234	0.026345	0.000295	0.973249	0.026457
SS5	0.007952	0.967364	0.024684	0.008529	0.966527	0.024944	0.001255	0.973921	0.024824
SS6	0.002165	0.974182	0.023653	0.002501	0.974009	0.02349	0.002581	0.97393	0.023489
SS7	0.002756	0.973904	0.02334	0.008614	0.967915	0.023471	0.001749	0.974982	0.023269
SS8	0.004313	0.970484	0.025204	0.002729	0.972089	0.025182	0.00188	0.973249	0.024872
SS9	0.002315	0.971047	0.026637	0.001818	0.97158	0.026602	0.003245	0.969943	0.026812
SS10	0.003197	0.969939	0.026864	0.004415	0.968756	0.026829	0.006897	0.965988	0.027115
SS11	0.004845	0.968832	0.026323	0.003179	0.970693	0.026128	0.000455	0.973795	0.025751
SS12	0.00446	0.969428	0.026112	0.004761	0.969825	0.025414	0.001642	0.971774	0.026584
Steady state	Bottom (m/m%)								
	1			2			3		
SS1	0.036589	0.046665	0.916746	0.039695	0.044942	0.915364	0.034752	0.047141	0.918107
SS2	0.036861	0.030993	0.932146	0.04029	0.03366	0.926051	0.034362	0.030692	0.934946
SS3	0.039093	0.031878	0.929029	0.043312	0.032298	0.92439	0.038241	0.032363	0.929396
SS4	0.040096	0.032329	0.927574	0.037906	0.030849	0.931245	0.038033	0.031457	0.93051
SS5	0.038782	0.029402	0.931815	0.041312	0.028724	0.929964	0.03769	0.029158	0.933153
SS6	0.04026	0.035215	0.924525	0.041292	0.042375	0.916334	0.037005	0.032209	0.930786
SS7	0.039215	0.035597	0.925187	0.039334	0.039529	0.921137	0.038483	0.032293	0.929223
SS8	0.039435	0.028198	0.932367	0.044212	0.028218	0.92757	0.036599	0.028644	0.934756
SS9	0.038782	0.029402	0.931815	0.041312	0.028724	0.929964	0.036565	0.029003	0.934432
SS10	0.038646	0.030863	0.930491	0.041703	0.031075	0.927222	0.036008	0.031057	0.932935
SS11	0.045486	0.03598	0.918535	0.04334	0.034944	0.921717	0.037341	0.036462	0.926197
SS12	0.038193	0.036247	0.92556	0.041842	0.036475	0.921683	0.034102	0.036549	0.929349

	1								
Steady state	Feed (m/m%)			Top (m/m%)			Bot (m/m%)		
	H2O	MeOH	PrOH	H2O	MeOH	PrOH	H2O	MeOH	PrOH
SS1	0.02293	0.434543	0.542527	0.005297	0.967612	0.027091	0.036589	0.046665	0.916746
SS2	0.02316	0.435939	0.540901	0.004667	0.969454	0.025878	0.036861	0.030993	0.932146
SS3	0.021923	0.435671	0.542406	0.00243	0.969874	0.027697	0.039093	0.031878	0.929029
SS4	0.021271	0.437324	0.541405	0.004317	0.969208	0.026474	0.040096	0.032329	0.927574
SS5	0.023816	0.424254	0.55193	0.007952	0.967364	0.024684	0.038782	0.029402	0.931815
SS6	0.022759	0.425316	0.551926	0.002165	0.974182	0.023653	0.04026	0.035215	0.924525
SS7	0.023136	0.42593	0.550934	0.002756	0.973904	0.02334	0.039215	0.035597	0.925187
SS8	0.023736	0.426775	0.549489	0.004313	0.970484	0.025204	0.039435	0.028198	0.932367
SS9	0.02791	0.416722	0.555368	0.002315	0.971047	0.026637	0.038782	0.029402	0.931815
SS10	0.024022	0.425729	0.550249	0.003197	0.969939	0.026864	0.038646	0.030863	0.930491
SS11	0.024726	0.42706	0.548214	0.004845	0.968832	0.026323	0.045486	0.03598	0.918535
SS12	0.022716	0.42862	0.548665	0.00446	0.969428	0.026112	0.038193	0.036247	0.92556
	2								
Steady state	Feed (m/m%)			Top (m/m%)			Bot (m/m%)		
	H2O	MeOH	PrOH	H2O	MeOH	PrOH	H2O	MeOH	PrOH
SS1	0.023544	0.437474	0.538983	0.004251	0.969874	0.025875	0.039695	0.044942	0.915364
SS2	0.0236	0.438266	0.538134	0.005627	0.968455	0.025917	0.04029	0.03366	0.926051
SS3	0.024474	0.438365	0.537161	0.003392	0.968983	0.027625	0.043312	0.032298	0.92439
SS4	0.024307	0.434352	0.541342	0.00342	0.970234	0.026345	0.037906	0.030849	0.931245
SS5	0.024657	0.424108	0.551235	0.008529	0.966527	0.024944	0.041312	0.028724	0.929964
SS6	0.023472	0.424532	0.551996	0.002501	0.974009	0.02349	0.041292	0.042375	0.916334
SS7	0.023037	0.424904	0.552059	0.008614	0.967915	0.023471	0.039334	0.039529	0.921137
SS8	0.024549	0.425216	0.550235	0.002729	0.972089	0.025182	0.044212	0.028218	0.92757
SS9	0.031033	0.414687	0.55428	0.001818	0.97158	0.026602	0.041312	0.028724	0.929964
SS10	0.024005	0.426951	0.549044	0.004415	0.968756	0.026829	0.041703	0.031075	0.927222
SS11	0.025604	0.425638	0.548757	0.003179	0.970693	0.026128	0.04334	0.034944	0.921717
SS12	0.024906	0.425555	0.549539	0.004761	0.969825	0.025414	0.041842	0.036475	0.921683
	3								
Steady state	Feed (m/m%)			Top (m/m%)			Bot (m/m%)		
	H2O	MeOH	PrOH	H2O	MeOH	PrOH	H2O	MeOH	PrOH
SS1	0.020506	0.452037	0.527457	0.002282	0.971778	0.02594	0.034752	0.047141	0.918107
SS2	0.020196	0.446059	0.533746	0.004026	0.970017	0.025958	0.034362	0.030692	0.934946
SS3	0.018782	0.44148	0.539738	0.002157	0.969944	0.027899	0.038241	0.032363	0.929396
SS4	0.019516	0.438521	0.541963	0.000295	0.973249	0.026457	0.038033	0.031457	0.93051
SS5	0.020576	0.436824	0.542599	0.001255	0.973921	0.024824	0.03769	0.029158	0.933153
SS6	0.021815	0.431703	0.546482	0.002581	0.97393	0.023489	0.037005	0.032209	0.930786
SS7	0.022587	0.431521	0.545892	0.001749	0.974982	0.023269	0.038483	0.032293	0.929223
SS8	0.020441	0.432966	0.546592	0.00188	0.973249	0.024872	0.036599	0.028644	0.934756
SS9	0.025125	0.424482	0.550394	0.003245	0.969943	0.026812	0.036565	0.029003	0.934432
SS10	0.02082	0.433506	0.545674	0.006897	0.965988	0.027115	0.036008	0.031057	0.932935
SS11	0.020452	0.432111	0.547437	0.000455	0.973795	0.025751	0.037341	0.036462	0.926197
SS12	0.021605	0.432288	0.546107	0.001642	0.971774	0.026584	0.034102	0.036549	0.929349

Steady state	Separator factor			L (L/min)	Separation factor
	1	2	3		
SS1	701.6714	763.4474	729.6261	17.41014	731.5816
SS2	1126.717	1028.057	1138.372	15.6139	1097.715
SS3	1020.531	1003.924	998.4107	13.61681	1007.622
SS4	1050.368	1111.71	1088.165	11.62327	1083.414
SS5	1242	1254.482	1255.575	10.16842	1250.686
SS6	1081.306	896.6714	1198.193	8.253712	1058.724
SS7	1084.485	960.9682	1205.644	8.209477	1083.699
SS8	1273.191	1268.925	1276.95	10.19308	1273.022
SS9	1155.311	1182.466	1165.554	11.63869	1167.777
SS10	1088.573	1077.391	1070.177	13.58157	1078.714
SS11	939.6338	979.9684	960.5968	15.66823	960.0663
SS12	947.9903	964.2954	929.5141	17.31478	947.2666

F 2. The separation factor calculated from the reconciliation data of GC (mole fraction)

F 2.1 Data reconciliation

F 2.1 Data reconciliation

In order to obtain the sets of data, the results from the GC – analysis and the on – line measure measurements of the external flows from the experiments were reconciled. This is done to ensure that the overall mass and component balance are respected from a steady state point of view. More details of this method can be seen from the reference (Toben, 2003).

The objective function for the measurements for the data reconciliation is:

$$F = \sum_i \left(\frac{y_i^m - y_i^f}{\sigma_i}\right)^2$$

Where y_i^m is the measured valued, y_i^f is the calculated fitted value and σ_i is the standard deviation of measurement i. The measured variables y_i^m are:

$$y^m = [\ x_{F,H2O}\ \ x_{F,MeOH}\ x_{F,\mathrm{Pr}OH}\ x_{D,H2O}\ x_{D,MeOH}\ x_{D,\mathrm{Pr}OH}\ \ x_{B,H2O}\ x_{B,MeOH}\ x_{B,\mathrm{Pr}OH}\ \mathrm{F\ D\ B}]^{\mathrm{T}}$$

$$0 = F - D - B$$
$$0 = Fx_{F,MeOH} - Dx_{D,MeOH} - Bx_{B,MeOH}$$
$$0 = Fx_{F,\mathrm{Pr}OH} - Dx_{D,\mathrm{Pr}OH} - Bx_{B,\mathrm{Pr}OH}$$
$$0 \le x_{k,j} \le 1$$
$$\sum_j^3 x_{k,j} = 1$$
$$0 \le F \le F_{Feed}$$

$$0 \le D \le F_{Feed}$$
$$0 \le B \le F_{Feed}$$

F 2.2 Data reconciliation results

The feed flow, top and bottom flow rate of each steady state (Kmol/hr)

	F (kmo/hr)	D (kmol/hr)	B (kmol/hr)
SS1	2.565443	1.066174	1.468367
SS2	2.563482	1.068128	1.455942
SS3	2.559691	1.075561	1.445209
SS4	2.554782	1.078308	1.438449
SS5	2.545107	1.048837	1.458691
SS6	2.542513	1.045347	1.479645
SS7	2.54558	1.039651	1.463552
SS8	2.544747	1.051859	1.461642
SS9	2.541696	1.049272	1.465888
SS10	2.547582	1.051032	1.460751
SS11	2.546231	1.039299	1.536249
SS12	2.545887	1.038458	1.494451

The deviation of each component, each steady state and the average deviation of all steady state of each component

Steady state	Feed			Top		
	H20	MeOH	PrOH	H20	MeOH	PrOH
SS1	0.0016065	0.0093697	0.007879	0.001531	0.002086	0.000684
SS2	0.0018514	0.0052999	0.003608	0.000806	0.000791	3.96E-05
SS3	0.0028512	0.0029071	0.002623	0.000649	0.000535	0.000142
SS4	0.0024236	0.0021465	0.000342	0.002112	0.0021	6.99E-05
SS5	0.0021546	0.0073	0.005198	0.004043	0.004049	0.00013
SS6	0.0008311	0.0039333	0.003163	0.00022	0.000129	9.42E-05
SS7	0.0002927	0.0035613	0.003284	0.003707	0.003807	0.000103
SS8	0.0021751	0.0040993	0.001924	0.001235	0.001388	0.000186
SS9	0.0029557	0.0051685	0.002615	0.000724	0.000835	0.000112
SS10	0.0018437	0.0041821	0.002371	0.001886	0.002028	0.000156
SS11	0.0027566	0.0034017	0.000663	0.002216	0.002507	0.000291
SS12	0.0016798	0.0033711	0.001784	0.001721	0.001256	0.000589
Av	0.002	0.0046	0.003	0.002	0.0018	0.0002

Steady state	Bottom		
	H20	MeOH	PrOH
SS1	0.002498	0.001157	0.001372
SS2	0.002976	0.001634	0.004548
SS3	0.002716	0.000263	0.00279
SS4	0.00123	0.000744	0.001942
SS5	0.001858	0.000344	0.001601
SS6	0.002238	0.005222	0.007248
SS7	0.000461	0.003622	0.004043
SS8	0.003847	0.000252	0.00366
SS9	0.002375	0.000341	0.002245
SS10	0.00285	0.000118	0.002867
SS11	0.004221	0.000776	0.003849
SS12	0.003872	0.000157	0.003833
Av	0.0026	0.0012	0.0033

Av: means average value

The deviation of each steady state for the feed, top and bottom

	F	D	B
SS1	0.000435	0.000147	0.00333
SS2	0.000644	0.00103	0.00413
SS3	0.000658	0.00117	0.00559
SS4	0.000919	0.00127	0.00315
SS5	0.00098	0.000891	0.00515
SS6	0.000576	0.00076	0.00531
SS7	0.000562	0.000366	0.00564
SS8	0.000628	0.000338	0.00379
SS9	0.000539	0.000834	0.00571
SS10	0.000525	0.000423	0.000915
SS11	0.000462	8.33E-05	0.00736
SS12	0.000441	0.000847	0.00486
Av	0.000614	0.00068	0.004578

The reconciliation GC data (Mole fraction)

	Feed			Top		
	H20	MeOH	PrOH	H20	MeOH	PrOH
SS1	0.031	0.4309	0.5381	0.0021	0.9715	0.0263
SS2	0.0337	0.4239	0.5423	0.0023	0.9718	0.0259
SS3	0.0335	0.4273	0.5392	0.0003	0.972	0.0278
SS4	0.0325	0.429	0.5386	0.0006	0.973	0.0265
SS5	0.0343	0.4177	0.5479	0.0037	0.9715	0.0248
SS6	0.0281	0.4225	0.5493	0.0013	0.9751	0.0236
SS7	0.0348	0.4192	0.546	0.0021	0.9745	0.0234
SS8	0.0321	0.4194	0.5485	0.0011	0.9738	0.0251
SS9	0.0317	0.4179	0.5504	0.0018	0.9715	0.0267
SS10	0.0334	0.4187	0.5479	0.0028	0.9703	0.027
SS11	0.0192	0.4183	0.5624	0.0033	0.9707	0.026
SS12	0.0275	0.4183	0.5542	0.0026	0.9714	0.026

	Bottom		
	H20	MeOH	PrOH
SS1	0.0316	0.0474	0.921
SS2	0.0307	0.0335	0.9358
SS3	0.0322	0.0335	0.9343
SS4	0.0308	0.0325	0.9367
SS5	0.0315	0.0303	0.9382
SS6	0.0356	0.0372	0.9273
SS7	0.0301	0.0368	0.9331
SS8	0.0338	0.0294	0.9368
SS9	0.0356	0.0292	0.9352
SS10	0.0317	0.0322	0.9362
SS11	0.0488	0.0367	0.9146
SS12	0.0365	0.0375	0.926

	F (kmo/hr)	D (kmol/hr)	B (kmol/hr)	L(L/min)	Separation factor
SS1	2.5649	1.0668	1.4981	17.41014	717.7419743
SS2	2.5628	1.069	1.4938	15.6139	1048.130513
SS3	2.559	1.0764	1.4826	13.61681	975.1311071
SS4	2.5541	1.0791	1.475	11.62327	1058.239884
SS5	2.5445	1.0496	1.4948	10.16842	1212.952864
SS6	2.5422	1.0457	1.4965	8.253712	1029.946043
SS7	2.5448	1.0406	1.5043	8.209477	1055.9573
SS8	2.5442	1.0525	1.4917	10.19308	1236.21953
SS9	2.5412	1.0498	1.4914	11.63869	1165.34144
SS10	2.547	1.0518	1.4952	13.58157	1044.852611
SS11	2.5467	1.0387	1.5081	15.66823	930.4152379
SS12	2.5457	1.0387	1.5069	17.31478	922.5809231

F 2.3 Separation factor versus reflux flow rate with the reconciled data

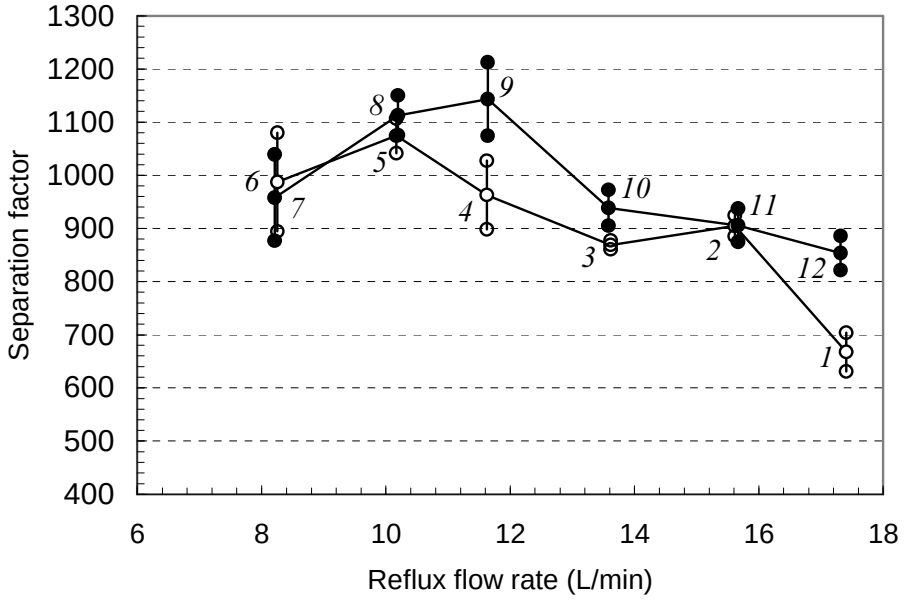

Figure F.1: Inherent separation factor with standard deviation vs. reflux flow rate with both top pressure and bottom pressure control for experiments IV. Steady states 1-6 have top pressure control, while steady states 7-12 have bottom pressure control.